GENERATING RELIABLE DATABASE FOR LOSS ESTIMATION AND MITIGATION PLANNING OF TSUNAMI EFFECTS
Case Study: Cilacap City, Indonesia

By:
Rahmat Ganda Pandapotan Sihombing

GENERATING RELIABLE DATABASE FOR LOSS ESTIMATION AND MITIGATION PLANNING OF TSUNAMI EFFECTS
Case Study: Cilacap City, Indonesia

Thesis submitted to the Graduate School, Faculty of Geography, Gadjah Mada University in partial fulfillment of the requirement for the degree of Master of Science in Geo-Information for Spatial Planning and Risk Management

UGM ITC

By:
Rahmat Ganda Pandapotan Sihombing
08/276581/PMU/5629
sihombing22614@itc.nl

Supervisors:
1. **Dr. Djati Mardiatno, MSi**
2. **Drs. M. C. J. Michiel Damen**

GADJAH MADA UNIVERSITY
INTERNATIONAL INSTITUTE FOR GEO-INFORMATION SCIENCE AND EARTH OBSERVATION
2010

THESIS

GENERATING RELIABLE DATABASE FOR LOSS ESTIMATION AND MITIGATION PLANNING OF TSUNAMI EFFECTS; Case Study: Cilacap City, Indonesia

By:
Rahmat Ganda Pandapotan Sihombing
08/276581/PMU/5629
22614

Has been approved in Yogyakarta
February 2010

By a team of supervisors:
Chairman

___________________.

External Examiner

Prof. Dr. Freek van der Meer ___________________.

Supervisor 1 Supervisor 2

Dr. Djati Mardiatno, MSi **Drs. M. C. J. Michiel Damen**

Certified by:
Program Director of Geo-Information for Spatial Planning and Risk Management
Graduate School Faculty of Geography, Gadjah Mada University

Dr. H. A. Sudibyakto, M. S.

DISCLAIMER

This document describes work undertaken as part of a program of study at the Double Degree International Program of Geo-Information for Spatial Planning and Risk Management, a Joint Program of International Institute for Geo-Information Science and Earth Observation (ITC) - The Netherlands and Gadjah Mada University - Indonesia. All views and opinions expressed therein remain the sole responsibility of the author, and do not necessarily represent those of the institute.

Sihombing, R. G. P.

Abstract

This research was intended to formulate efficient and effective methods in developing reliable database for loss estimation and mitigation planning of tsunami impact. The existing maps are usually not sufficient for loss estimation and mitigation planning purposes in terms of geometrical aspect. New maps can be generated utilizing high spatial resolution satellite imagery. For loss estimation and mitigation planning in the basis of individual buildings, the positional accuracy of the imagery must be improved through geometrical correction. In accordance with the sub-meter pixel size, the GCPs to be used in the rectification process are highly recommended to have horizontal precision of sub-meter also. Differential GPS measurement must be conducted to provide GCPs of the expected horizontal precision. The corrected imagery and the spatial arrangements of the features in the existing maps are combined to develop new maps for the database of elements at risk. A good database can be used as the basis for accurate loss estimation and effective mitigation planning.

Ideally, a complete identification of all elements at risk exposed to certain hazards must be established for loss estimation and mitigation planning. This study will focus on the population and buildings where the community live and do their activities. Land parcels will also be taken into account because mitigation planning is usually arranged in the basis of individual building or individual land parcel. A site-specific study on the vulnerability of elements at risk will result more accurate loss estimation and more effective mitigation planning. For this reason, the vulnerability curves of buildings constructed by the 2006 South Java tsunami reconnaissance survey team are used for this study. The behavior of a building under the effects of certain hazards will determine whether the people in the building might be injured or killed. Therefore, the vulnerability of people inside or nearby a building is determined based on the vulnerability of individual building. Dynamic distribution of population is estimated based on architectural space requirements and several reasonable assumptions.

Loss estimation and mitigation planning were conducted two times, based on the original imagery and the corrected imagery. Comparison of the final results of the works will show whether or not geometrical correction conducted upon the imagery changed the estimated loss significantly. Furthermore, the comparison will show whether or not the proposed methods for developing the database of elements at risk are useful for loss estimation and mitigation planning.

Acknowledgements

I would like to acknowledge and give thanks to:

- My beloved wife Sysca and my lovely little daughter Amanda. You give me the reasons to fight for.
- Sihombing family and Hasibuan family for their full support during my study.
- Badan Perencanaan Pembangunan Nasional (BAPPENAS) and Netherlands Education Support Office (NESO) for providing the scholarship so that the author was able to take a part in the Joint Education Program of UGM and ITC.
- Badan Pertanahan Nasional (BPN) that gave the author permission to join the education program and to leave the office during the study.
- My supervisors: Dr. Djati Mardiatno and Drs. Michiel Damen. I thank you for your inputs and guidance from the beginning of the work.
- Dr. David G. Rossiter for the tough discussions during the fieldwork and the mid term evaluation. I appreciate your constructive criticisms.
- Dr. Junun Sartohadi, Dr. Aris Marfai, and Drs. Robert Voskuil for their assistance during my proposal writing in Enschede.
- All the lecturers in the Geo-Information for Spatial Planning and Risk Management Joint Education Program from UGM and ITC for their support during my study in the program.
- All of my Geo-Info classmates. Tandang, Bang Bona, Bang Emba, Kang Zein, and Mas Wahyu for their support. Mbak Dewi; my partner during the fieldwork in Cilacap. Mbak Fetty, Arie, Echa, Mbak Diah, and Mbah Sigit. We did it..!!
- All of my ITC friends. Special thanks to Fajar for the discussions during my proposal writing in Enschede.
- Bapak Firman Fahada and the staffs of Balai Pemantapan Kawasan Hutan (BPKH) Wilayah XI Jawa – Madura for providing the complete set of Mapping grade GPS equipments.
- Bapak Atim Bukhori of Kantor Pelayanan Pajak Pratama Cilacap. The Block map and the document of the Tax Office are critical inputs for the works.
- Bapak Pujo Hartoyo, Bapak Bambang Riyadi, and Bapak Gatot of Kantor Pertanahan Cilacap for the Land Office's land parcel maps.
- My fieldwork crews in Cilacap; Bang Hamdani of MPKD UGM-Japan Batch 7, Mas Anto, Mas Tujung, and Ajie.
- Saut Sagala for the discussions to improve my thesis writing.
- Bapak Widjokongko of BPPT for the cooperation during the fieldwork in Cilacap.

Finally, I give thanks to Jesus Christ my Lord for the blessings I have received for all my life. With His Will, I am able to finish this study.

Rahmat Ganda Pandapotan Sihombing
2010

Table of contents

List of figures

List of tables

1. Introduction

This chapter is discussing the background of the research, problem statement, research objectives, research questions, and hypothesis. The research aims to formulate efficient and effective methods in developing reliable database for loss estimation and mitigation planning of tsunami effects. Most of the works in the research were conducted by making use of the geo-information technology.

1.1. Background

Tsunami is an exceptional marine event characterized by high energy waves triggered by an earthquake, a volcanic eruption, or a submarine landslide (Lavigne *et al.*, 2007). The July 2006 South Java tsunami caused damage and casualties along an approximately 200 km segment of the south coast of Java. Early reports stated that there were about 500 deaths, 400 injuries, 300 missing and 50.000 displaced persons, as revealed in Figure 1.1 below.

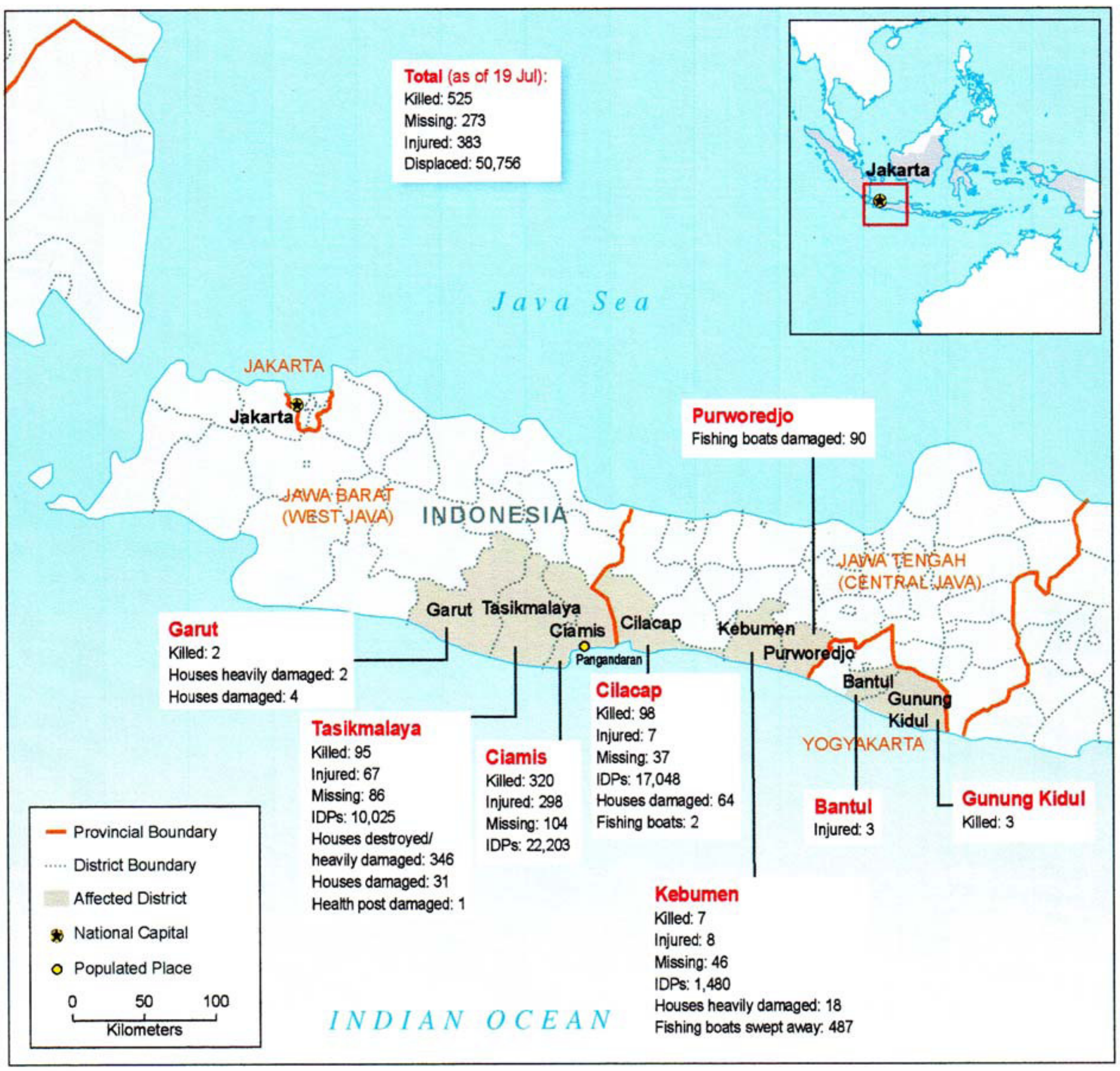

Figure 1-1. Report of the 19th July 2006 South Java tsunami (ReliefWeb, 2006)

Indonesia is located at one of the most active geological subduction zones in the world (Post *et al.*, 2007). Considering the most recent seaquakes and the consequent tsunamis in Aceh (December 2004) and South Java (July 2006), it is expected that in the near future tsunamis are likely to occur in Indonesia. At the same time, Indonesia's population is increasingly growing in coastal areas. The growing population in the coastal area is threatened by tsunamis. Since the tsunami hazard can not be reduced or avoided, mitigation measures must be undertaken to reduce the impact of tsunami events to the population.

1.2. Problem Statement

There are three basic elements for tsunami mitigation planning:

1. Future tsunami extent
   Knowing the extent of future tsunami is the foundation for mitigation planning. Information about the extent of a tsunami event is usually provided by a tsunami inundation model.
2. Vulnerability of elements at risk
   Elements at risk are population, buildings and engineering works, infrastructure, environmental features and economic activities in the area affected by a hazard (ISDR, 2004). Information about the vulnerability of the elements at risk is a critical input for loss estimation and mitigation planning. Identification of the highly vulnerable elements at risk is the basis in determining the sufficient mitigation measures. The result of vulnerability assessment on various elements at risk is commonly presented as vulnerability curves.
3. Exposure of the elements at risk
   The elements at risk will be directly affected by a tsunami event if they are located in the tsunami extent area. Locations of the elements at risk are also critical inputs for loss estimation and mitigation planning. Maps related to the elements at risk of adequate accuracy must be provided for those purposes.

This study will focus mainly on buildings and population as the elements at risk. Therefore, an accurate individual building map is required. Since mitigation planning is commonly arranged in the basis of individual building and individual land parcel, an accurate land parcel map is also required for this study. Unfortunately, those maps of adequate accuracy for loss estimation and mitigation planning are not always available.

1.3. Research Objectives

The main objective of the research is to develop a reliable database of elements at risk for accurate loss estimation and effective mitigation planning. An accurate land parcel map, an accurate individual building map, and a well defined tsunami buffer zone are critical inputs to propose mitigation plans in reducing the future losses due to tsunami effects. The main objective can be detailed in several specific objectives:

1. This study will develop methods to create a reliable database of elements at risk by making use of:
   a. Land parcel map of the Land Office
   b. Block map of the Tax Office
   c. Record of Land Parcel and Building Data developed by the Tax Office
   d. High spatial resolution imagery
   e. High precision Ground Control Points (GCPs)
2. This study will provide potential loss estimation of buildings and population located within the tsunami inundation area.
3. This study will propose non structural mitigation measure through land use policy; acquisition of tsunami buffer zone for open-space uses.
4. This study will propose structural mitigation measure; retrofitting
5. This study will determine whether correction of maps and imageries utilizing high precision GCPs changes the final result of loss estimation significantly or not.

1.4. Research Questions

The research questions of this study are detailed in Table 1.1 below:

Table 1-1. Research objectives and research questions

No	Objectives	Research Questions
1.	To develop methods in creating a database of elements at risk by making use of: existing maps and databases, high spatial resolution satellite imagery, and high precision GCPs.	1. How reliable are the existing maps and databases for loss estimation and mitigation planning purposes? 2. How to obtain high precision GCPs ? 3. How to combine existing maps, high spatial resolution satellite imagery, and high precision GCPs in generating reliable land parcel map and individual building map?
2.	To provide loss estimation of buildings and loss estimation of population for day time and night time scenarios.	1. How to identify the buildings located within the classes of tsunami inundation area? 2. How to determine the physical vulnerability and the economic value of the buildings? 3. How to estimate the dynamic distribution of population? 4. How to determine the vulnerability of the people to tsunami effects?
3.	To propose non structural mitigation planning through land use policy: acquisition of the tsunami buffer zone	1. How to determine a tsunami buffer zone based on a tsunami inundation model? 2. How to estimate the replacement cost?
4.	To propose structural mitigation planning: retrofitting	1. How to identify the buildings subjected to retrofitting? 2. How to determine the effective retrofitting measure?

5.	To determine whether or not improvement of maps and imageries utilizing GPS measurement of high precision changes the final result of loss estimation	1. How much is the difference of building loss estimation calculated using maps generated based on original imagery and loss estimation calculated using maps generated based on accurately corrected imagery? 2. How significant does image correction change the results of population loss estimation?

1.5. Hypothesis

The losses estimated using the existing individual building map will differ significantly to the losses estimated using the new individual building map to be generated.

2. Literature Review

This chapter contains some reviews of the literatures related to the works in the study. Brief explanations are given on the tsunami inundation modelling, risk assessment and loss estimation, vulnerability of building and population to tsunami effects, the use of high spatial resolution satellite imagery, and the use of GPS measurement. The theoretical background in the literatures will be used as the basis in conducting the works of the research.

2.1. Tsunami inundation modelling

The nature and extent of tsunami hazard is usually predicted by making use of modelling approach. The common output of the approach is the tsunami inundation model. A tsunami inundation model can be generated using simple model, roughness coefficient based model, and numerical model. There are many numerical techniques with specific characteristics. The application of each model depends on the objective of the study, the availability of data and the physical conditions of the study area.

1. The simple model
   In the simple model, the data of wave height for the worst occurrence will be the bench mark for the inundation model (Papathoma *et al.*, 2003). The tsunami force, tsunami direction, and off shore bathymetry are not taken into account. The inundation area is considered to be the area between the shoreline and the contour line which value is the same with the wave height. The flow depth will differ by the ground elevation.
2. Roughness Coefficient-Based Model
   According to Hill and Mader (1997) in Gerardi *et al*. (2007), the probable distance of tsunami inundation is calculated based on surface roughness coefficient and the wave height at the coast. The formula is revealed below:
   $X_{max} = 0.006 \times ((H_o^{4/3}) / n^2)$; where:
   X_{max} = Maximum flow distance
   H_o = Tsunami wave height at the coastline
   n = Coefficient of surface roughness
   Like the simple model, this model does not consider the hydrodynamic aspect of tsunami wave. This model is good for coastal area with homogenous slope. One of the models based on the above theory is The Non Linier Shallow Water Model (Yeh, 2006).
3. The Numerical Model
   The numerical model includes the generation of hydrodynamic processes based on 4 main aspects in near shore zone:
   1. seabed topography
   2. refraction, diffraction, and reflection effects
   3. wave circulation
   4. energy accumulation

Tsunami inundation models are not expected to provide precise prediction on the nature and extent of tsunamis. Due to the inherent uncertainties in tsunami models; the parameters used in calculations (models, topography, etc) and the judgment to infer inundation, the resulting error is difficult to quantify (Alpar *et al.*, 2004). Those uncertainties result fuzzy boundaries of tsunami inundation models. Though with fuzzy boundaries, the outcome of tsunami modelling is a critical input for loss estimation and mitigation planning.

2.2. Risk assessment and loss estimation

Tsunami risk is a function of three factors: 1) the nature and extent of the tsunami hazard; 2) the vulnerability of facilities and people to damage; and 3) the amount of development or number of people exposed to the hazard (Eisner, 2001). The tsunami risk exists only if there is a vulnerable society within the tsunami hazard area. Degree of losses and the number of casualties are determined by the amount of facilities and the number of people exposed to the tsunami hazard within the tsunami hazard area.

Hazard is a potentially damaging physical event, phenomenon or human activity that may cause the loss of life or injury, property damage, social and economic disruption or environmental degradation (ISDR, 2004). Hazard has a temporal probability and spatial probability. Many studies have been undertaken to model the nature and extend of tsunami hazard. The outcome of the mapping and modelling processes are tsunami inundation models that support decision making for tsunami threatened communities.

Vulnerability is the degree of loss to a given element at risk or set of elements at risk resulting from the occurrence of a natural phenomenon of a given magnitude and expressed on a scale from 0 (no damage) to 1 (total damage) (UNDRO, 1991). Vulnerability represents the conditions determined by physical, social, economic and environmental factors or processes, which increase the susceptibility of a community to the impact of hazards. Vulnerability can be subdivided in physical, social, economical, and environmental vulnerability.

The amount of losses can be quantified in various ways. It can be revealed in the number of buildings damaged, number of people affected, or the amount of economic losses due to tsunami impact. The way the amount is quantified also the risk is quantified (Westen, 2009).

Quantitative assessment of tsunami risk can be conducted utilizing the following formula (Westen, 2009):

$R = P_T * P_L * V * A$

in which:

$\mathbf{P_T}$ is the temporal probability of occurrence of a tsunami hazard with certain intensity

$\mathbf{P_L}$ is the spatial probability of occurrence of a tsunami hazard with certain intensity

V is the physical vulnerability, specified as the degree of damage to a specific element at risk at certain tsunami intensity

A is the quantification of the specific type of element at risk evaluated.

The required data for a quantitative risk assessment as mentioned above are not always available. Tsunami is a very rare event. In the case of South Java tsunami, no extrapolation can be conducted to determine the temporal probability. Without the data of temporal probability, a quantitative risk assessment is not possible to be conducted. Future loss estimation can be conducted instead, utilizing the following formula:

Losses = V * A

in which:

V is the physical vulnerability, specified as the degree of damage to a specific element at risk at certain tsunami intensity

A is the quantification of the specific type of element at risk evaluated

2.3. Vulnerability of buildings and people to tsunami effects

The study will concentrate only on the physical vulnerability of the elements at risk. Physical vulnerability is the degree of loss to built environment or infrastructure and population resulting from the occurrence of a natural phenomenon of a given magnitude and expressed on a scale from 0 (no damage) to 1 (total damage) (Kingma and Westen, 2009). The methods for physical vulnerability assessment are revealed in Table 2.1 below.

Table 2-1. Overview of methods used for measuring physical vulnerability

Group	Method	Description
Empirical Methods	Analysis of observed damage	Based on the collection and analysis of statistics of damage that occurred in recent and historic events. Relating vulnerability to different hazard intensities.
	Expert opinion	Based on asking groups of expert on vulnerability to give their opinion e.g. on the percentage damage they expect for the different structural types having different intensities of hazard. In order to come to a good assessment of the vulnerability, many expert have to be asked and this is time consuming, and subjective in general. Re-assessments of vulnerability after building upgrading or repair are difficult to accommodate.
	Score Assignment	Method using a questionnaire with different parameters to assess the potential damages in relation to different hazard levels. The score assignment method is easier to update e.g. if we think about earthquake vulnerability before and after application of retrofitting.
Analytical models	Simple Analytical models	Studying the behavior of buildings and structures based on engineering design criteria, analyzing e.g. seismic load and to derive the likelihood of failure, using computer based methods from geotechnical engineering. Using e.g. shake tables and wind tunnels, as well as computer simulation techniques;
	Detailed Analytical methods	Using complex methods. It is time consuming, needs a lot of detailed data and will be used for assessment of individual structures

Source: Kingma and Westen (2009)

Buildings are one of the most important groups of elements at risk. People live and do many of their activities in buildings. The behavior of a building under the effects of certain hazards will determine whether the people in the building might be injured or killed (Kingma, 2009). Papathoma and Dominey-Howes ((2003) calculated the vulnerability of individual buildings within the inundation zone in Gulf of Corinth, Greece. A multi criteria evaluation method is used to develop the so called *Papathoma Tsunami Vulnerability Assessment Model* (PTVAM). Field surveys of tsunami events such as the 1992 Flores tsunami, the 1993 Hokkaido tsunami and the 1994 Java tsunami were used as the basis to determine several characteristics of buildings that contribute to their vulnerability. Those criteria were then ranked and weighted based on their levels of importance for the vulnerability value.

Table 2-2. The criteria of building vulnerability, their ranking and weight factors

Criteria	Code	Weight factor
Building material	a	7
Row	b	6
Surroundings	c	5
Condition of ground floor	d	4
Number of floors	e	3
Sea defence	f	2
Natural environment	g	1

Source: Papathoma and Dominey-Howes (2003)

The vulnerability of each building (BV) in the inundation zone is then calculated as follows:
BV = (7xa)+(6xb)+(5xc)+(4xd)+(3xe)+(2xf)+(1xg)
The Human Vulnerability (HV) of each building is calculated using the following equation:
HV = BV x P (where P = Population).

Dominey-Howes and Papathoma (2007) evaluated the appropriateness of the PTVAM model by making use of the results from post-tsunami surveys in the Maldives following the December 26, 2004 Indian Ocean tsunami. A revised version of the PTVAM (PTVAM 2) was proposed. Evaluation was conducted upon each PTVAM attribute, to determine the relevance of each attribute to loss or damage caused by the tsunami.

Table 2-3. Contribution of the criteria to building vulnerability

Criteria	Contribution to vulnerability
Building material	Significantly important
Surroundings	Significantly important but needs further assessment to determine
Condition of ground floor	Needs further assessment to determine
Number of floors	Significantly important
Sea defence	Significantly important
Natural environment	Significantly important but needs further assessment to determine

Source: Dominey-Howes and Papathoma (2007)

Dall'Osso *et al*. (2009) revised the PTVA model for assessing the vulnerability of buildings to tsunami damage. The structural vulnerability "*SV*" of a building is determined by the:

1. Attributes of the building structure (*Bv*);
2. Depth of flood water (*Ex*) at the point where the building is located; and
3. The degree of protection (*Prot*) that is provided to that building by any barriers.

$SV = (Bv) \cdot (Ex) \cdot (Prot)$

The attributes of each variable are as follows:

Table 2-4. Attributes of each variable for structural vulnerability calculation

Variable for structural vulnerability calculation		
Building structure	**Degree of protection**	**Depth of flood water**
Building material	Building row	0 – 1
Condition of ground floor	Presence of seawall	1 – 2
Number of floors	Natural barriers	2 - 3
Foundation	Presence of a brick wall around the building	3 – 4
Shape and Orientation		> 4
Movable Objects		
Preservation Condition		

Source: Dall'Osso *et al*. (2009)

Reese *et al*. (2007) conducted a reconnaissance survey to the South Java area affected by the tsunami of 17 July 2006. The purpose of the work was to acquire data for calibration of models used to estimate tsunami inundations, casualty rates and damage levels. The level of damage observed was diverse and was primarily depended on water depth and the building construction type. Tsunami waves accounted for all surveyed damage since there was no significant ground shaking from the earthquake.

A site-specific study on the vulnerability of elements at risk will result accurate loss estimation and effective mitigation planning. The area of this study was also affected by the 2006 South Java tsunami. Construction types and overall situation of the area for this study are similar to the areas observed by the reconnaissance survey team. The vulnerability curves constructed by the reconnaissance survey team are very suitable to be used for this study. Detailed explanation on the result of the reconnaissance survey will be revealed in Sub-chapter 5.5.

2.4. The use of high spatial resolution satellite imagery

Taubenbock *et al*. (2008) utilized high spatial resolution satellite data for risk and vulnerability assessment to tsunami hazard in Padang, Indonesia. Spatial distribution of built-up densities and land use were derived from IKONOS imagery. High spatial resolution satellite imagery has been widely used for such works. It is less time consuming and much cheaper compared to terrestrial mapping.

Providers of high spatial resolution satellite imageries have produced imageries of sub-meter pixel size. These data are of a resolution comparable with aerial photographs, but are already in digital format and usually include several spectral bands as well. Multi-spectral channels are of lower resolution, usually at 4 times the resolution of the pan-chromatic band. Table 2.5 below describe briefly about the available high spatial resolution satellite imageries and the prices.

Table 2-5. Brief description of the available high spatial resolution satellite imagery

Satellite imagery	Spatial resolution (meter)	Price * (US $ per square kilometer)
GEOEYE-1	0.5 (panchromatic) 2.0 (multi-spectral)	12.5 – 40
IKONOS	1.0 (panchromatic) 4.0 (multi-spectral)	10 – 38
WorldView-1	0.5 (panchromatic)	28 – 70
QuickBird	0.6 and 0.7 (panchromatic) 2.4 and 2.8 (multi-spectral)	14 - 83

* The price varies by the specifications

Source: Eurimage (2009)

A QuickBird imagery data covering the extent area of Cilacap City is available for this study. *Digital Globe*, the provider of QuickBird data, offers different image data products with various corrections applied. They are “Basic” imagery, “Ortho-rectified” imagery, and “Standard” imagery. Basic imagery is the least processed image product of the Digital Globe product suite; only corrections for radiometric distortions and adjustments for internal sensor geometry, optical and sensor distortions have been performed on each scene ordered. Ortho-rectified imagery products are designed for users who require an imagery product that is GIS-ready or for users that require a high degree of absolute geometric accuracy for analytical applications. It is accurate at the same level as the base map. Standard Imagery products are designed for users with knowledge of remote sensing applications and image processing tools that require data of modest absolute geometric accuracy and/or large area coverage. Geometrical aspects of those three types of QuickBird imagery are shown in Table 2.6 below:

Table 2-6. Table QuickBird imagery products and associated accuracies

Product Level	Processing	Absolute Accuracy		Geographic Availability
		CE90%	RMSE	
Basic Imagery	Sensor Corrected (Raw)	23-meters*	14-meters*	Worldwide
Standard Imagery	Georectified	23-meters**	14-meters**	Worldwide
Ortho 1:50,000	Orthorectified	25.4-meters	15.4-meters	Worldwide
Ortho 1:12,000	Orthorectified	10.2-meters	6.2-meters	US and Canada
Ortho 1:5,000	Orthorectified	4.23-meters	2.6-meters	Worldwide
Ortho 1:4,800	Orthorectified	4.1-meters	2.5-meters	US and Canada
Custom Ortho	Orthorectified	variable***	variable***	Worldwide

*Attained using supplied Image Support Data files and a user supplied DEM, excluding sensor and viewing geometry and topographic displacement

**Excluding viewing geometry and topographic displacement

*** Accuracy of the Custom Ortho is determined by the accuracy and quality of customer supplied support data.

Source: Digital Globe (2009)

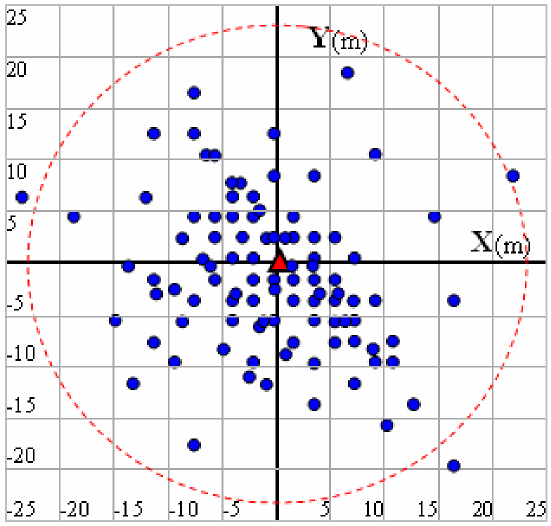

Figure 2-1. Illustration of positional accuracy specified by CE90

Positional accuracies of QuickBird imageries are specified by CE90; circular error at 90% probability. If the position of a feature is measured from an image and compared to its true position, then the radial difference should be less than the CE90 accuracy for 90% of the well defined, photo-identifiable features (Dial, 2000).

Figure 2.1 illustrates the positional accuracy of a QuickBird standard imagery; 23 meters at CE90. For a number of check points on the image, 90% are expected to have positional error < 23 meters.

2.5. The use of GPS measurement

The use of Global Navigation Satellite Systems (GNSS) and Inertial Navigation Systems (INS) on satellite and airborne platforms with imaging sensors means that the geo-referencing can be provided with a minimum number of ground control points, thus allowing the data to be merged with map data, ground positions and other image data in a very short time (Dowman, 2005). However, the positional errors of the imageries established in such method are still significant. For example, the positional accuracies of the ortho-rectified QuickBird imageries range from 4.1 to 25.4 meters.

In practice, positional accuracy of an image may not suit the expectation of some users whose works are in detailed scale. Users may improve the positional accuracy of the imagery through geometrical correction. Geometrical correction is carried out by conducting a geo-referencing process upon the satellite imagery. Ground control points (GCPs) of high accuracy are required to validate and to correct the high spatial resolution imagery. Most of the panchromatic high spatial resolution imageries have the pixel size of sub-meter. In accordance with the sub-meter pixel size, the GCPs to be used in the rectification process are highly recommended to have horizontal precision of sub-meter also. Such high precision GCPs are usually not extractable from standard topographic maps and must be taken by geodetic surveys including differential GPS measurement techniques.

Geodetic grade of dual frequency GPS receiver set is not necessary to be employed in the GCPs measurement. It can achieve millimeters to centimeters horizontal precision but there is no need of such accuracy in rectifying imagery of 50 to 70 cm pixel size. A mapping grade/ mid grade single frequency can be utilized instead.

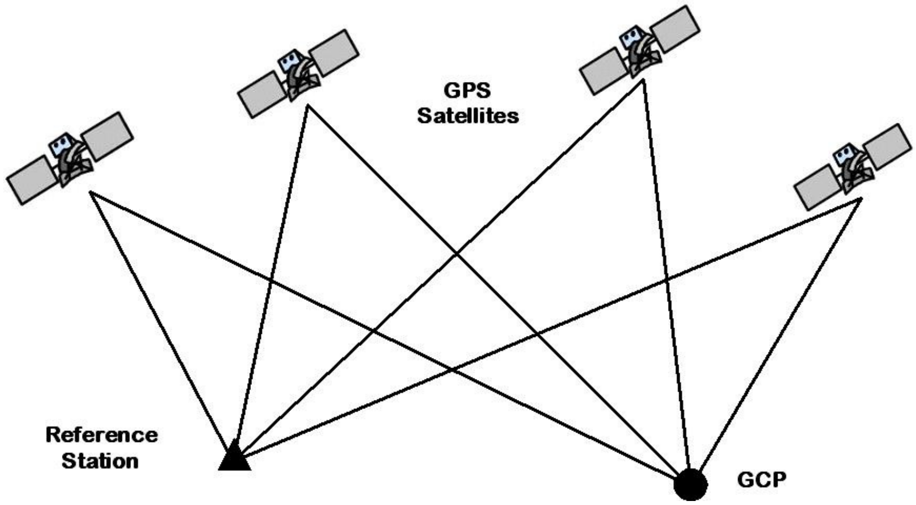

Figure 2-2. Illustration of Differential GPS measurement

Differential GPS measurement using mid grade/ mapping grade single frequency receivers followed by post processing differential correction is expected to result sub-meter horizontal precision. Post processing is reported to have a horizontal accuracy within 0.5 meters (Jones and Jones, 2004). Since the mapping grade receiver use only one frequency (L1), the data involved in post processing is only the code phase. The code phase produces less precise positioning than the carrier phase. Both code phase and carrier phase are involved in GPS measurements using dual frequency (L1 and L2) geodetic grade receiver.

The *base receiver* is located at a reference station of a defined true coordinates, whilst the *rover receiver* is located at the proposed ground control point (GCP). Both receivers, the base and the rover, must "look" at the same satellites at the same time period to allow differential post processing correction. Differential correction is the practice of comparing position data collected by the rover receiver to position data collected by a base station receiver, and applying a correction factor based on this comparison. Differential post processing will eliminate or reduce several errors of the measurement as shown in Table 2.7 below.

Table 2-7. Effects of differential reduction

Error and bias	Eliminated	Reduced	Not eliminated nor reduced
Satellite clock	√		
Receiver clock	√		
Orbit (ephemeris)		√	
Ionosfer bias		√	
Troposfer bias		√	
Multipath			√
Noise			√
Selective availability	√	√	

Source: (Abidin, 2007)

The raw field data can be logged for five to ten seconds occupation time (short-duration post processing) as well as for longer occupation times of 20 to 30 minutes (long- duration post processing). Short-duration post-processing usually does not offer sub-meter horizontal accuracies, whilst long-duration post-processing usually offers a mean horizontal accuracy of sub-meter (Jones and Jones, 2004).

The accuracy is very much depends on the satellite constellation during the measurement. The strength of satellite constellation geometry is represented by the value of PDOP (Positional Dilution of Precision). The long duration gives many more chances to log code phase of low PDOP (≤ 4.0). In order to achieve ≤ 60 cm horizontal precision, the author operated long-duration occupation time and set the filter only to record the readings of PDOP ≤ 4.0.

Setting the filter not to record the readings taken when PDOP (Positional Dilution of Precision) and SNR (Signal to Noise Ratio) are above some minimum level is possible in the mapping grade GPS receiver. Statistical information can be analyzed in a post-processing step that lets the surveyor decide about the quality of the data used in a measured point.

3. Research Methodology

The data requirement, research design, and limitation of the research are revealed in this chapter. There are five main works in the research: assessment of the satellite imagery and existing maps, generating the database of elements at risk, loss estimation of buildings and population, non-structural mitigation planning, and structural mitigation planning. General processes of the main works are described in flowcharts to give clear overviews of each of the works. The source of each data, the processes applied upon them, and the expected outputs are also explained in this chapter.

The research involves several works in order to reach the objectives. The works are grouped into three main stages; pre-fieldwork, fieldwork, and post-fieldwork. Identification of data requirements and selection of the methods for data analysis are carried out in the pre-fieldwork stage. Secondary data and primary data are collected during the fieldwork stage. Database development, loss estimation of buildings and population, and mitigation planning are conducted in the post-fieldwork stage. The general processes of the works in the research are revealed in Figure 3.1 below:

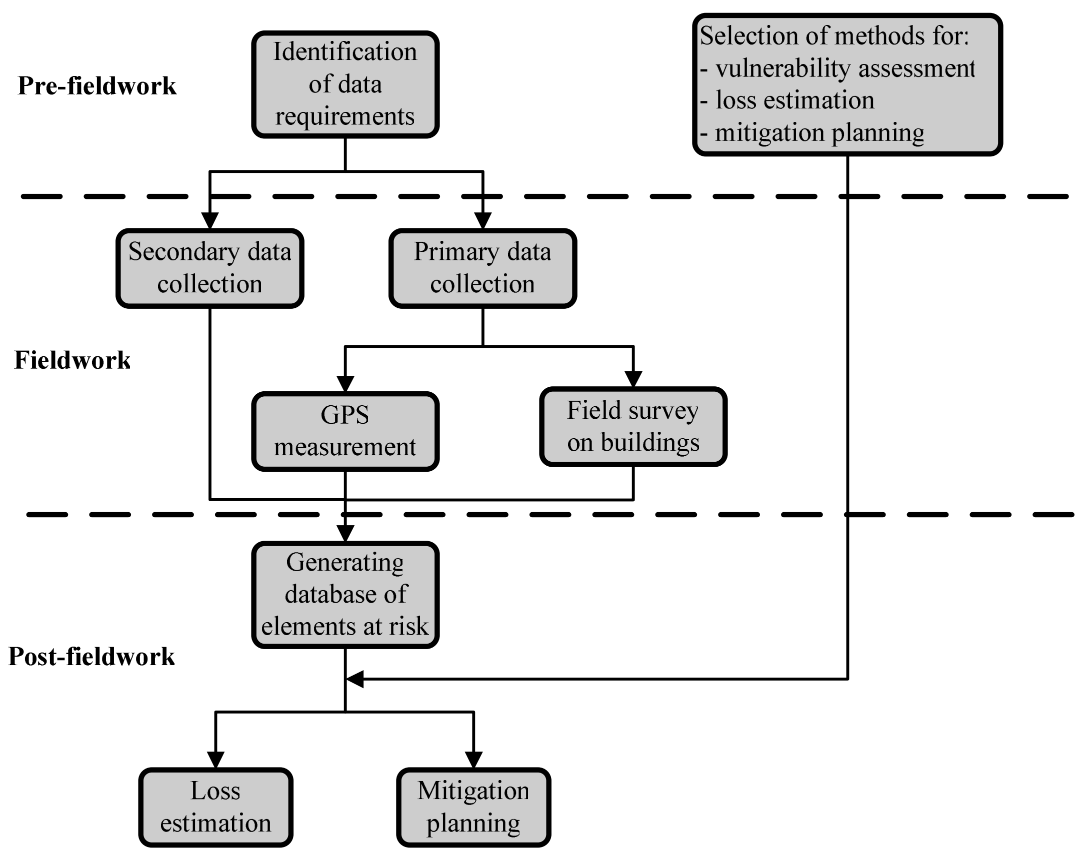

Figure 3-1. The main stages of the research

3.1. Data Requirement

The secondary data available for the study are shown in Table 3.1 below:

Table 3-1. Secondary data requirements for the study

Secondary data requirements	Source	Format
Land parcel map	Land Office	Digital
Block map	Tax Office	Digital
The Record of Land Parcel and Building Data	Tax Office	Soft copy document
Panchromatic QuickBird imagery of 0.6 m pixel size	GITEWS (German Indonesian Tsunami Early Warning System) project	Digital
Tsunami inundation model	Previous research of Dr. Mardiatno	Digital
Topographic map scale 1 : 25000	BAKOSURTANAL (National Coordination Agency for Survey and Mapping)	Hard copy

The primary data collected during the fieldwork are as follows:

Table 3-2. Primary data requirements for the study

Primary data requirements	Method for data collection
Inventory on the physical characteristics of buildings	Data extraction from the Tax Office document and field survey
Coordinates of ground control points (GCPs)	Differential GPS measurement

3.2. Research Design

The main works in the research are as follows:

1. Generating the database of elements at risk
   a. Assessment of the satellite imagery and the existing maps
   b. Generating new land parcel map and individual building map
   c. Determining the vulnerability and amount of elements at risk
2. Loss estimation due to tsunami effects
   a. Loss estimation of buildings
   b. Loss estimation of population
3. Mitigation planning of tsunami effect:
   a. Non structural mitigation planning through land use policy
   b. Structural mitigation planning: retrofitting scheme

3.2.1. Generating the database of elements at risk

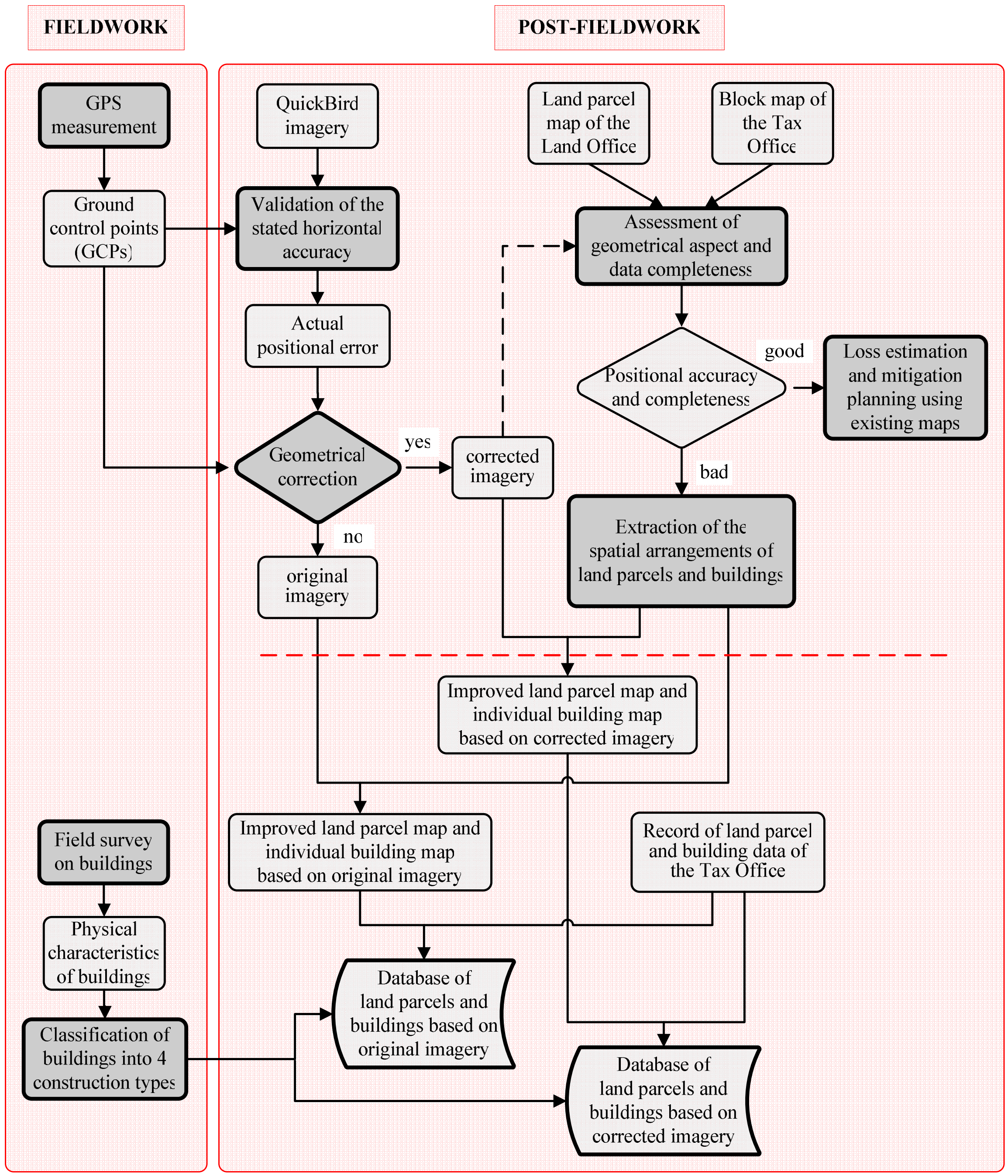

Figure 3-2. Generating the database of elements at risk

Ideally, a complete identification of all elements at risk exposed to tsunamis must be established for loss estimation. In fact, loss estimation studies nearly always focus on specific groups of elements at risk, such as buildings or population. This study will also focus on buildings and population. Land parcels will also be taken into account because mitigation planning is usually arranged in the basis of individual building or individual land parcel.

The existing maps available for loss estimation and tsunami mitigation planning are the land parcel map of the Land Office and the block map of the Tax Office. Assessment of their positional accuracy and feature completeness must be conducted to ensure whether or not they are reliable for loss estimation and tsunami mitigation planning.

If the existing maps are not reliable for those purposes, new maps must be generated. Satellite imagery is commonly used as the basis in generating maps. Since loss estimation and mitigation planning are going to be conducted in the basis of individual land parcel and individual building, the satellite imagery must be of high spatial resolution. A panchromatic QuickBird imagery with 0.60 m of spatial resolution is available for this study.

The horizontal accuracy of the imagery is 10 m and the total RMS of the rectification of the panchromatic channel is 2.3287 m. Even if the image data has a stated positional accuracy, it is always recommended to validate the image to ensure that the image meets the stated positional accuracy. A positional accuracy of 10 m is considered to be good enough compared to the positional accuracy of most of the maps available in Indonesia. The original imagery can be directly used as the basis in generating new maps. In the other hand, positional error up to 10 m may lead to significant error for loss estimation and mitigation planning. Geometrical correction should be conducted upon the imagery to improve its positional accuracy.

The useful thing can be extracted from the existing maps is the spatial arrangement of the land parcels and the buildings. The new maps will be generated based on both the original imagery and the corrected imagery. By comparing the final results of the works, conclusions can be drawn whether or not the geometrical correction on the imagery gives significant changes for loss estimation and mitigation planning.

Attribute data of land parcel and building are already established in the *Record of Land Parcel and Building Data* (census data) developed by the Tax Office, as revealed in Table 3.3 below.

Table 3-3. Attribute data of land parcels and buildings established by the Tax Office

Attribute data on land parcels	Attribute data on buildings
• Area of land parcels • Values of land parcels • etc	• Area of buildings • Values of buildings • Building type (Building use) • Construction type • Roof type • Wall material • Floor material • Number of storey • Age of building • Electrical capacity • etc

Not all of the required data for buildings are available in the record. There are no data on the column material and the dimension of the column. Field survey must be conducted to make adequate inventory on the physical characteristics of buildings.

The prices of land parcels and buildings are listed in the *Record of Land Parcel and Building Data* developed by the Tax Office. The listed prices may differ from the market price. Since the complete data of the prices of land parcels and buildings are only available in this document, loss estimation and the cost for mitigation planning will be based on this document.

Population data in Indonesia is usually established on the basis of administrative units. Estimation of population number per household is usually carried out by dividing the total population in a village by the number of households. Since the sample areas are not in administrative units, this approach is not appropriate to conduct. In the absence of census data, estimation of population distribution will be based on the space requirements of individual buildings and several reasonable assumptions.

3.2.2. Loss estimation of buildings and population

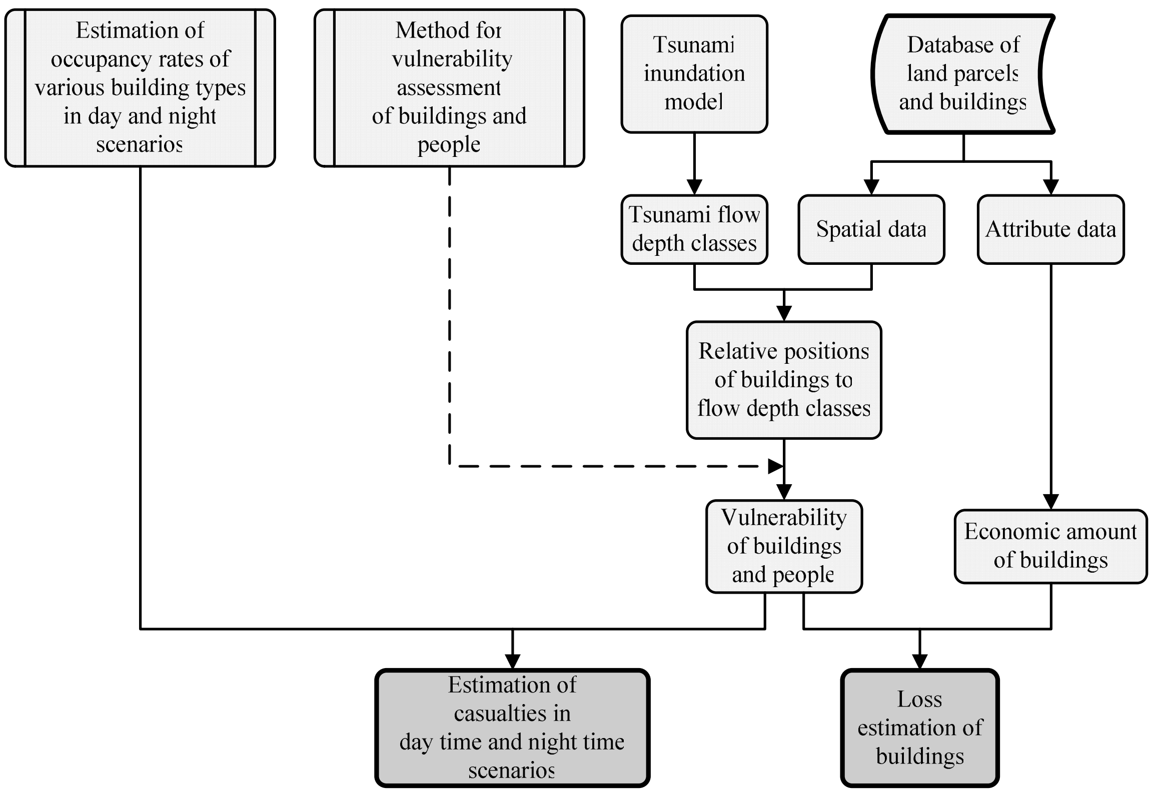

Figure 3-3. Loss estimation of buildings and population

Future loss estimation can be conducted the following formula:

Losses = V * A

in which:

V is the vulnerability, specified as the degree of damage to a specific element at risk at certain tsunami intensity

A is the quantification of the specific type of element at risk evaluated

Assessment of physical vulnerability (V) of buildings is based on vulnerability curves developed by a reconnaissance survey team of the South Java July 2006 tsunami. An empirical approach was applied to define the relation between the flow depth and damage observed during the survey. The economic value (A) of each building is available in the Record *of Land Parcel and Building Data* developed by the Tax Office. The price of an unregistered building will be approximated based on the closest registered buildings with the same construction type.

The behavior of a building under a tsunami event, determines whether the people in the building might be injured or killed. Assumptions are used to determine the casualties to tsunami event. In the case of 2006 south Java tsunami, all deaths and injuries occurred in or near totally and badly damaged buildings. The vulnerability of buildings will determine the vulnerability of people within or nearby.

If the physical vulnerability and economic value of buildings can be determined, the loss estimation on buildings is possible to be conducted. The estimation of occupancy rates for various building types that have the potential to be badly damaged or to collapse will be used for the estimation of casualties. Since the occupancy rates of buildings will differ in day and night time, estimation of casualties will be conducted in day and night scenarios. The loss estimation will be conducted two times, utilizing the database developed based on original imagery and utilizing the database developed based on the corrected imagery. The difference of final results will show how significant the image correction contributes for loss estimation.

3.2.3. Non-structural mitigation planning through land use policy

Defining the tsunami buffer zone is the first step in non structural mitigation planning. A tsunami inundation model of a worst case scenario in Cilacap city developed by Mardiatno in 2006 will be used as the basis in determining the tsunami buffer zone in the study area.

The land parcel map, the individual building map, and the well defined tsunami buffer zone are the primary inputs for acquisition plan. The relative positions of the land parcels or buildings to the buffer zone can be simply determined by overlaying analysis. The accuracy of each spatial data is critical in determining whether or not a land parcel or building is located partially or completely within the tsunami buffer zone. The replacement cost for tsunami buffer zone acquisition is assumed to be the total compensation for land parcels and buildings located in the tsunami buffer zone.

If the tsunami buffer zone is acquired and fully controlled by the local authority, the population at risk will be relocated to safer area. This approach will directly decrease the number of potential casualties to tsunami effects. Non structural mitigation planning will be conducted two times, utilizing the database developed based on original imagery and utilizing the database developed based on the corrected imagery. The difference of final results will show how significant the image correction contributes for non structural mitigation measures.

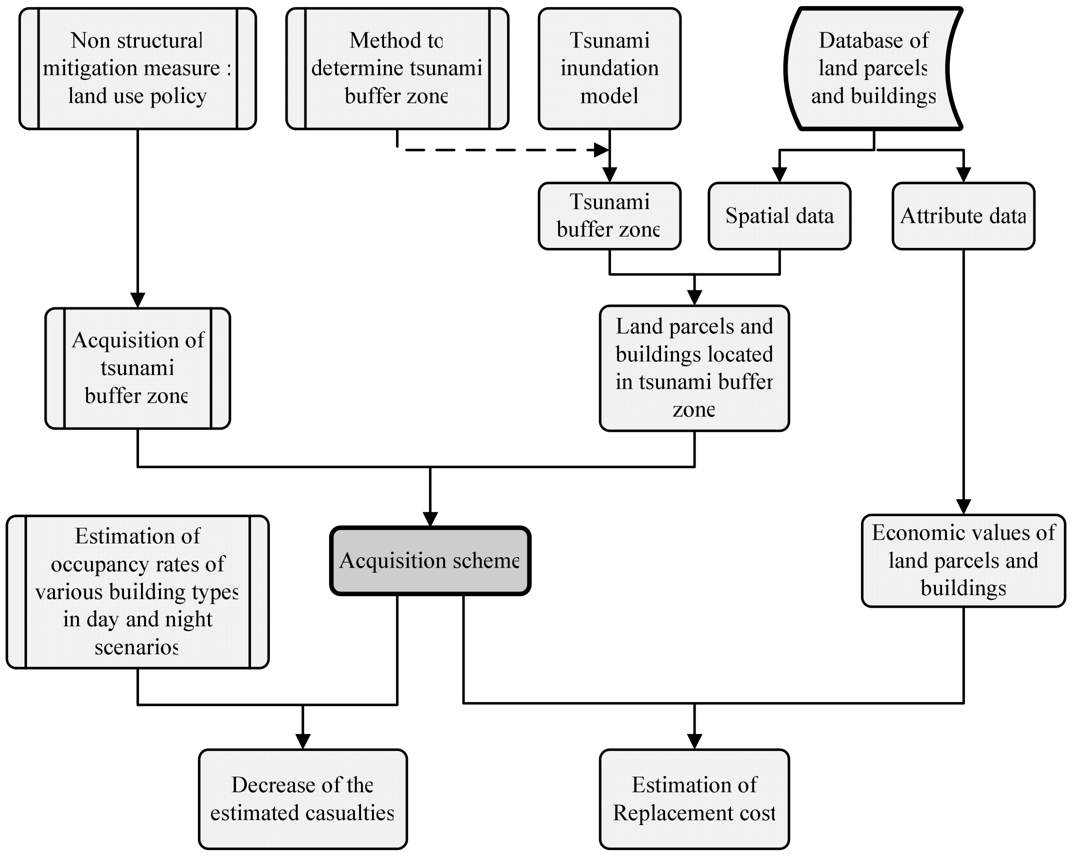

Figure 3-4. Non-structural mitigation planning through land use policy

3.2.4. Structural mitigation planning: retrofitting

A minimum structural adequacy for each flow depth classes must be defined to establish a sufficient retrofitting strategy. The study on the observed damages of the July 2006 South Java tsunami can be used to determine the minimum retrofitting measure addressed to each highly threatened building. The vulnerability value of a building is the basis to determine whether a building is subjected to retrofitting or not.

The retrofitting measures addressed to buildings are expected to increase the performance of the buildings under a given flow depth. The change on the behavior of buildings under tsunami event will directly affect the people living in or nearby. The retrofitting measures are expected to decrease the number of potential casualties.

The scheme for retrofitting was developed two times utilizing two individual building maps, the one developed based on the original imagery and the other one developed based on the corrected imagery. The difference of final results will show how significant the image correction contributes for retrofitting scheme. Whether or not image correction is useful for a structural mitigation planning will be concluded by analyzing the final results.

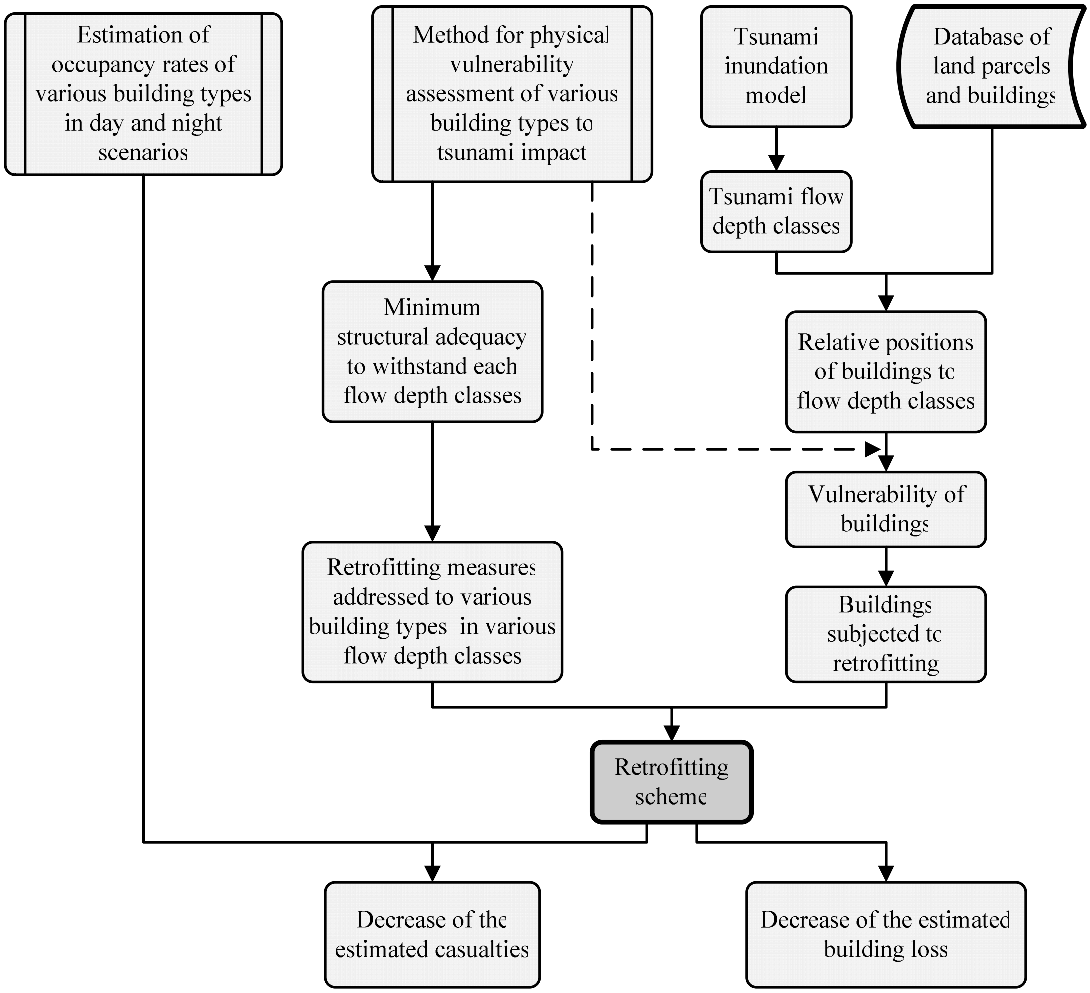

Figure 3-5. Structural mitigation planning: retrofitting

3.3. Limitation of the research

There are two main limitations in the research:

- The positional accuracy of the tsunami inundation model was not assessed. The maps used as the basis to develop the tsunami inundation model was not assessed either. The model is assumed to have adequate positional accuracy. If the model was assessed in terms of positional accuracy, the research would give more objective results.
- The prices of land parcels and buildings listed in the *Record of Land Parcel and Building Data* of the Tax Office are for taxation purpose. Those prices do not represent the actual values as the market values do. In fact, they are much lower than the market values. Loss estimation and calculation of replacement cost should use the market values instead of the values available in the document of the Tax Office. In that way the results of loss estimation and replacement cost estimation will be more accurate.

4. Cilacap City and tsunami threat

Brief explanation about the tsunami inundation model of Cilacap City is given in this chapter. The model represents the tsunami threat in Cilacap City of the worst case scenario. This chapter also provides brief overviews on the geomorphology of the coast and the socio-economic condition of the population living in the coastal area of Cilacap City.

The location for the study on the tsunami loss estimation should be selected where the highest impact of tsunami occurrence is expected. Within the GITEWS (German Indonesian Tsunami Early Warning System) project, it has been agreed that for Java and Bali; the rural region around Cilacap/ Pangandaran (Java) and Kuta (Bali) are classified as highly at risk to tsunamis (Post *et al.*, 2007). This study will take place on the coastal area of Cilacap city, Central Java, Indonesia. Cilacap city lies between latitude 7°39’01.92”S – 7°45’09.53”S and longitude 108°59’27.21”E – 109°06’04.25”E.

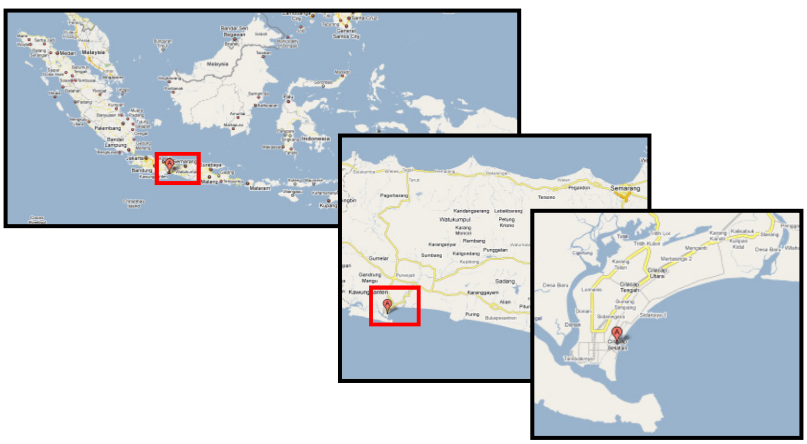

Figure 4-1. Location of study area

Figure 4-2. The two sample areas

The two sample areas for the study are located in two different villages. Those villages are also located in two different sub-districts. The urban sample area is located in *Tegalkamulyan* Village (*Cilacap Selatan* Sub-district), whilst the rural sample area is located in Mertasinga Village (*Cilacap Utara* Sub-district). Tegalkamulyan Village is a populated area. Settlements and industrial uses occupy most of the land in the area. Contrary, Mertasinga Village is less populated. The predominant land use in the area is for agricultural use; paddy field.

4.1. Tsunami inundation model of Cilacap City

Understanding the tsunami threat is the first step in reducing potential losses. Efforts to characterize the nature and extent of tsunami hazard must be undertaken at the first place. Information about the area extent of tsunami hazard is a critical input to determine whether there is a vulnerable society within the tsunami hazard area or not. A tsunami occurrence is not considered a disaster when it occurs in uninhabited areas. It is considered a disaster when it occurs in a populated area, and brings loss or destruction to the vulnerable society.

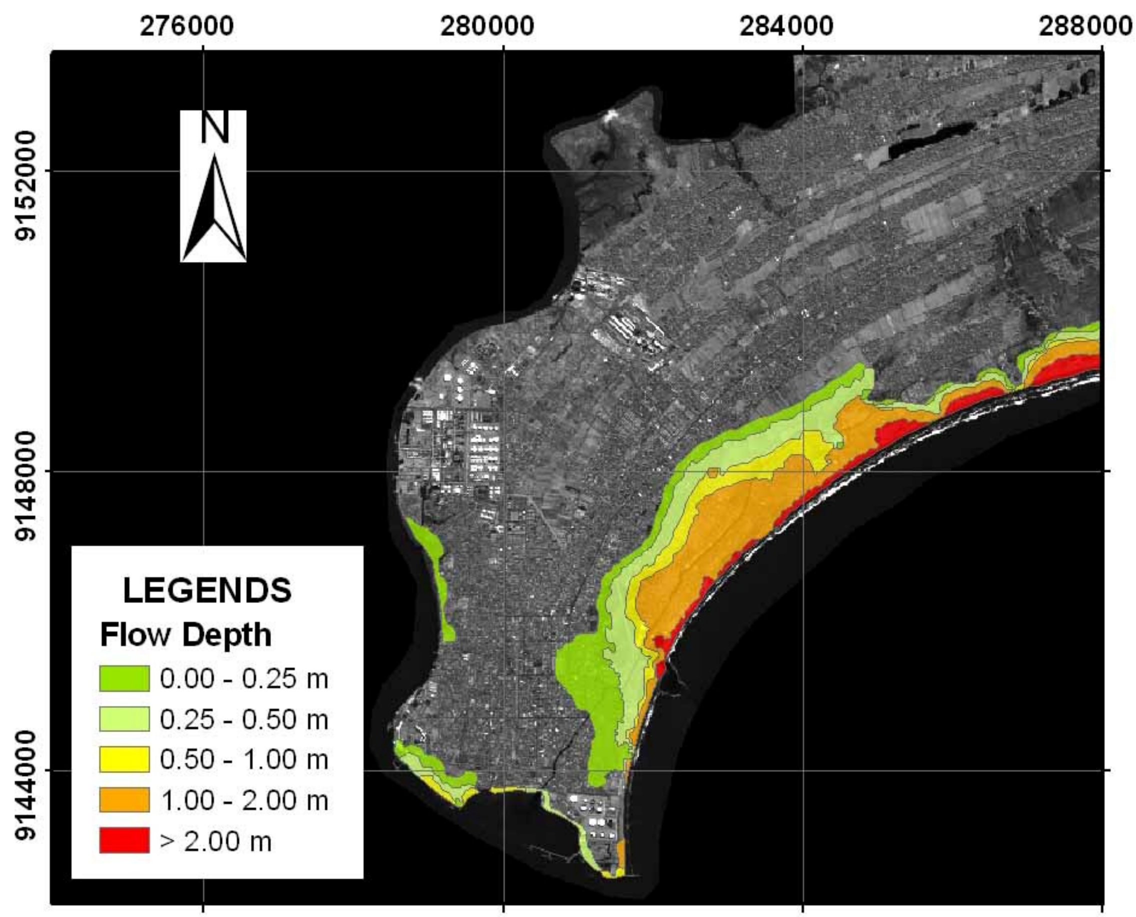

Figure 4-3. The tsunami inundation model of Mardiatno overlaying the QuickBird imagery

Information on the nature and the extent of tsunami hazard is commonly represented by a tsunami inundation model, as shown in Figure 4.3. The tsunami inundation model used in this study was developed by Mardiatno in 2008 under the TUNAMI numerical model. TUNAMI provides a complete analysis of hazard potential, i.e. the tsunami source (initial condition), tsunami propagation, and inundation. The model was based on a hypothetic epicenter location (110.0º E; -9.5° S) and earthquake magnitudes of Mw = 8.5. The earthquake of Mw = 8.5 was selected as the worst-case scenario of tsunami hazard potential.

The vulnerability values of elements at risk are directly affected by the relative positions of the elements at risk to the tsunami flow depth. For loss estimation and mitigation planning purposes, a tsunami inundation model is usually divided into classes of flow depth.

There were 31 virtual gauges employed in developing this tsunami inundation model. Those virtual gauges were evenly distributed along the coast of Cilacap City:

- 11 virtual gauges were located inland
- 6 virtual gauges were located at the shoreline, and
- 14 virtual gauges were located off shore

The six virtual gauges located at the shoreline showed the wave height of 3.47 m – 3.75 m.

Studies on the relation between the wave height, tsunami intensity and the level of damages have been conducted by many scientists. The tsunami intensity scale was first devised by August Sieberg (1927) and was modified by Nicholas Ambraseys (1962). There are 6 classes of tsunami intensity range from very light to disastrous. Correlation between wave height and level of damages was not clearly defined in the scales. Nowadays, this intensity scale is considered to be too crude.

Papadopoulos and Imammura (2001) arranged tsunami scale according to a tsunami's effects on humans (a), effects on objects including boats (b), and damage to buildings (c). The correlation between the wave height and the potential level of damages was defined in the scale. Based on this tsunami intensity scale, the estimated future tsunami event in Cilacap can be put in scale VII (damaging). Papadopoulos-Imammura tsunami intensity scale is available in appendix 2.

4.2. Geomorphology of the coast

Cilacap coast is formed of alluvium which contains coastal sediments and river deposits. Coastal deposits consist of unconsolidated sand deposited as regular beach ridges. These beach ridges form a more or less parallel banding along the coast in the Cilacap area (Sutikno, 1981). Recently, the ridges have been used as settlement areas and the lower parts have been used for paddy fields. Cilacap area is characterized by former spit form, crescentic shoreline, and has swampy area. Mardiatno (2008) created a geo-morphological map which was mainly based on image interpretation. Interpretation was emphasized on the landform elements, i.e. landform types, shoreline configuration, and material contents.

Visual interpretation technique was performed on the satellite images to delineate landform types, supported by morphological analysis to classify the landform types. Based on image interpretation and field survey, the landforms in Cilacap can be classified into abandoned valley, alluvial plain, backswamp, beach, coastal plain (former beach), colluvial footslope, colluvio-alluvial footslope, floodplain, karst hills, mature beachridge, mature swale, mudflat, old beachridge, old swale, saltmarsh, spit, swamp (former swale), young beach ridge and young swale (Mardiatno, 2008).

Cilacap city is situated less than 12 m above sea level. It has a flat to gentle topography, thus is exposed to any tsunami source. The terrain elevation in the lowland area is higher in the northern and north eastern part and becomes lower in the western and south western part. The surface water flows mainly from north east to south west. Physiographically, the area of Cilacap City as a whole is relatively flat, with a pattern of low ridges and shallow depressions parallel to the coast.

Sutikno (1981) in Mardiatno (2008) distinguished the coastal alluvial plain of Cilacap into a number of smaller landform units as follows:

1. *Sand dune units (currently, these have disappeared)*

   These units are parallel to the coast and their elevations are about 7 m above sea level. The typical width of these dunes is about 100 m. The material consists of non-weathered coarse sands of volcanic origin with dark colour. The natural forms of these sand dunes are no longer found due to the exploitation of such iron-rich sands.
2. *Beach ridge units*

   Remains of the beach ridges are now used for settlement. The beach ridges are parallel to the coast and are variable in width (0.2 - 1.0 km). The features of the ridges are only evident from the Gumilir village eastward and are no longer observed in the city area. The beach ridges are predominantly formed by sand, with a rather fine texture compared to that of the ridges near the coast.
3. *Lagoon units*

   These units, which are now used as paddy fields, are in relatively low position as they form depressions alternating with the beach ridges. The width varies from 0.2 to 3.0 km. The material comprises of fine-textured sediment and even clays. These fine materials possibly originate from the weathering processes of the ridges and from the suspended loam of the Serayu River brought by the irrigation channels.
4. *Alluvial plain units*

   These units consist of the alluvial plain and the flood plain. The flood plain was developed under the influence of the Serayu River and the Donan River. Material of the Donan River banks is clayey while that of the Serayu river bank is sandy. Some features that are typical of abandoned meander belts are visible in the Serayu River flood plain.

4.3. Population in the coastal area of Cilacap City

There are four sub-districts located at the coast: Cilacap Selatan, Cilacap Tengah, Cilacap Utara, and Kesugihan. Some of the villages in those sub-districts are directly exposed to the sea. For loss estimation and mitigation planning, the data of the population in the coastal area must be taken into account. Table 4.1 shows the population number and population density while Table 4.2 shows the classification of residential houses based on the wall material.

Table 4-1. Population density of villages located at the coast

No	Sub-district	Village	Area (square km)	Population	Population Density (per square km)
1	Cilacap Selatan	Tambakreja	1.56	22,051	14,135
		Tegalreja	1.59	13,368	8,408
		Sidakaya	1.31	12,049	9,198
		Cilacap	1.71	16,050	9,386
		Tegalkamulyan	2.94	13,927	4,737
2	Cilacap Tengah	Kutawaru	8.44	10,115	1,198
		Lomanis	3.62	4,945	1,366
		Donan	4.55	24,701	5,429
		Sidanegara	3.38	30,638	9,064
		Gunungsimping	2.17	14,541	6,701
3	Cilacap Utara	Kebon Manis	1.99	10,412	5,084
		Gumilir	3.36	14,049	4,074
		Mertasinga	4.93	15,493	3,077
		Tritih Kulon	5.03	16,719	3,324
		Karang Talun	3.53	10,813	3,063
4	Kesugihan	Menganti	6.55	10,002	1,527
		Karang Kadri	4.07	6,109	1,501
		Slarang	7.32	8,269	1,130

Source: BPS (2007)

Part of the area of Tegalkamulyan Village was chosen as the urban sample area. The village is directly exposed to the tsunami threat; threatened by the >2 m flow depth class, highly populated, and has many buildings. Part of the area of Mertasinga Village represents the rural sample area. Mertasinga Village is also directly exposed to the tsunami threat and threatened by the >2 m flow depth class. Contrary, this village is less populated.

Loss estimation and mitigation planning will be conducted upon both sample areas using the similar methods. The final results of the works will show how the methods work in a populated area and a less populated area. Conclusions will be drawn based on the comparison of the results. Recommendation for Cilacap City and other coastal cities will be given based on the conclusions.

Table 4-2. Classification of residential houses based on wall material

No	Sub-district	Village	Number of houses based on the wall material			
			Brick infill	Partly brick infill	Timber	Bamboo
1	Cilacap Selatan	Tambakreja	2,810	1,072	821	410
		Tegalreja	1,542	910	453	185
		Sidakaya	1,671	421	216	201
		Cilacap	1,453	925	832	915
		Tegalkamulyan	2,245	541	212	131
2	Cilacap Tengah	Kutawaru	1,103	275	275	243
		Lomanis	676	415	28	18
		Donan	3,110	1,053	937	527
		Sidanegara	5,011	1,857	113	53
		Gunungsimping	1,873	829	342	44
3	Cilacap Utara	Kebon Manis	1,258	604	63	229
		Gumilir	1,824	921	58	351
		Mertasinga	1,699	1,137	71	508
		Tritih Kulon	1,636	1,193	112	711
		Karang Talun	1,166	751	70	436
4	Kesugihan	Menganti	371	679	612	532
		Karang Kadri	258	437	196	296
		Slarang	454	859	232	426

Source: BPS (2007)

5. Generating the database of elements at risk

The main stages in developing the database of elements at risk are explained in this chapter. Assessment and correction of the QuickBird imagery must be conducted at the first place before it is used to assess the geometrical aspects of the existing maps. The differential GPS measurement to provide GCPs of pixel size horizontal precision is also described in this chapter. The next stages are: determining the vulnerability of buildings and people inside or nearby a building, determining the economic value of buildings, and determining the dynamic distribution of people in the basis of individual building for day time and night time scenarios.

Elements at risk are all objects, persons, animals, activities and processes that may be adversely affected by hazardous phenomena, in a particular area, either directly or indirectly (Kingma, 2009). Comprehensive data about the elements at risk will be the critical input for the evaluation of the vulnerability of the elements at risk of certain hazards.

Ideally, a complete identification of all elements at risk exposed to certain hazards must be established for loss estimation. In fact, surveys of elements at risk in many studies are always incomplete. Therefore loss estimation studies nearly always focus on specific groups of elements at risk, such as buildings or population. Buildings are one of the most important groups of elements at risk. The behavior of a building under a hazard event, determines whether the people in the building might be injured or killed (Kingma, 2009). The data on land parcels will also be taken into account because mitigation planning is usually arranged in the basis of individual building or individual land parcel.

The spatial data and attribute data related to land parcels and buildings are already established in the Land Office and the Tax Office. The existing maps are usually not sufficient for loss estimation and mitigation planning purposes in terms of geometrical aspect. Overlaying analysis of those maps with the QuickBird imagery will reveal the level of positional errors of those maps. Unfortunately, the QuickBird imagery itself also contains significant positional error. Assessment and correction of the QuickBird imagery must be conducted at the first place.

5.1. Assessment and correction of the satellite imagery

Panchromatic QuickBird imagery of 0.60 m spatial resolution is used in this study. Geometrical aspect of the imagery must be assessed to ensure that image meets the positional accuracy stated in the metadata. Geometrical correction is usually required to improve the positional accuracy of image data. The corrected imagery will be used as the basis to assess the accuracy of existing maps available for the study. If the existing maps are not reliable for loss estimation and mitigation planning, new maps will be generated based on the image data.

5.1.1. Positional accuracy of the QuickBird imagery

The QuickBird imagery used in this study is the *custom ortho*. Its positional accuracy is determined by the accuracy and quality of customer supplied support data. The detailed information about the positional accuracy of the QuickBird imagery used in this study is stated in the metadata as shown in appendix 4. It is stated that the horizontal accuracy is 10 m and the total RMS of the rectification of the panchromatic channel is 2.3287. Even if the image data has a stated positional accuracy, it is always recommended to validate the image to ensure that the image bundle meets the stated positional accuracy. Several check points must be provided over the study area for the validation process. Those ground control points are real world features that could easily be located on the ground and in the corresponding QuickBird image.

Coordinates of the ground control points can be obtained from existing maps or through measurement. Ground control points (GCPs) of high positional precision are required to validate and to correct the panchromatic QuickBird imagery, in accordance with the high spatial resolution of the imagery. Since the pixel size of the QuickBird imagery is 60 cm, the GCPs used in the rectification are highly recommended to have horizontal precision ≤ 60 cm. Such high precision GCPs are usually not extractable from standard topographic maps and must be taken by geodetic surveys including differential GPS measurement techniques.

The validation and improvement processes can be conducted all at once. The GCPs used for validation process can also be used to geo-reference the QuickBird imagery. Geometrical aspect of the QuickBird imagery is put on the top of priority because it will be used as the bench mark in generating the improved land parcel map and the improved individual building map in the study area. The improved land parcel map will be used to determine the land parcels located within the tsunami buffer zone, whilst the improved individual building map will be used to determine the potential loss in case a tsunami of worst case scenario take place.

5.1.2. Measurement of ground control points (GCPs)

As previously mentioned, the GCPs require horizontal precision ≤ 60 cm. This level of accuracy is usually not extractable from standard topographic maps. It can be achieved by making use of differential GPS measurement techniques with post processing differential correction upon the recorded field measurement data. The differential GPS measurement was conducted during the fieldwork. The author used a Trimble ProXH™ mapping grade single frequency receiver which acts as a rover. The base station is also a Trimble L1 5000 single frequency receiver which is located at the office of *Forest Zone Strengthening Bureau Region XI Jawa – Madura* in Yogyakarta. In order to achieve ≤ 60 cm horizontal precision, the author operated long-duration occupation time (20 to 30 minutes) and set the filter only to record the readings of PDOP ≤ 4.0. The long duration occupation time gives many more chances to log code phase of low PDOP (≤ 4.0).

Figure 5-1. The base receiver at the reference station mounted on the top of a tower (left) and the GCP located on the edge of a structure identifiable on the imagery (right) (fieldwork doc.)

Position of the rover is determined based on the fixed position of the reference point at the base station. Data recorded by the rover and the base station were compiled to perform differential correction. GPS Pathfinder Office 3.10 software was used to perform the data post processing. Horizontal precisions of a GCP before and after correction are shown in Figure 5.2 below.

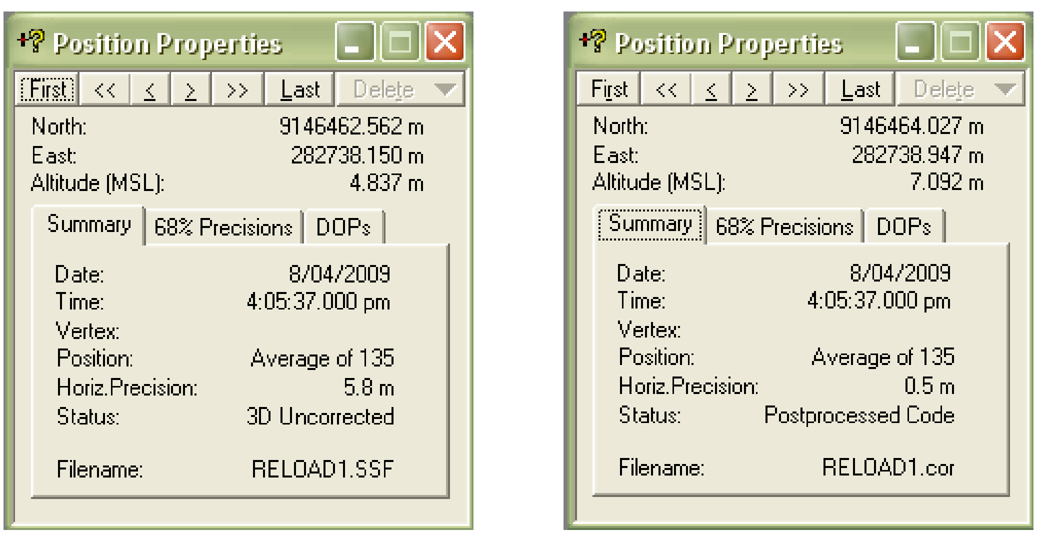

Figure 5-2. Horizontal precision of GCP before correction (left) and after correction (right)

There were 32 GCPs measured during the fieldwork. 8 GCPs were spread over the Cilacap city, 11 extra GCPs were spread over the urban sample area, and 13 other extra GCPs were spread over the rural sample area. Unfortunately, the base station was sometimes turned off during the field measurement. Some GCPs did not have base station logging data, thus differential correction could not be applied upon them. Those points did not achieve sub meter horizontal precision. There are only 25 GCPs with sub meter horizontal precision as shown in Table 5.1.

Table 5-1. GCPs with sub meter horizontal precision

Tie Points	X	Y	Horizontal Precision
urban1	281895.319	9145989.461	0,6 m
urban2	282039.371	9145899.300	0,6 m
urban3	282200.628	9145949.364	0,6 m
urban11	282244.452	9146458.202	0,6 m
urban12	282172.339	9146238.773	0,5 m
urban9	282188.678	9146639.050	0,6 m
urban6	282738.947	9146464.027	0,5 m
rural11	286935.04	9149395.666	0,5 m
rural4	287058.771	9149250.157	0,5 m
rural8	287306.772	9149877.623	0,5 m
rural10	287343.064	9149586.863	0,5 m
rural5	287444.435	9149389.702	0,6 m
rural7	287609.813	9149764.002	0,6 m
rural6	287854.294	9149551.565	0,5 m
rural3	286657.503	9149570.735	0,5 m
rural1	286802.984	9149176.549	0,5 m
rural12	286011.186	9149193.987	0,5 m
rural13	286525.248	9149085.159	0,5 m
rural14	286197.659	9148973.061	0,5 m
extend1	280562.595	9143777.617	0,6 m
extend2	280342.626	9146047.873	0,5 m
extend3	282610.068	9148754.028	0,7 m
extend4	283958.863	9149947.816	0,6 m
extend5	285072.482	9149104.814	0,6 m
extend6	283779.521	9148337.200	0,5 m

Source: Data Analysis

5.1.3. Validating and correcting the QuickBird imagery

The measured GCPs were used as the bench mark in validating the positional accuracy of the image data. Comparing the coordinates of GCPs to the corresponding points on the image is a simple method to judge whether the image meets the stated positional accuracy or not. Validation process was conducted at the same time with the on screen geo-referencing process.

A geo-reference defines the relation between rows and columns in a raster map and XY-coordinates (Kerle and Damen, 2009). The coordinates of pixels in a raster map is defined by making use of a coordinate system which may contain projection information. The coordinates of GCPs shown in Table 5.1 and their corresponding points on the image can be used to determine the shifting distance of each tie point.

At least 4 GCPs are required in geo-referencing satellite imagery, but it is always good to provide more than 4 GCPs on the image to have better geometrical control. The GCPs should be evenly distributed over the area of interest on the image to make to the image represents the real world better. There are 25 GCPs available for the on screen geo-referencing of QuickBird satellite imagery. 8 GCPs are spread over the Cilacap city, 6 extra GCPs are available over the urban sample area, and 11 other extra GCPs are spread over the rural sample area.

Geo-referencing process using 8 GCPs which are spread over the Cilacap city is considered to be adequate to improve the positional accuracy of the QuickBird satellite imagery. Geo-referencing process using 8 GCPs spread over the Cilacap city and 17 extra GCPs spread over the urban and rural sample areas is expected to give better geometrical control. The result of the two geo-referencing processes upon the same image bundle will be compared to see how significant those 17 extra GCPs on the two sample areas contribute to the improve the positional accuracy of the image.

1. *Geo-referencing method 1: using GCPs spread over the Cilacap city*

Eight GCPs are spread over the sea shore area because it is the area of interest in the study. The spreading of the GCPs is shown in Figure 5.3 below. The RMSE (Root Mean Square Error) achieved in the geo-referencing process is 0.87342 m. RMSE is a mathematical formula that compares the actual location of the map coordinates on the control layer to the transformed positions in the raster (ESRI-Canada, 2006). The distance between these two sets of coordinates is the residual error. A high residual error on a particular point could indicate a misplaced link. Human error also has the potential to contribute to the RMSE since it is almost impossible to pick the exact corresponding points on the raster image. A sub meter RMSE is usually considered to be acceptable in geo-referencing process.

Figure 5-3. Geo-referencing method 1

Table 5-2. The coordinates of GCPs and their corresponding points on the image

GCPs	Coordinates of corresponding points on the QuickBird image		Coordinates of GCPs	
	X	Y	X	Y
extend1	280558.698	9143773.826	280562.595	9143777.617
extend2	280347.931	9146055.852	280353.910	9146060.854
extend3	282597.580	9148739.301	282604.851	9148743.332
extend4	283948.372	9149938.265	283955.084	9149940.708
rural5	287453.501	9149386.659	287458.712	9149384.786
urban3	282195.117	9145948.195	282200.628	9145949.364
extend6	283774.104	9148334.985	283779.521	9148337.200
extend5	285101.423	9149123.671	285106.404	9149126.011

Source: Data Analysis

Table 5-3. Shifting distances of GCPs to their corresponding points on the image

GCPs	Coordinates of corresponding points on the QuickBird image VS Coordinates of GCPs		
	ΔX (m)	ΔY (m)	shifting distance (m)
extend1	3.897	3.791	5.437
extend2	5.979	5.002	7.796
extend3	7.272	4.031	8.314
extend4	6.711	2.443	7.142
rural5	5.211	1.873	5.537
urban3	5.511	1.169	5.633
extend6	5.417	2.215	5.853
extend5	4.981	2.340	5.503

Source: Data Analysis

The coordinates of GCPs and their corresponding points on the image are shown in Table 5.2. The shifting distances of the tie points are shown in Table 5.3. The points shift from 5.437 m to 8.314 m. The QuickBird imagery used in this study is stated to have a 10 m positional accuracy. Considering the 0.87342 m RMSE, it can be concluded that the image does meet the 10 m positional accuracy. Considering the 5.437 m to 8.314 m shifting distances, a geo-referencing process is recommended to be applied upon the original QuickBird imagery.

2. *Geo-referencing method 2: using GCPs spread over the Cilacap city and extra GCPs spread over the sample areas*

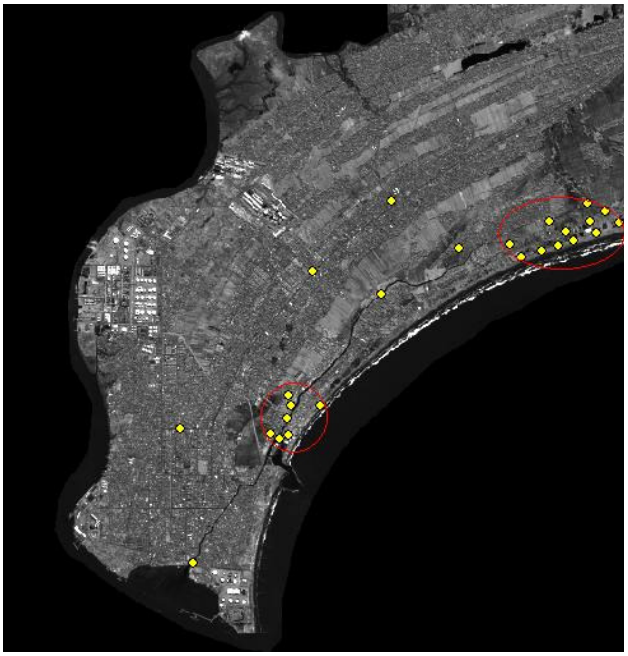

Figure 5-4. Geo-referencing method 2

Eight GCPs which are spread over the study area and 17 extra GCPs located in the two sample areas are used for the second geo-referencing method. Extra GCPs are expected to reduce the positional error to the minimum. The spreading of the GPS is shown in Figure 5.4 on the left.

The coordinates of GCPs and their corresponding points are shown in Table 5.4 below. The RMSE (Root Mean Square Error) achieved in the second geo-referencing process is 0.80136 m. As stated earlier, a sub meter RMSE is usually considered to be acceptable in geo-referencing process.

Table 5-4. The coordinates of GCPs and their corresponding points on the image

GCPs	Coordinates of corresponding points on the QuickBird image		Coordinates of GCPs	
	X	Y	X	Y
extend2	280347.918	9146055.567	280353.910	9146060.854
extend3	282597.838	9148739.135	282604.851	9148743.332
extend4	283948.820	9149938.161	283955.084	9149940.708
urban1	281888.691	9145986.899	281895.319	9145989.461
urban2	282033.205	9145896.974	282039.371	9145899.300
urban3	282194.923	9145947.676	282200.628	9145949.364
urban6	282730.005	9146458.211	282736.522	9146459.827
urban9	282189.794	9146637.953	282196.985	9146641.276
urban12	282163.448	9146236.490	282170.084	9146237.952
rural1	286799.570	9149179.039	286804.117	9149177.948
rural3	286650.778	9149573.797	286655.294	9149574.010
rural4	287053.158	9149258.345	287058.506	9149257.752
rural5	287452.886	9149387.177	287458.712	9149384.786
rural6	287850.513	9149554.367	287854.294	9149551.565
rural7	287603.647	9149757.334	287608.004	9149755.492
rural8	287302.016	9149878.855	287306.772	9149877.623

rural10	287335.425	9149585.088	287340.390	9149583.182
rural11	286935.075	9149406.405	286940.518	9149405.549
rural12	285978.754	9149192.104	285984.040	9149191.612
rural13	286508.683	9149083.543	286514.816	9149082.364
rural14	286174.412	9148970.627	286179.008	9148969.436
extend5	285101.102	9149125.372	285106.404	9149126.011
extend1	280557.289	9143774.789	280562.595	9143777.617
extend6	283774.404	9148334.481	283779.521	9148337.200
urban11	282242.586	9146452.598	282249.278	9146454.152

Source: Data Analysis

Table 5-5. Shifting distances of GCPs to their corresponding points on the image

GCPs	Coordinates of corresponding points on the QuickBird image VS Coordinates of GCPs		
	ΔX (m)	ΔY (m)	shifting distance (m)
extend2	5.992	5.287	7.992
extend3	7.014	4.197	8.174
extend4	6.264	2.547	6.762
urban1	6.628	2.562	7.106
urban2	6.166	2.326	6.590
urban3	5.705	1.688	5.950
urban6	6.517	1.616	6.714
urban9	7.191	3.323	7.922
urban12	6.635	1.462	6.794
rural1	4.546	1.091	4.675
rural3	4.516	0.213	4.521
rural4	5.347	0.593	5.380
rural5	5.826	2.391	6.298
rural6	3.781	2.802	4.706
rural7	4.357	1.842	4.731
rural8	4.756	1.232	4.913
rural10	4.965	1.906	5.318
rural11	5.443	0.856	5.510
rural12	5.286	0.492	5.308
rural13	6.133	1.179	6.246
rural14	4.597	1.191	4.748
extend5	5.302	0.639	5.340
extend1	5.306	2.828	6.012
extend6	5.117	2.719	5.794
urban11	6.692	1.554	6.870

Source: Data Analysis

Coordinates of GCPs and their corresponding points on the image are shown in Table 5.4. The shifting distances of the tie points are shown in Table 5.5. The points shift from 4.521 m to 8.174 m. The QuickBird imagery used in this study is stated to have a 10 m positional accuracy. Considering the 0.80136 m RMSE, it can be concluded that the image does meet the 10 m positional accuracy. Considering the 4.521 m to 8.174 m shifting distances, it can be obviously concluded once again that a geo-referencing process should be applied upon the original QuickBird imagery.

Geo-referencing method 1 and geo-referencing method 2 are then compared to determine the difference of positional error resulted from both methods.

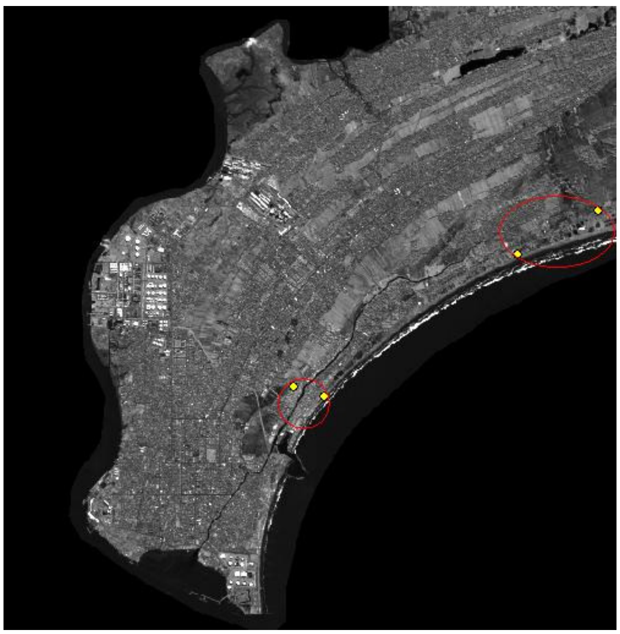

Figure 5-5. Check points in the two sample areas

Four check points are chosen to compare the positional accuracy given by the two aforementioned geo-referencing methods. The comparison of the positional accuracy will show how significant those 17 extra GCPs on the sample areas contribute to improve the positional accuracy of the image. Two check points are located in the urban sample area and other two check points are located in the rural sample area, as shown in Figure 5.5.

Table 5-6. The coordinates of check points resulted from two geo-referencing processes

Check Points	Georeferencing using 8 GCPs spread over Cilacap city		Georeferencing using 8 GCPs spread over cilacap city and 17 extra GCPs spread over the sample areas	
	X	Y	X	Y
check point 1	282736.522	9146459.827	282735.513	9146460.279
check point 2	282196.985	9146641.276	282196.159	9146641.623
check point 3	287608.0042	9149755.492	287608.121	9149755.846
check point 4	286179.0081	9148969.436	286178.914	9148969.205

Source: Data Analysis

Table 5-7. The shifting distances of check points resulted from two geo-referencing process

Check Points	Georeferencing using 8 GCPs spread over Cilacap city VS Georeferencing using 8 GCPs spread over cilacap city and 17 extra GCPs spread over the sample areas		
	ΔX (m)	ΔY (m)	shifting distance (m)
check point 1	1.009	0.452	1.106
check point 2	0.826	0.347	0.896
check point 3	0.117	0.354	0.373
check point 4	0.094	0.231	0.249

Source: Data Analysis

The coordinates of checkpoints resulted from two geo-referencing processes are shown in Table 5.6. The shifting distances of the check points are shown in Table 5.7. The points shift from 0.249 m to 1.106 m. 3 out of 4 check points are of sub meter shifting distance. Considering the 0.60 m pixel size of the panchromatic QuickBird imagery, it can be concluded that the geo-referencing process using 8 GCPs which are spread over the Cilacap city gives adequate positional accuracy for the whole study area. Extra GCPs spread over the urban and rural sample areas will surely give better positional accuracy but they are not always necessary. This conclusion can be used as a bench mark for other similar researches.

5.2. Assessment of the existing maps

The existing spatial data available to identify the elements at risk are the Land Office's land parcel map and the Tax Office's block map. Those data are available in digital format. A single layer for land parcels and another single layer for individual buildings are available in the Tax Office's block map. The existing maps are in different data formats and different coordinate systems. Conversions of data format and conversions of coordinate system are required to have the data in the same data format and the same coordinate system.

5.2.1. The land parcel map of the Land Office

The Land Office's land parcel map is usually created using Autodesk or AutoCad program. The map is in dwg format. Actually, there are many layers in the map. Each layer contains a single feature data type e.g. river, railway, road, footpath, land parcel, boundary of village, etc. It is also possible to create layers containing textual data corresponding to the feature data. In order to work with this data in the ArcGIS program, the map must be converted from dwg format to shp format. The conversion tool is available in the Autodesk Map program. The step wise processes of conversion are available in appendix 2.

The projection system of the Land Office's land parcel map is the TM3º (Transverse Mercator 3 degrees) projection system. Basically, the TM3º projection system is derived from the UTM (Universal Transverse Mercator) projection system. A 6 º zone in the UTM projection system is divided into two 3 º zones. Thus, in a single UTM zone there will be 2 TM3º zones. For instance, for a UTM 49 S zone there will be TM3º 49.1 and TM3º 49.2 zones. Other principal differences between the UTM coordinate system and the TM3º coordinate system are the scale factor at the central meridian and the false coordinates.

A scale factor is the ratio of the true scale at a given point to the stated scale (Knippers, 1999). A map projection without distortions would have a scale factor of 1.0000. Unfortunately, there is no map projection that maintains correct scale all over the map. At any point of the map the scale may vary from the stated scale. For example, the scale factor at the central meridian of a UTM zone is 0.9996. Thus, 1000 meters measured along the central meridian on the Earth's surface will become 999.6 meters on the projection. This is a contraction of 40 cm per kilometer.

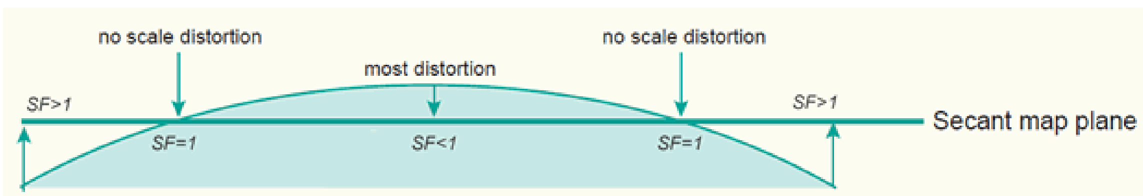

Figure 5-6. Scale factor on a secant map plane (Knippers, 1999)

The scale factor at the central meridian of a TM3º zone is 0.9999. Compared to the scale factor at the central meridian of a UTM zone, a TM3º zone has smaller scale distortion. It means that a TM3º zone represents shapes, angles, areas, distances and directions, everywhere on the map better than a UTM zone. This is the main reason for the Land Office (National Land Agency) to use the TM3º map projection system.

The natural origin of a Transverse Mercator projected coordinate system is at the intersection of a chosen parallel (usually the equator) and the central meridian of a zone. Under normal circumstances, the projection will give negative coordinates over parts of the map. Hence each natural origin will is usually given the False Easting and False Northing values to avoid using negative numbers in the coordinates.

Table 5-8. Properties of coordinate systems

Properties of Coordinate System	UTM Coordinate System	TM3º Coordinate System
Datum	WGS 1984	WGS 1984
Projection	Transverse Mercator	Transverse Mercator
Zone Width	6 º	3 º
Scale Factor	0.9996	0.9999
False Easting	500000	200000
False Northing	10000000	1500000

Source: BPN (1996)

Most of the maps produced by government's agencies in Indonesia usually have poor positional accuracy. The land parcel map of the Land Office is well known to have the best positional accuracy among the maps produced by government's agencies. Though with a good reputation, the positional accuracy of the Land Office's land parcel map is poor, as revealed by overlaying operation with the corrected QuickBird imagery. Beside the positional accuracy, the incompleteness of spatial data makes the map unreliable for loss estimation.

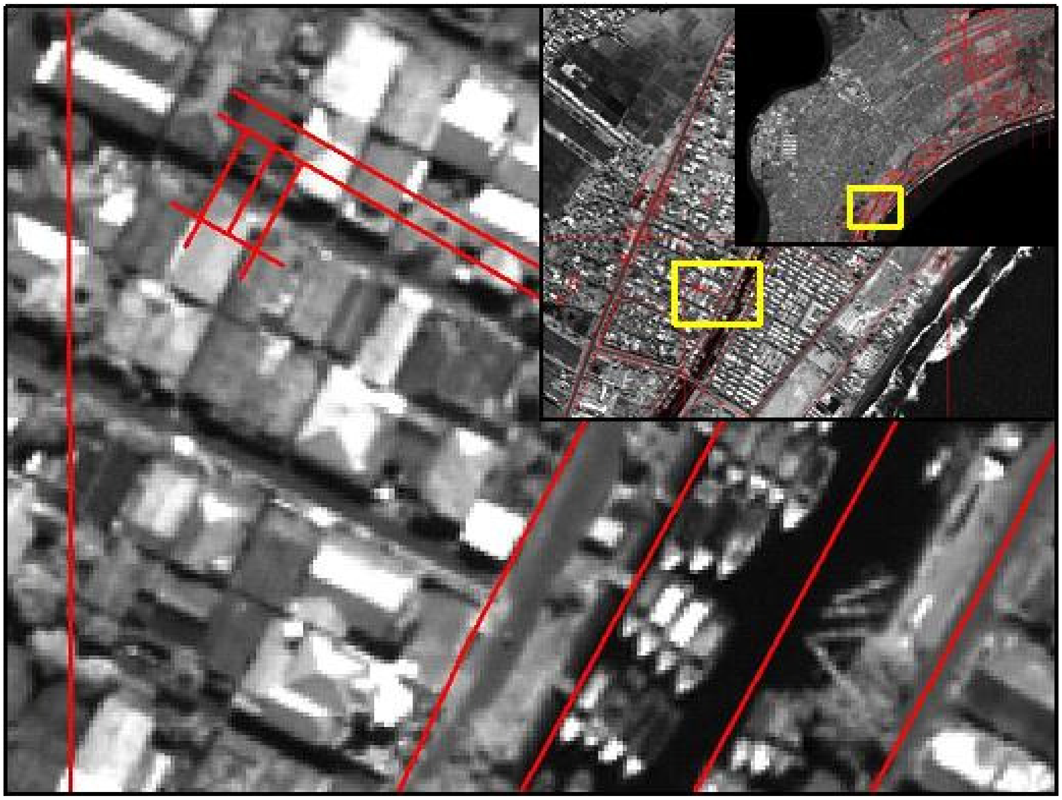

Figure 5-7. Land Office's land parcel map overlaying the QuickBird imagery

The land parcel map developed by The Land Office contains only the registered land parcels, the ones equipped with land certificates. In most of cities in Indonesia, there are much more unregistered land parcels than the registered ones. As the result, the land parcel map in the land office usually only covers low percentage of the total land parcels in an area.

The same situation is found in Cilacap city. In the urban sample area, there are only 9 out of 1724 land parcels equipped with land certificate. In other words, there are only 9 land parcels in the Land Office's Land Parcel Map over the sample area. In the rural sample area, there are only 6 out of 308 land parcels are mapped. The incompleteness of the land parcel map and the poor positional accuracy are shown in the Figure 5.7. In spatial analysis, the whole land parcels in the area of interest must be included. The block map developed by The Tax Office can be used to accelerate the process of generating the improved land parcel map.

5.2.2. The block map of the Tax Office

Figure 5-8. The Tax Office's block map overlaying QuickBird imagery (1)

A single layer for land parcels and another single layer for individual buildings are available in the Tax Office's block map. The block map developed by The Tax Office covers the whole land parcels and buildings registered to the Tax Office in the area of interest. The problem is that it usually has very bad positional accuracy as shown in Figure 5.8.

By making use of the *off set* tool in the AutoCad Map Program, the land parcel layer of the block map can be *dragged* to best fit the corrected QuickBird image as revealed in Figure 5.9.

Figure 5-9. The Tax Office's block map overlaying the QuickBird imagery (2)

It is obvious that there is no way that the land parcel layer or the individual building layer in the block map will fit the QuickBird imagery. The useful things can be extracted from this map is the spatial arrangement of the land parcels and the buildings.

The shape of the land parcels and the relative location among land parcels can be used as the pattern in digitizing an improved land parcel map based on QuickBird imagery. A new individual building map can be developed in the same manner.

5.3. Generating new land parcel map and new individual building map

It is obvious that there's no way that the land parcel maps of the Land Office and the block map of the Tax Office are reliable for loss estimation and mitigation planning of tsunami effects. New maps of better accuracy must be generated for those purposes. The useful thing can be extracted from those existing maps is the spatial arrangement of the land parcels and buildings.

New maps for the study can be generated based on the original QuickBird imagery or based on the improved QuickBird imagery. The land parcel map will cover only the land parcels registered to the Tax Office because replacement cost will only be addressed to land parcels with legal ownerships. The individual building map will cover the whole buildings located in the study area, whether they are registered or not. Loss estimation will include all the buildings located in the tsunami inundation area, whether they are registered or not.

5.3.1. Generating maps based on the original QuickBird imagery

Figure 5-10. On screen digitizing land parcel layer based on QuickBird imagery

The land parcels and the buildings will be digitized based on visual interpretation upon satellite imagery. High spatial resolution satellite imagery is very useful for the work because visual interpretation can be well conducted upon images with small pixel size.

The shape of the land parcels and the relative location among land parcels extracted from the existing maps can be used as the pattern in digitizing a new land parcel map based on QuickBird imagery. A new individual building map can be developed in the same manner.

Although it can be simply concluded that a shifting distance of 10 meters is big enough to affect the final result of loss estimation and site planning for tsunami mitigation, many researchers may neglect it. Improving the positional accuracy of high spatial resolution satellite imagery is not a simple work. In order to save the time and the cost allocated for the loss estimation and mitigation planning, researchers may use the original image data.

The public facilities such as schools, mosques, and government's offices are not available in the individual building layer of the Block map. The data on those buildings are also not available in the Record *of Land Parcel and Building Data* developed by the Tax Office. Those buildings are not included as the objects of taxation. Visual interpretation is used to recognize those special buildings on the imagery. Validations on the use of those buildings are also conducted in the field survey during the fieldwork.

5.3.2. Generating maps based on the corrected QuickBird imagery

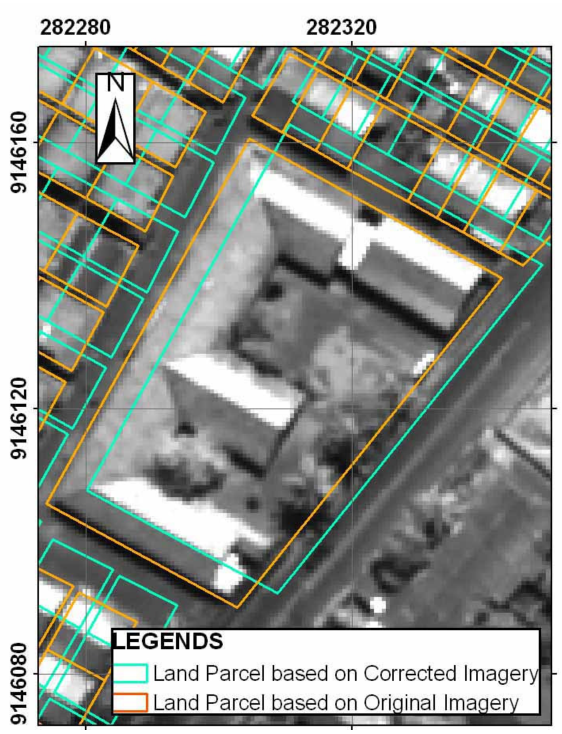

Figure 5-11. Shifting of land parcel based on original image to land parcel based on corrected image

The land parcel map and the individual building map will be generated in the same manner with the ones generated based on the original imagery. The shape of the land parcels and buildings and the relative location among them are extracted from the existing maps to be used as the pattern in digitizing a new land parcel map and individual building map based on the corrected QuickBird imagery.

The QuickBird imagery which will be used as the basis in generating the improved maps must be previously geo-referenced. The shifting distances between the land parcels digitized based on the original imagery to the land parcels digitized based on the corrected imagery are shown in Figure 5.11

5.4. Determining the economic values of land parcels

The land parcel map consists of 1724 polygons in the urban sample area and 308 polygons in the rural sample area. The price of each land parcel is available in the *Record of Land Parcel and Building Data* developed by the Tax Office. The prices of land parcels listed in the document are for taxation purpose, thus may differ from the market price. Obtaining the data about the market price of land parcels in the study area will be a complicated work since real estate agencies are not common in the area. Since the complete data of land prices is only available in the *Record of Land Parcel and Building Data* developed by the Tax Office, the land prices for replacement cost will be based on this document.

5.5. Classification of buildings based on their physical vulnerabilities

A team of scientists from New Zealand and Indonesia conducted a reconnaissance survey to the South Java area affected by the tsunami of 17 July 2006. The purpose of the work was to acquire data for calibration of models used to estimate tsunami inundations, casualty rates and damage levels. The level of damage observed was diverse and was primarily depended on water depth and the building construction type (Reese *et al.*, 2007). Tsunami waves accounted for all surveyed damage since there was no significant ground shaking from the earthquake. Buildings were classified under four main categories: timber/ bamboo, traditional brick, traditional brick with reinforced-concrete (RC) columns, and RC-frame with brick infill walls.

- *Timber/ bamboo*


Figure 5-12. Damage to timber/ bamboo construction type after inundation to nearly 1 meter depth (left) and 3 meters depth (right) (Reese *et al.*, 2007)

This construction type consists of wood frame. Plaited bamboo sheet or timber is used as the wall material. In nearly all cases a flow depth of less than a meter caused light to moderate damage, a flow dept of 1.5 to 2 m resulted in roughly 70% destroyed and 30% lightly to heavily damaged but repairable, and a flow depth exceeding 2 m caused total destruction.

- *Traditional brick*


Figure 5-13. Most of the traditional brick construction type collapsed after inundation of 3 meters (left). There were a few partially intact (right) (Reese *et al.*, 2007)

The *traditional brick* are buildings made of un-reinforced brick walls on concrete foundations. The construction was weak, with single-skin brick walls, often plastered on both sides. Most of the buildings are covered with clay tiles or corrugated concrete sheet. The observed damage levels were not much different from the timber/ bamboo ones. The main difference was that slightly more houses remained upright where the flood depth was greater than 2 m. Most of them are not repairable. Only the concrete floor which often remained intact.

- *Traditional brick with RC-columns*

Figure 5-14. Debris field inland of the damaged buildings (left) the damage of t*raditional brick with RC-columns* to a flow depth of 3.8 meters (right) (Reese *et al.*, 2007)

The structure has rudimentary reinforced concrete columns. Columns range from 100 mm × 100 mm with 4 wires of 3 mm diameter, to 200 mm × 200 mm with 4 smooth bars of 8 to 12 mm diameter at the four corners. The walls suffered from punching, often with holes punched through multiple walls. Even though the reinforcement was rudimentary, it improved the performance significantly. The observed damage levels were minor for a sub meter flow depth. A flow depth of 1.5 to 2m of water caused light to moderate damage (repairable), and a flow depth 3 to 4 m resulted serious damage, but buildings were upright and probably repairable.

- *RC-frame with brick infill walls*

Figure 5-15. Damages on a well engineered *RC-frame with brick infill walls* building after inundation to a depth of 3.8 meters (left) and the detail of the reinforcement (right) (Reese *et al.*, 2007)

This robust construction type is often with two or more storeys, they had brick infill walls with plastering on both sides, reinforced concrete columns of at least 200 mm × 200 mm, at least 6 bars of 12 mm reinforcement, and concrete floors. The construction experienced zero to light damage to ground floor for a sub meter flow depth. A flow depth 1.5 to 2 m caused light to moderate damage to ground floor (repairable), and 3 to 4 m of flow depth resulted moderate damage to ground floor (holes punched through 1 or more walls). Upper storeys were untouched and provided refuge to people. Since the minor damage is only experienced by the ground floor, the overall damage levels were low.

An empirical approach was applied to define the relation between the flow depth and damage observed during the survey. Vulnerability curves were constructed based on analysis of observed damages for different types of constructions. Those curves show that the increase of flow depth will increase the level of damages. Different types of constructions will suffer from different level of damages at the same flow depth. The vulnerability curves developed by Reese et al are shown in Figure 5.16 below.

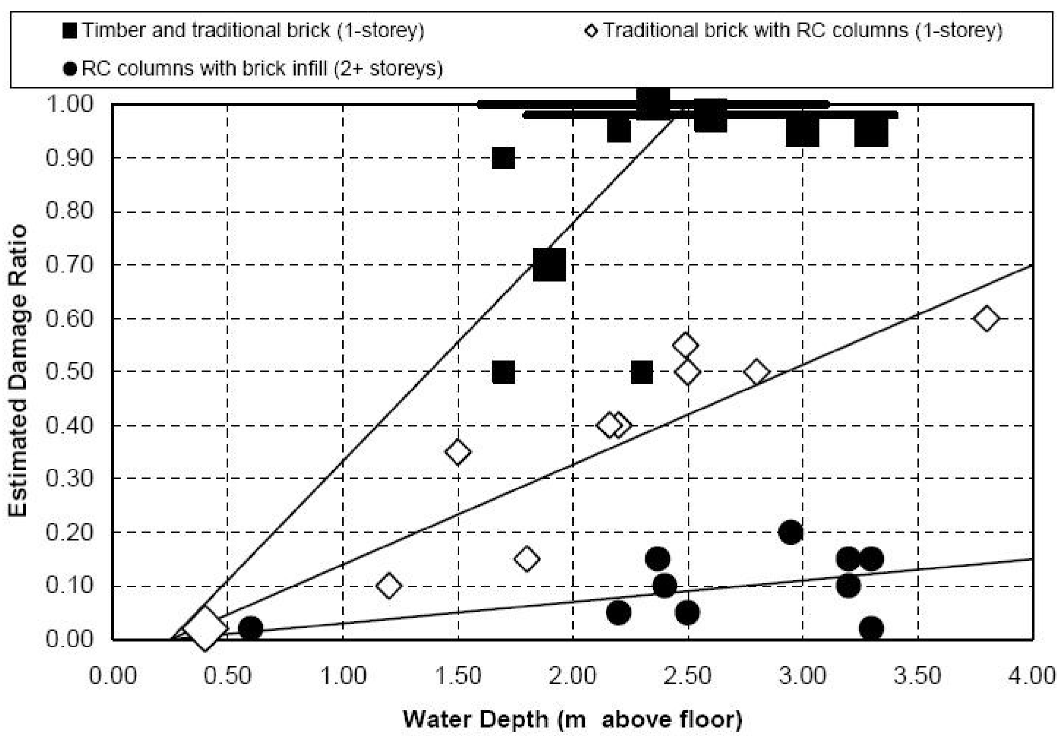

Figure 5-16. Estimated damage ratios and fragility curves as a function of inundation depth for various types of constructions (Reese *et al.*, 2007)

The observation showed that the shielded buildings experience lower damage level to the ones exposed to tsunami wave. The existence of other buildings in front of a building will provide shielding to the building.. All of the inspected buildings were surveyed in this respect as well. Shielded t*raditional brick with RC-columns* buildings experienced damage not greater than 20%, similar construction type exposed to tsunami wave suffered above 40 % of damage.

Figure 5-17. In a flow depth of about 2 m, the buildings in the first row toward the sea were heavily damaged (left) while those in the third row had suffered little structural damage (right) (Reese *et al.*, 2007)

Comparison of the fragility curves of the exposed to the shielded buildings are as follows.

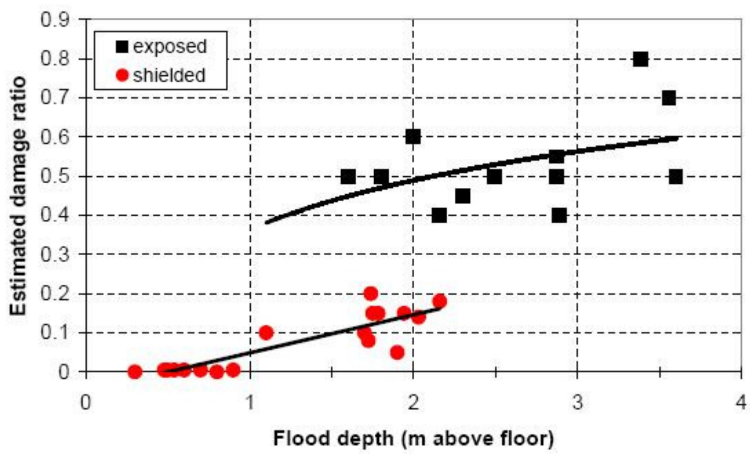

Figure 5-18. Damage ratios and fragility curves as a function of inundation depth and exposure for traditional brick buildings with RC-columns (Reese *et al.*, 2007)

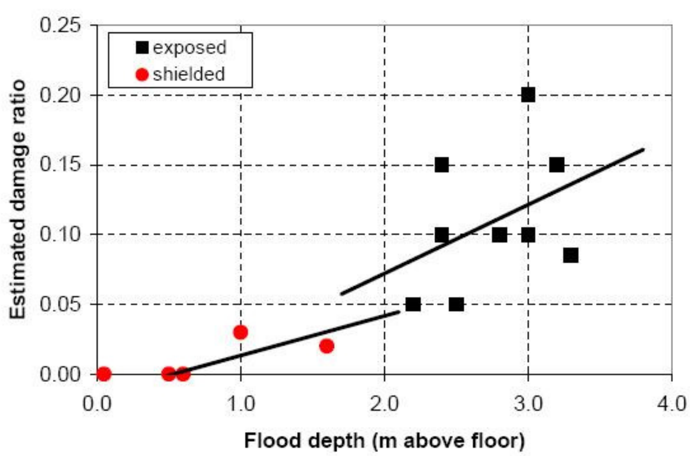

Figure 5-19. Damage ratios and fragility curves as a function of inundation depth and exposure for RC-frame with brick infill (Reese *et al.*, 2007)

The classification method developed by Reese *et al*. is used in this research. Buildings in the urban and rural sample areas were surveyed during the fieldwork. Basic information about the structural characteristic was recorded, including the foundation type/ floor material, wall type, roof type, number of floor post/ pile type, and post/ pile dimension.

The attribute data of the registered buildings are available in the Tax Office's block map. The useful data for building classification available are floor material, wall material, number of storey, and roof material. The data of post/ pile material and the dimension of the post/ pile for the registered buildings are collected during the fieldwork. For the unregistered buildings, all of the construction data are collected during the fieldwork. The buildings classified by the construction type are shown in Figure 5.20 below.

Figure 5-20. Various construction types in the newly generated individual building map overlaying the QuickBird imagery

5.6. Determining the economic values of buildings

The individual building map consists of 1141 polygons in the urban sample area and 104 polygons in the rural sample area. The prices of the buildings registered to the Tax Office are also available in the *Record of Land Parcel and Building Data* developed by the Tax Office.

There are buildings which are not registered to the Tax Office. Those buildings are not found in the individual building map of the Tax Office. It might be that the owners do not pay the tax of their buildings or the data in the document are not well updated. Public facilities such as schools, mosques, and government's offices are also not available in the individual building map of the Tax Office. The prices of those buildings are also not found in the *Record of Land Parcel and Building Data* of the Tax Office. The unregistered buildings were identified by making use of QuickBird imagery and by conducting field survey. For complete loss estimation, the prices of those unregistered buildings must also be determined.

Beside the Tax Office, there are no other reliable sources to obtain the data about the price of buildings in the study area. Real estate agencies are not common in the area. People in the area are not accustomed to sell or buy buildings through real estate agencies. There are 647 buildings out of 1245 buildings in the study area are registered to the Tax Office. Since the data about the prices of buildings are only available in the *Record of Land Parcel and Building Data* of the Tax Office, the prices of the unregistered buildings will be approximated based on this document. The price of an unregistered building will be determined based on the closest registered buildings with the same construction type. The price of public facilities such as state schools, mosques, temples, or government's offices will be determined in the same manner.

$$\mathbf{P_j} = \frac{\mathbf{A_j}}{\mathbf{A_i}} \ \mathbf{x} \ \mathbf{P_i}$$

in which:

P_j is the price of the unregistered building

P_i is the price of the closest registered buildings with the same construction type

A_j is the area of the unregistered building

A_i is the area of the closest registered buildings with the same construction type

5.7. Determining the vulnerability of the population in the basis of individual building

The behavior of a building under the effects of certain hazards will determine whether the people in the building might be injured or killed. The study on the effects of July 2006 South Java tsunami in 22 villages shows the correlation between the death toll and the number of houses destroyed. Casualties are assumed to be restricted to the destroyed group of houses. A similar assumption is that all deaths and injuries occurred in or near totally and badly damaged buildings. The physical vulnerability of a building to tsunami event will directly affect the vulnerability of people inside or nearby the building. Values of building vulnerability will be used as the basis in determining the vulnerability of people to tsunami effects. The expected extent of damage to a building at a certain vulnerability value must be defined at the first place.

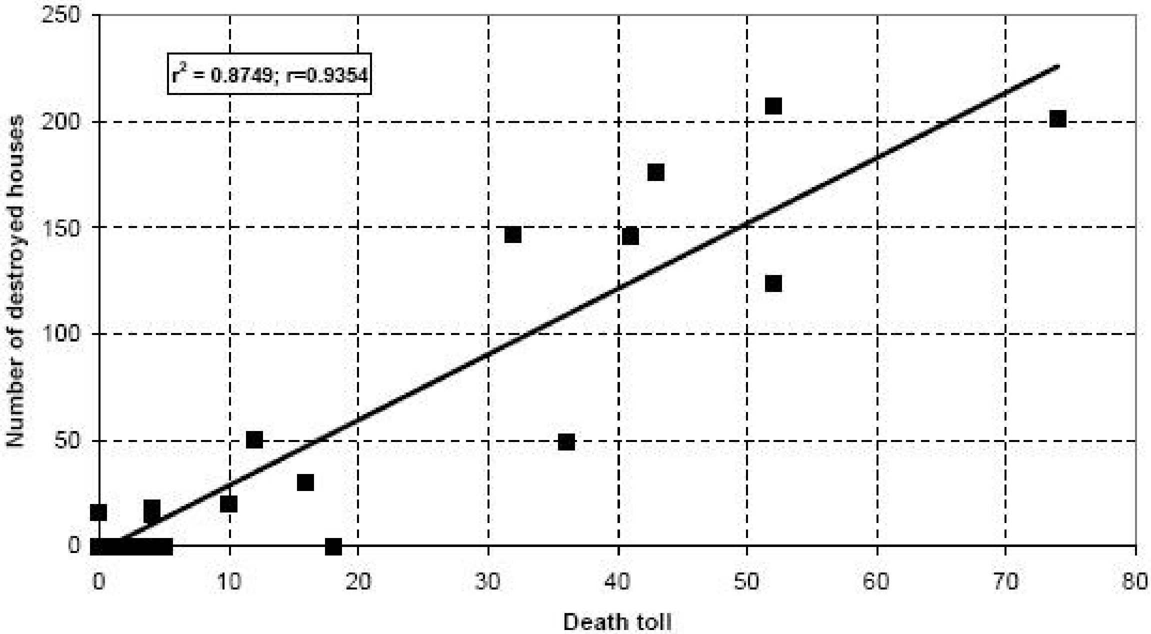

Figure 5-21. Death rates as a function of building destruction in the July 2006 South Java tsunami (Reese *et al.*, 2007)

The number of floors is critically important for determining the vulnerability of people occupying a structure (Dominey-Howes and Papathoma, 2007). For multi storey buildings, the upper storey allows the occupants to evacuate vertically. Where vertical evacuation is not possible, occupants are more vulnerable of suffering injury or death. In fact, the multi storey buildings are usually the well-engineered ones. The vulnerability values of this type of construction are very low. The very low building vulnerability values will result low vulnerability of the people inside or nearby.

Investigation of tsunami-induced damage and fragility of buildings in Thailand after the December 2004 Indian Ocean tsunami was also conducted by a group of scientist from Thailand and Japan. Southern Thailand has been considered a region that is not prone to seismic activity. The observed damages of buildings are primarily contributed by tsunami. The damage level of RC buildings in southern Thailand is quite similar with the damage level of traditional brick with RC column in southern Java. The overall result of the study is in line with the observation of July 2006 South Java tsunami conducted by a group of scientist from Indonesia and New Zealand. Each damage level of the RC buildings observed in southern Thailand is quantified as shown in Table 5.9. The quantification can be adopted to define the damage level of traditional brick with RC column buildings in southern Java whose vulnerability values have been previously determined.

There is no similar table to Table 5.9 found for other types of buildings in the study area. The values in table will be adopted to define the potential extent of damage for timber/ bamboo, traditional brick and RC frame with brick infill wall construction type.

Table 5-9. Values assigned to the damage levels

Damage level	**Vulnerability value**
No damage	0
Damage to secondary members (Damage to wall and roof)	0.33
Damage to primary members (Damage to foundation, column, and beam)	0.67
Collapse	1.00

Source: Ruangrassamee *et al*. (2006)

A number of assumptions are required to determine the vulnerability of people based on the extent of damage of buildings:

- Buildings with vulnerability values between < 0.33 are potential to experience from minor damage to damage of secondary members. Due to the light damage, people who are inside the building will only suffer from light injury.
- Buildings with vulnerability values between 0.33 and 0.67 ($0.33 \leq V < 0.67$) are potential to experience damage from secondary members to primary members. The falling of walls and roof will cause injury to inhabitants. When the damage start to reach the foundation, columns, or beams, the people inside or nearby are very likely to suffer from severe injury.
- Buildings with vulnerability values ≥ 0.67 are potential to experience damage to primary members or to collapse. The damage of foundation, columns, and beams is very likely to cause the building to be partially or totally collapsed. This level of damage is assumed to cause death to people inside or nearby the building.

Those assumptions prevail in most of flow depth classes. An exception should be addressed to the > 2 m flow depth class. The study on the effects of July 2006 South Java tsunami shows that higher flow depth tends to have higher flow velocity, as shown in Table 5.10 below.

Table 5-10. Estimation of tsunami flow velocity

Water depth front (m)	Water depth rear (m)	Distance from shore (m)	Flow velocity (m/s) Eq. (2)	Max velocity (m/s) Eq. (1)
1.05	0.89	90	1.8	3.2
3.00	2.00	165	4.4	5.4
2.23	1.30	190	4.3	4.7
2.35	1.30	175	4.5	4.8
1.92	1.75	205	1.8	4.3
1.39	1.08	210	2.4	3.7
2.71	2.16	90	3.4	5.2

Source: Reese *et al*. (2007)

The higher flow velocity results more damaging scouring effect of tsunami flow. With debris load, the scouring effect will be deadly. In addition, the flow depth of > 2 m has the higher potential to drown the people inside or nearby the building. Different assumptions should be made in the > 2 m flow depth class. The assumptions were summarized in Table 5.11.

Table 5-11. Vulnerability of people based on the vulnerability of buildings and flow depth classes

Vulnerability of building	**Damage extent on building**	**Effect on human inside or nearby**				
		Flow depth 0 – 0.25 m	**Flow depth 0.25 – 0.5 m**	**Flow depth 0.5 – 1.0 m**	**Flow depth 1 – 2 m**	**Flow depth > 2 m**
0 – 0.33	No damage – Damage to wall and roof	x	x	Light injury	Light injury	Severe injury
0.33 – 0.67	Damage to wall and roof – Damage to foundation, column, and beam	x	x	x	Severe injury	Death
0.67 - 1	Damage to foundation, column, and beam – Collapse	x	x	x	Death	Death

Source: Data Analysis

5.8. Determining the population distribution in individual buildings

No census data on the population distribution is available for the study. Population data in Indonesia is usually established in the basis of administrative units. Estimation of population number per household is usually carried out by dividing the total population number in a village by the number of households. Since the sample areas are not in administrative units, this approach is not appropriate to conduct. In the absence of census data, estimation of population distribution will be based on the individual building map with several reasonable assumptions.

The existence of people in every building will differ during the day time and night time. Accurate population loss estimation and an effective mitigation planning require the information of the dynamic population distribution in the day time and night time. Regarding different concentration of people in day time and night time, the population distribution is calculated in two scenarios: day time and night time.

Estimation of population number in buildings is conducted based on two approaches:

1. Architectural space requirement approach

The approach of architectural space requirement is actually estimating the number of building occupants from the area of building space using the norms or standards of architectural design (Budiarjo, 2006). For example, the norms or standard of space requirement in designing a mosque is 1.8 m^2/ person. It implies that a 180 m^2 mosque can accommodate 100 persons at its full capacity (180/1.8=100). The space requirement values used by Budiarjo (2006) are adopted for some building types for this study:

a. Mosque : 1.8 m^2 / person
  - Day time scenario : 10 % of the capacity
    It is assumed that in day time, a mosque is filled by people to 10 % of its capacity.
  - Night time scenario : 1 person
    It is assumed that only 1 attendant who stays in the mosque at night.

b. School : 4.0 m^2 / person
  - Day time scenario : 110 % of the capacity
    It is assumed that the number of teachers, staffs, and merchants is 10 % of the number of students.
  - Night time scenario : 1 person
    It is assumed that only 1 security guard who stays in the school at night.

c. Office : 8.5 m^2 / person
  - Day time scenario : 100 % of the capacity
    In day time, an office is assumed to be filled to its regular occupancy (100 %).
  - Night time scenario : 1 person
    It is assumed that only 1 security guard who stays in the office at night.

d. Warehouse : 40.0 persons (in 1 hectare site)
  - Day time scenario : 100 % of the capacity
    In day time, a warehouse is assumed to be filled to its regular occupancy (100 %).
  - Night time scenario : 2 person
    It is assumed that there are 2 security guards who stay in the warehouse at night.

The area of buildings extracted from the satellite imagery is the planar-roof area. Buildings in Indonesia generally have overhang roof structure of approximately 1m length surrounding the building. The percentage of area below overhang structure is around 15 % of the whole planar-roof area. The area of buildings used as the building area in estimating the number of occupants is 85 % of the planar-roof area.

2. Assumptions and field observations

For some building types, direct observation was conducted to give more objective occupancy rates rather than space requirement approach.

a. Residential house

The predominant number of family member is 4 persons/ household, whether the family live in a large house or a small house. A family generally consists of a father, a mother, and 2 children. The size of the house rarely affects the number of population in the household. The number of family member per household is assumed to be 4 persons/ household.

- Day time scenario : 50 % of occupants
  It is assumed that the mother and a child stay at home, whilst the father is at work and the other child is at school.
- Night time scenario : 100 % of occupants
  It is assumed that all of the family members are at home at night.

b. Shop

Most of the shops in the area are *ruko* (*rumah-toko*). It is assumed that there are averagely 4 persons in a shop including the employee(s) and visitors.

- For a single storey *ruko*, the shop is situated at the front of the building and the family live at the back of the building. The dynamic distribution of the occupants is as follows:
- Day time scenario : 50 % of family members + 4 (employee(s) and/ or visitors)
  It is assumed that half of the family members do their activities outside the house.
- Night time scenario : 100 % of family member
  It is assumed that all of the family members are at home at night, and the shop is closed at night.
- For a multi storey *ruko*, the shop is situated in the ground floor of the building and the family live in the upper storey of the building. The construction type of multi storey *ruko* is considered to withstand the tsunami effect. Only the occupants in the shop (ground floor) will be taken into account because the family members who stay in upper storey are considered not vulnerable to tsunami impact.
- Day time scenario : 50 % of family members + 4 (employee(s) and/ or visitors)
  It is assumed that half of the family members do their activities outside the house. The ones who are at home will stay to help in the shop (in the ground floor)
- Night time scenario : -
  It is assumed that the shop is closed at night. All of the family members are at home at night, and they stay in the upper storey. No one is in the ground floor.

c. Temple

The temple is used only on Sunday and religious festal days. In ordinary days, there are only the attendant, cleaning service staff, and a security guard.

- Day time scenario : 1 attendant, 1 cleaning service, and 1 security guard
- Night time scenario : 1 cleaning service and 1 security guard

5.9. Conclusion

- Differential GPS measurement with post-processing differential correction have resulted 25 GCPs of sub meter horizontal precision. 24 out of 25 GCPs reached the horizontal precision $\leq$ pixel size (0.6 m).
- The panchromatic ortho-rectified QuickBird imagery met the stated positional accuracy of 10 m. The shifting distances of check points in the image range from 4.521 to 8.314 m.
- Geo-referencing process utilizing 8 GCPs evenly spread over the City is adequate for image correction. Considering the 0.6 m pixel size, extra GCPs in the sample areas do not contribute significant changes for positional accuracy.
- The positional accuracy of the Land Office's land parcel map is poor. In some points, the positional accuracy is > 10 m. The map is not reliable for loss estimation and mitigation planning.
- The positional accuracy of the Tax Office's block map is very poor. In some points, the positional accuracy is > 50 m. The map is also not reliable for loss estimation and mitigation planning.
- New land parcel map and individual building map must be generated based on the corrected QuickBird imagery. The spatial arrangements of land parcels and buildings in the existing maps are used for screen digitizing of the new maps.
- The complete data of land and building prices is only available in the *Record of Land Parcel and Building Data* developed by the Tax Office. The prices are for taxation purposes, thus do not represent the market price.
- The predominant construction type in the study area is traditional brick with RC column. 1049 out of 1141 (91.94 %) buildings in the urban sample area are of this construction type. In the rural sample area 70.19 % of the buildings are of this construction type.
- Based on the architectural space requirement approach, there is only one building of very high occupancy rate in day time scenario. A state school is estimated to be occupied by 340 people during the day time.

6. Loss estimation, mitigation planning, and post-tsunami reconstruction

The developed database is very useful for loss estimation and mitigation planning. Loss estimation is conducted upon buildings and population. Mitigation planning includes non-structural mitigation planning through land use policy and structural mitigation planning: retrofitting of the existing buildings. This chapter also contains a sub chapter that reveals the usefulness of the database for post-tsunami reconstruction process.

6.1. Loss estimation of buildings and population

Without the data of temporal probability, a quantitative risk assessment is not possible to be conducted. Future loss estimation can be conducted instead, utilizing the following formula:

Losses = V * A

in which:

V is the vulnerability of elements at risk, specified as the degree of damage to a specific element at risk at certain tsunami intensity

A is the quantification of the specific type of element at risk evaluated.

6.1.1. Loss estimation of buildings

The physical vulnerability (V) and the economic value (A) of the buildings have been determined in Chapter 5. In the following, a 2- dimensional table was developed based on the vulnerability curves for each construction type (see Figure 5.16 in Sub-chapter 5.5). With this table, the potential damages of the buildings to tsunami flow depth are calculated.

The 2-dimensional table integrates the data from two different maps into one output map. The flow depth data in the tsunami inundation model will be joint with the construction type data in the individual building map. The output map will show the potential damage of various construction types due to various classes of tsunami flow depth.

Table 6-1. Estimated damage ratios of buildings to tsunami flow depth

		Tsunami flow depth (m)				
		0 - 0.25	0.25 - 0.50	0.50 - 1.00	1.00 - 2.00	> 2.00
Construction type	Timber/bamboo	0	0.11	0.33	0.78	1
	Brick traditional	0	0.11	0.33	0.78	1
	Brick traditional with RC-columns	0	0.05 (0*)	0.14 (0.05*)	0.33 (0.14*)	0.7 (0.33*)
	RC-frame with brick infill walls	0	0.01 (0*)	0.03 (0*)	0.07 (0.02*)	0.15 (0.1*)

* shielded buildings

Source: Data Analysis

The interactions between the classes of flow depth and the types of constructions to determine the various levels of damages are visualized in Figure 6.1 and Figure 6.2 below.

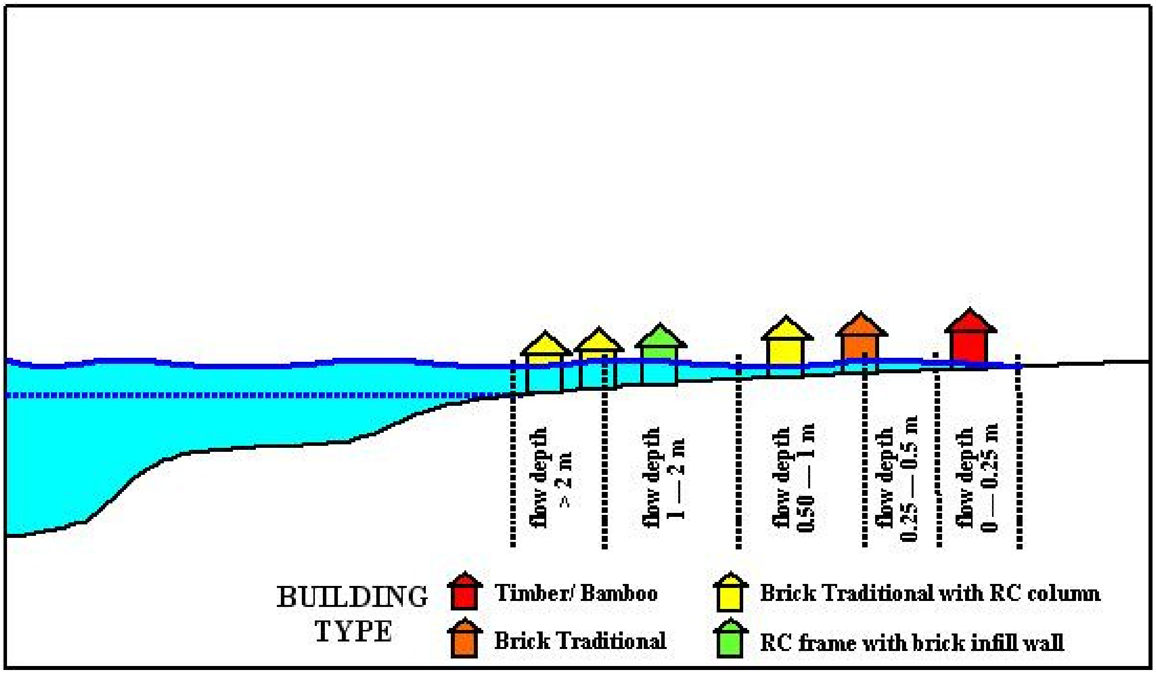

Figure 6-1. Illustration: various construction types inundated by various flow depth classes

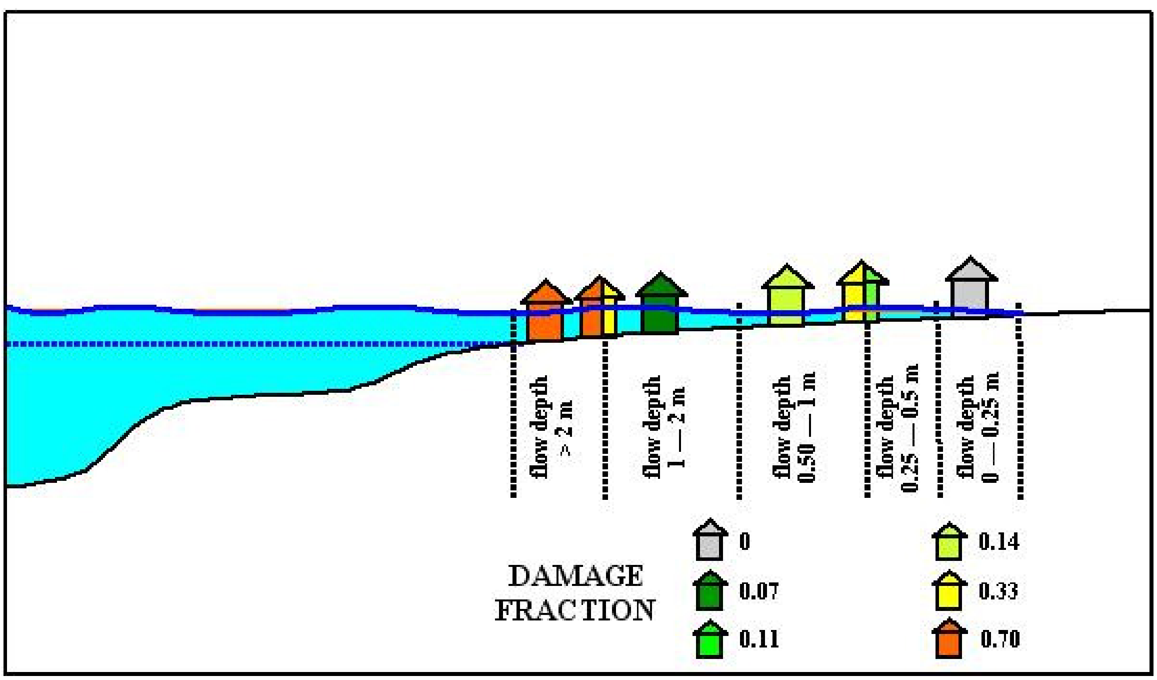

Figure 6-2. Illustration: various damage levels of buildings to tsunami flow depth

As clearly visualized in the figures above, the *brick traditional with RC column* located in the 0.5 - 1 m flow depth has different damage fraction compared to the same construction type located in the > 2 m flow depth. A *brick traditional with RC column* crossed by the boundary of the 1 - 2 m flow depth and the > 2 m flow depth is sliced into two parts of different damage ratios. The area of each part must be previously determined before conducting loss estimation.

An estimated loss of each individual building is calculated as follows:
Loss = V * A
in which:
V is the physical vulnerability of the building
A is the economic value (price) of the building

The processes of loss estimation are described in Figure 6.3 and Figure 6.4 below:

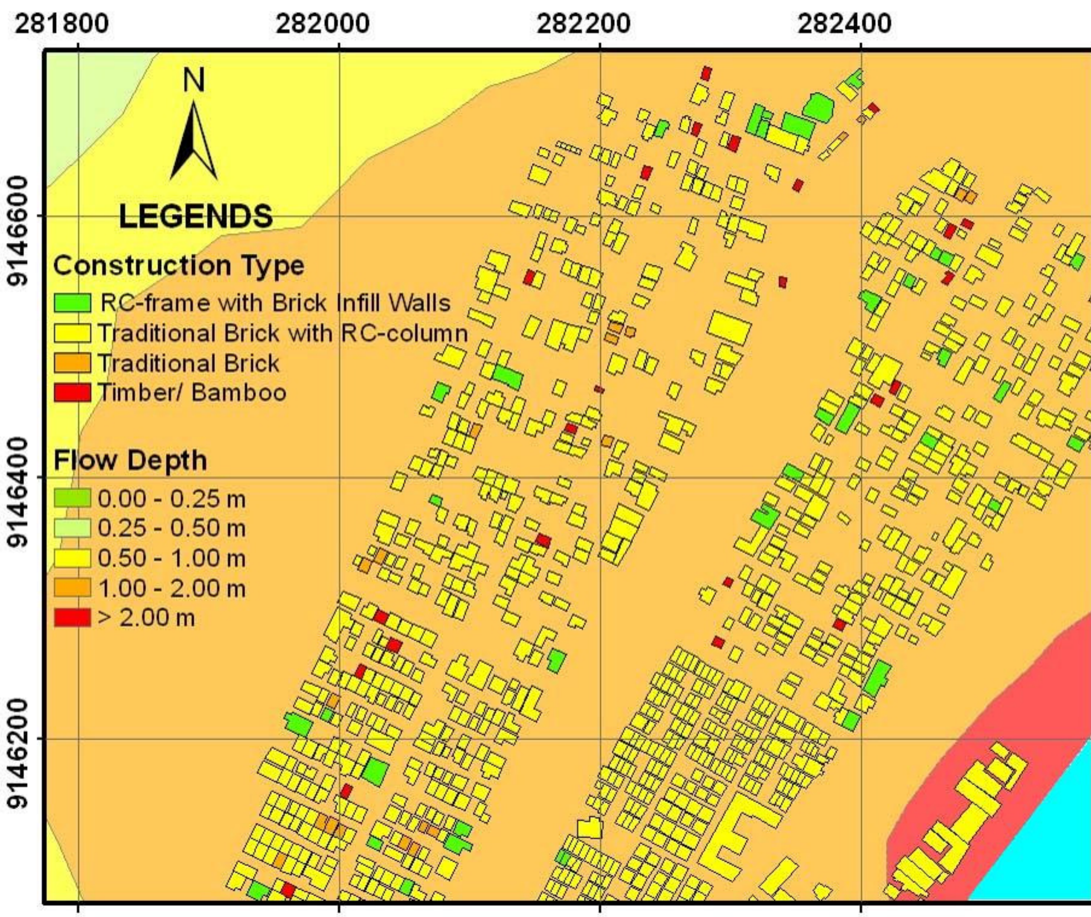

Figure 6-3. Various construction types located in various flow depth classes

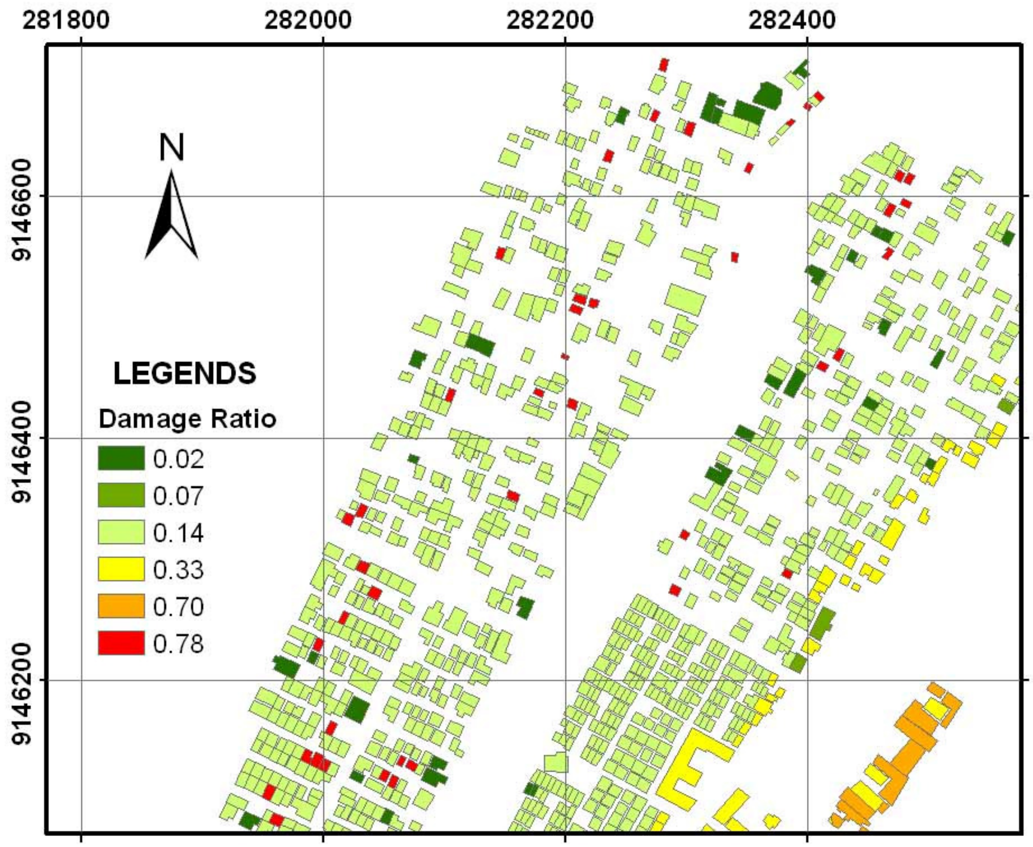

Figure 6-4. Various estimated damage levels of buildings

6.1.2. Loss estimation of population

As aforementioned, the behavior of a building under the effects of tsunami will determine whether the people in the building might be injured or killed. For defining the vulnerability of people inside or nearby a building, the vulnerability of the building must be determined at the first place.

There are buildings which are completely located within certain depth class and there are also buildings which are crossed by the boundary of two flow depth classes. Vulnerability value of a building crossed by the boundary of two flow depth class is defined as follow:

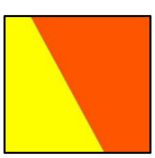

43.15 % of the building is located in the 1 – 2 m flow depth class and 56.85 % is located in the > 2 m flow depth class. The building has two vulnerability values, 0.33 and 0.70. The accumulative vulnerability value is:
(43.15 % * 0.33) + (56.85 % * 0.70) = 0.54

If the vulnerability values of buildings are determined, the vulnerability of people will able to be estimated. The vulnerability of people as the function of the vulnerability of buildings and the flow depth classes were determined in Sub-chapter 5.7. The results are revealed in Table 6.2 below:

Table 6-2. Vulnerability of people as the function the vulnerability of buildings and flow depth classes

Vulnerability of building	Damage extent on building	Effect on human inside or nearby				
		Flow depth 0 – 0.25 m	Flow depth 0.25 – 0.5 m	Flow depth 0.5 – 1.0 m	Flow depth 1 – 2 m	Flow depth > 2 m
0 – 0.33	No damage – Damage to wall and roof	x	x	Light injury	Light injury	Severe injury
0.33 – 0.67	Damage to wall and roof – Damage to foundation, column, and beam	x	x	x	Severe injury	Death
0.67 - 1	Damage to foundation, column, and beam – Collapse	x	x	x	Death	Death

Source: Data Analysis

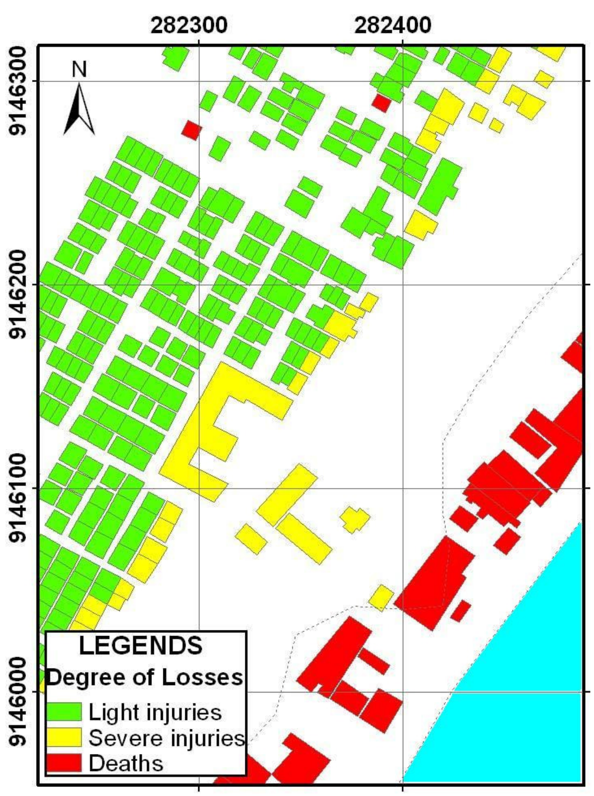

Figure 6-5. Vulnerability of people as the function of the vulnerability of buildings and flow depth classes

Based on Table 6.2 above, the vulnerability of the people inside or nearby a building can be estimated as functions of building's vulnerability and the depth of inundation. For example, a building with vulnerability value = 0.70 and inundated by > 2 m flow depth will cause death to all of the people inside or nearby the building.

The rates of deaths and injuries are determined as the function of the people's vulnerability and the occupancy rate of the building. For example, a warehouse is predicted to be badly damaged due to > 2 m tsunami inundation and cause death to the people inside and nearby. Usually, there are 4 people in the warehouse in day time and 2 people in night time. The death rate is 4 in a day time tsunami event, and is 2 in a night time tsunami event.

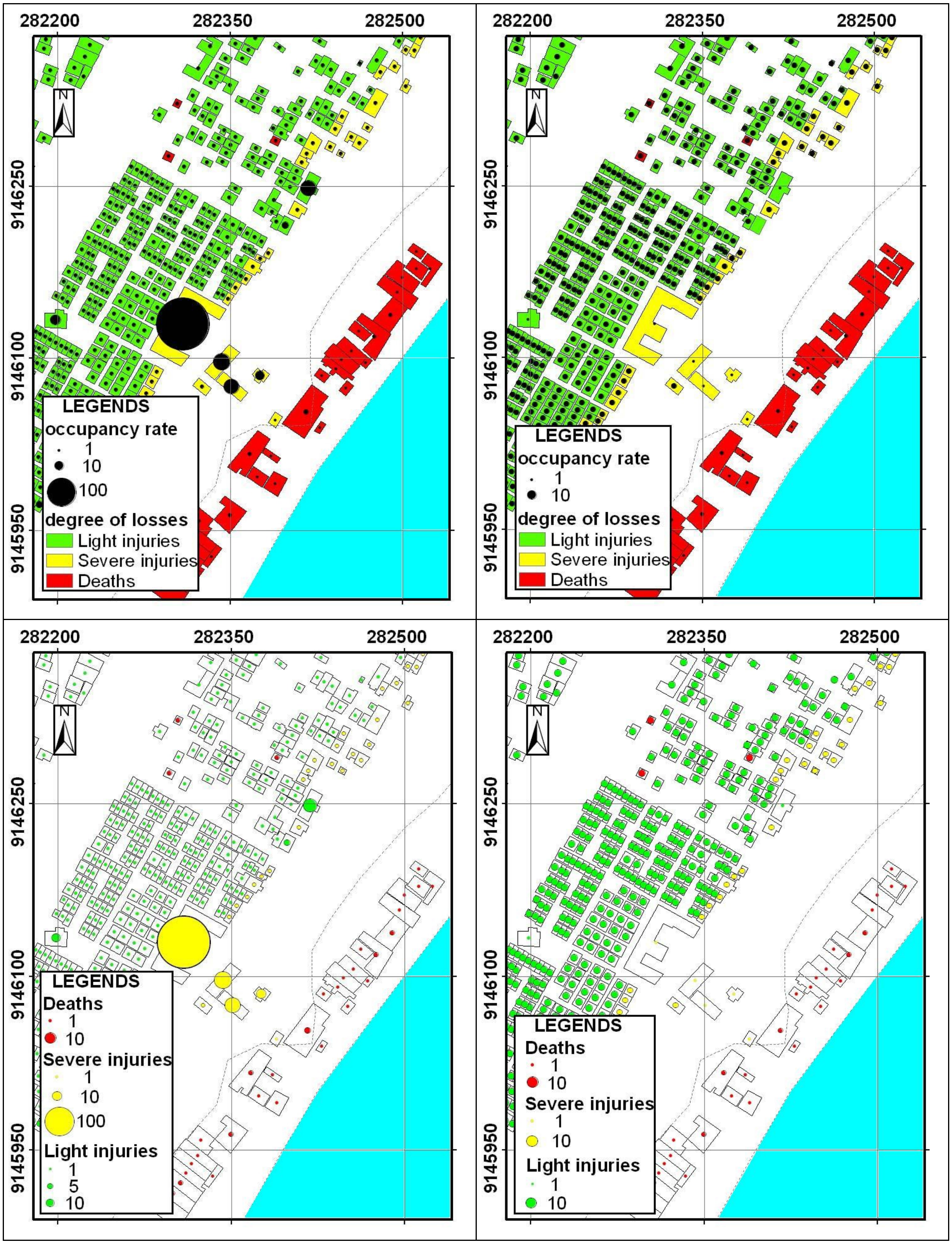

Figure 6-6. Occupancy rates of buildings in day time (top left), occupancy rates of buildings in night time (top right), estimated rates of death, severe injuries, and light injuries in day time scenario (bottom left), and estimated rates of death, severe injuries, and light injuries in night time scenario (bottom right)

6.2. Mitigation planning of tsunami effects

Mitigation is defined as structural and non-structural measures undertaken to limit the adverse impact of natural hazards, environmental degradation and technological hazards (ISDR, 2004). Structural measures refer to any physical construction to reduce or avoid possible impacts of hazards, which include engineering measures and construction of hazard-resistant and protective structures and infrastructure. Whilst, non-structural measures refer to policies, awareness, knowledge development, public commitment, and methods and operating practices, include participatory mechanisms and the provision of information, which can reduce risk and related impacts.

6.2.1. Non structural mitigation planning through land policy

Avoiding a tsunami hazard area is the most effective mitigation method (Eisner, 2001). Land use planning must put the extent of tsunami hazard into account.

1. *Determining the tsunami buffer zone in Cilacap City*

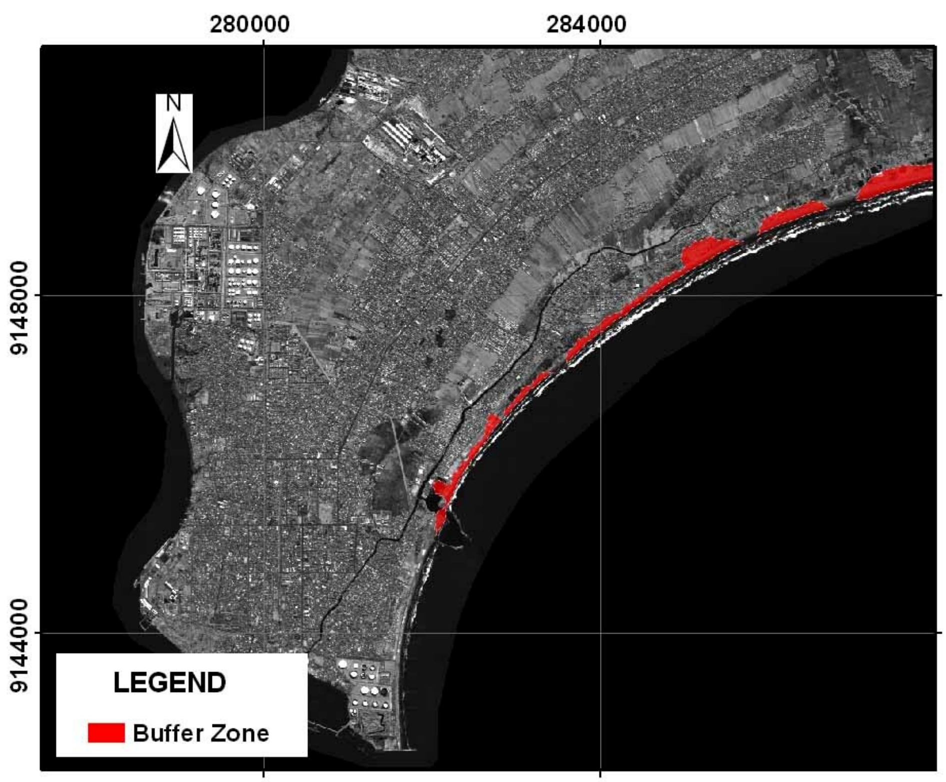

Figure 6-7. The proposed tsunami buffer zone

The tsunami inundation model developed by Mardiatno (2008) will be used as the bench mark in determining the area proposed as tsunami buffer zone. Previous study on the vulnerability of buildings in Sub-chapter 5.5 shows that the *timber/ bamboo* and *traditional brick* construction types will be partially or totally collapse after tsunami flow depth of > 2 m.

The *traditional building with RC column* will experience damage to secondary members up to primary members after tsunami flow depth of > 2 m. The potential death toll is also predominantly contributed by the > 2 m flow depth class, as revealed in Sub-chapter 5.7. Based on those considerations, special policy must be undertaken for the area that has the potential to be inundated by > 2 meters tsunami flow depth. The area should be proposed as a tsunami buffer zone.

2. Acquisition of the tsunami buffer zone for open space uses

The land parcel map, the individual building map, and the well defined tsunami buffer zone are the primary inputs for acquisition plan. The accuracy of each spatial data is critical in determining whether or not a land parcel or building is located partially or completely within the tsunami buffer zone.

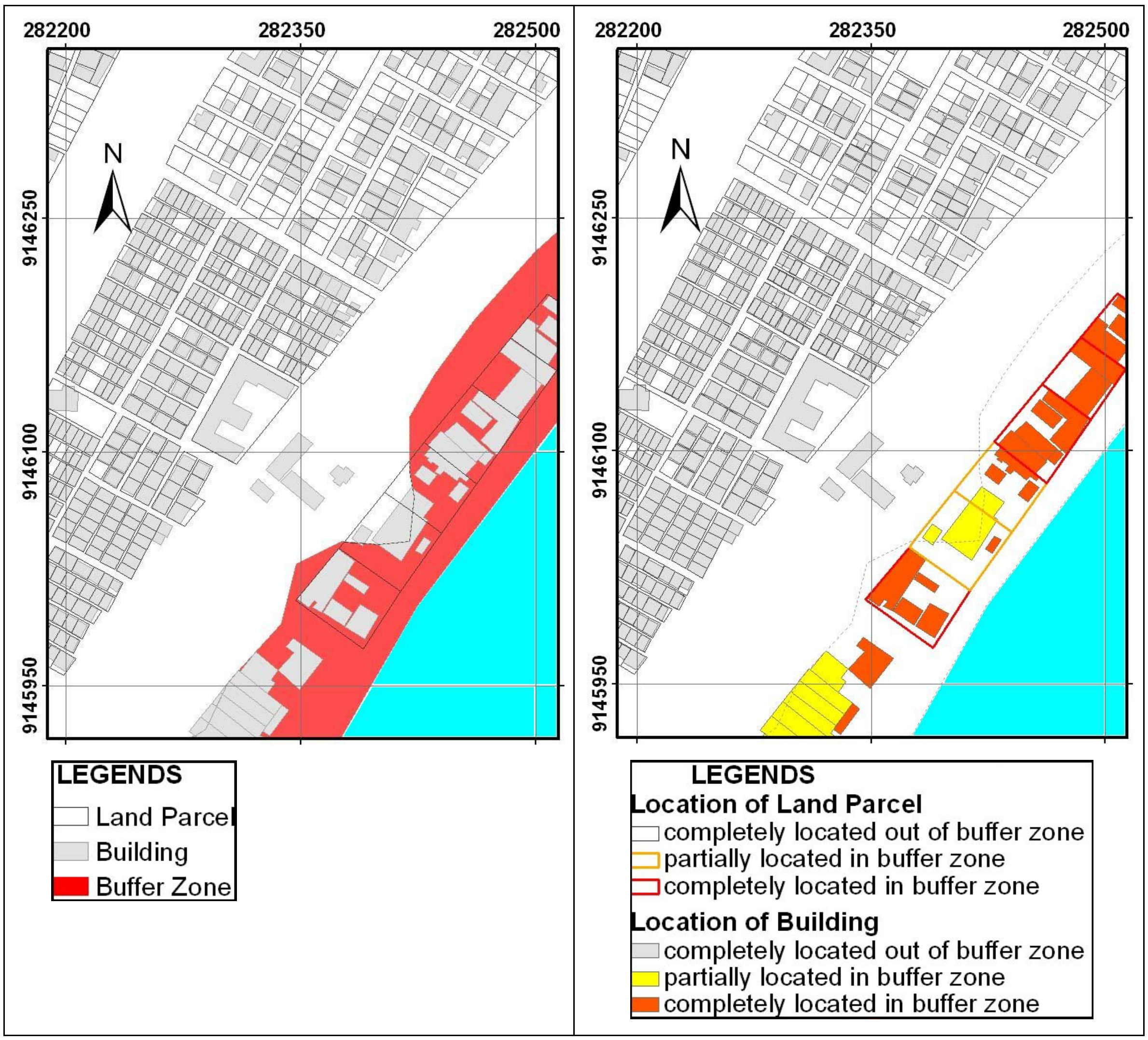

Figure 6-8. Relative positions of land parcels and buildings to tsunami buffer zone (left), and land parcels and buildings partially or completely located in the tsunami buffer zone (right)

All of the land parcels and buildings affected by the tsunami buffer zone should be subjected to acquisition, whether they are completely or partially located in the tsunami buffer zone. Compensation in this study will only be based on the data of the Tax Office. Values of land parcels and buildings have been included in the newly developed database of elements at risk as explained in Sub-chapter 5.4 and Sub-chapter 5.6. The replacement cost for tsunami buffer zone acquisition is calculated as the total compensation for land parcels and buildings located in the tsunami buffer zone.

The process of designing new development in the tsunami buffer zone must really emphasize in public safety goals. The following figures show two examples of land use design to reduce the impact of tsunami waves to coastal cities in Japan.

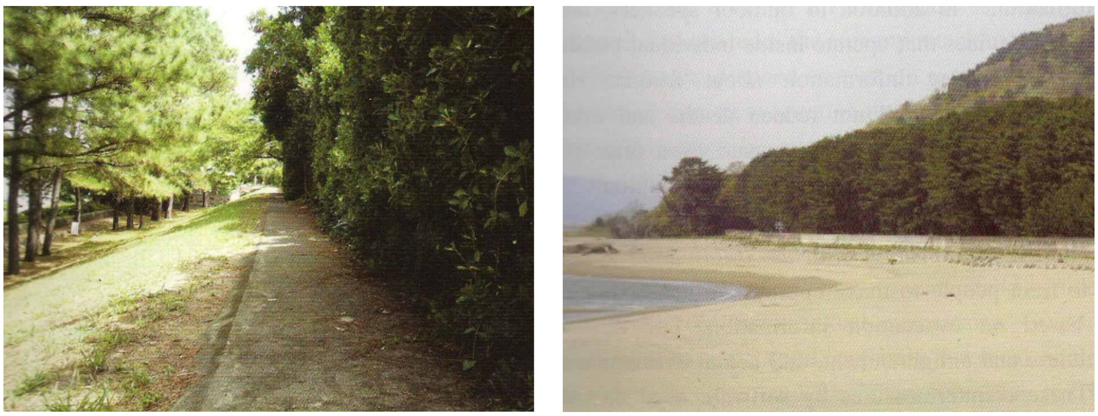

Figure 6-9. Coastal park and embankment (left) and *tsunami forest* (right) (Murata *et al.*, 2010)

The coastal park and embankment shown in Figure 6.9 above is in Hiromura Village, Hirogawa Town, Wakayama Prefecture, Japan. The entire village was heavily damaged by tsunami wave in 1605, 1707, and1854. After the tsunami in 1845, the local authority acquired the outmost part of the coastal area. The villagers previously lived in the area were relocated to safer area. Have the area been acquired by the local authority, coastal park and coastal embankment were established in the area.

Another good example of land use design to reduce the impact of tsunami waves is the tsunami forest. The tsunami forest acts as a shielding protector against the tsunami waves. Being blocked by the tsunami forest, the velocity and the energy of tsunami waves can be reduced. The big trees provide the "trapping effect" (Murata *et al.*, 2010). Many floating objects carried inland by tsunami waves can be trapped in the tsunami forest. The tress can also prevent the people from being swept away by the tsunami return flow because the people may have the chance to cling to the trees.

Implementation of those special land use designs require wide space of the outmost coastal area. Designation of tsunami buffer zone for coastal park or tsunami forest not only will avoid the people from the area of the highest tsunami threat, but will also reduce the potential losses of the population living behind the coastal park or the tsunami forest.

The United Nations Environment Programme (2005) stated that there has been a program in Indonesia similar to the ones in Japan. The “Program Pantai Lestari” (Sustainable Coast Programme) has been carried out by the Ministry of Environment since 1996. It is a national programme organized by local governments. Unfortunately, the programme is not implemented in all provinces of Indonesia. The most advanced example of the programme implementation is the Bali Demonstration Project for Integrated Coastal Management. This model can be used as a basis for the future coastal zone management of the tsunami prone areas in Indonesia.

6.2.2. Structural mitigation planning: retrofitting planning

Interventions must be conducted upon the highly threatened buildings to reduce the potential losses. The types of intervention necessary to enhance the performance of the building can be broadly grouped under the following three categories - Repair, Restoration and Strengthening (Santhanam, 2006). A more common term for the purpose is “retrofitting” which is divided into 3 concepts; Repair, Restoration and Strengthening (Boen, 2006). Retrofitting usually focuses on the existing buildings that are vulnerable to failure/collapse to an expected inundation depth.

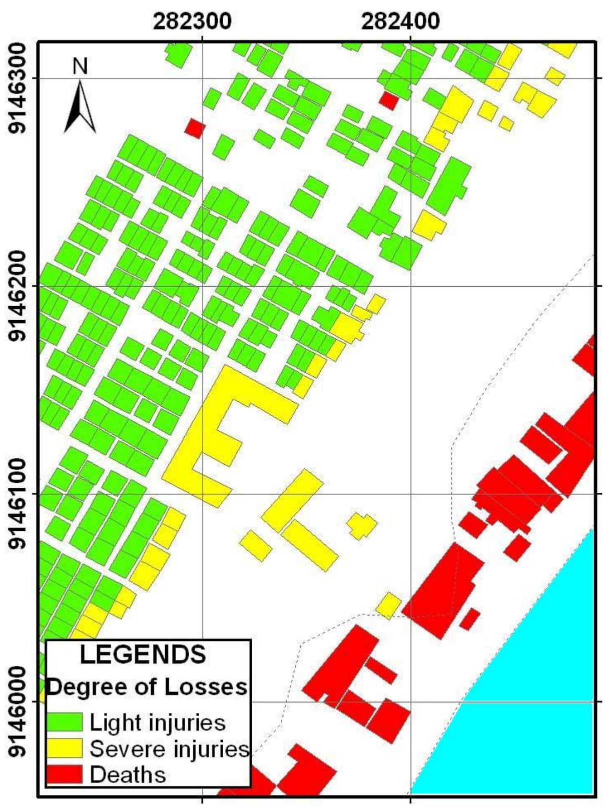

Figure 6-10. Vulnerability of people in the basis of individual building

Sufficient retrofitting measures must be addressed to the buildings which required them the most. The right retrofitting measures must be addressed to the right building. An effective retrofitting scheme is expected to lessen the vulnerability of buildings and the people as well, to the minimum at minimum the cost.

Buildings that have the potential to contribute deaths, buildings that have the potential to contribute severe injuries, and buildings that have the potential to contribute light injuries are put in the list of priorities respectively. Have the buildings subjected to retrofitting been determined; the next step is to determine the sufficient retrofitting measures for each building.

1. *Retrofitting scheme to avoid death toll*

Extracting the information from the database of elements and risk, the construction types that have the potential to contribute deaths due to the given tsunami intensity are:

- *Timber/ bamboo or traditional brick* located in the 1 – 2 m flow depth class.
  Those buildings must be upgraded to *traditional brick with RC column*.
- *Traditional brick with RC column* located in the > 2 m flow depth class.
  Those buildings must be upgraded to *RC frame with brick infill wall.*


Figure 6-11. *Traditional brick* construction type (left) and reinforced concrete column added to strengthen the structure and to create a *traditional brick with RC column* (right) (Boen, 2006)

RC frame with brick infill wall (located in > 2 m flow depth class) will contribute to severe injuries after retrofitting. Since the damage is only experienced by the ground floor, only the people who stay in the ground floor will suffer from severe injuries. The upper storey will provide refuge to people inside or nearby the building. Evacuation time will be decreased to the minimum if all the buildings located in > 2 m flow depth class are upgraded to well-engineered RC *frame with brick infill wall* construction type.


Figure 6-12. 10 cm x 10 cm to 20 cm x 20 cm column dimension for *traditional brick with RC-column* construction type (left) and at least 20 cm x 20 cm column dimension for *RC-frame with brick infill wall* (right) (fieldwork doc.)

2. *Retrofitting scheme to reduce severe injuries*

Extracting the information from the database of elements and risk, the construction types that have the potential to contribute severe injuries is:

- *Traditional brick with RC column* located in the 1 – 2 m flow depth class and exposed to the tsunami wave.

Implementation of both retrofitting schemes above is expected to avoid death toll and severe injuries. Distribution of the buildings subjected to retrofitting and the expected changes on construction types are shown in Figure 6.13 below.

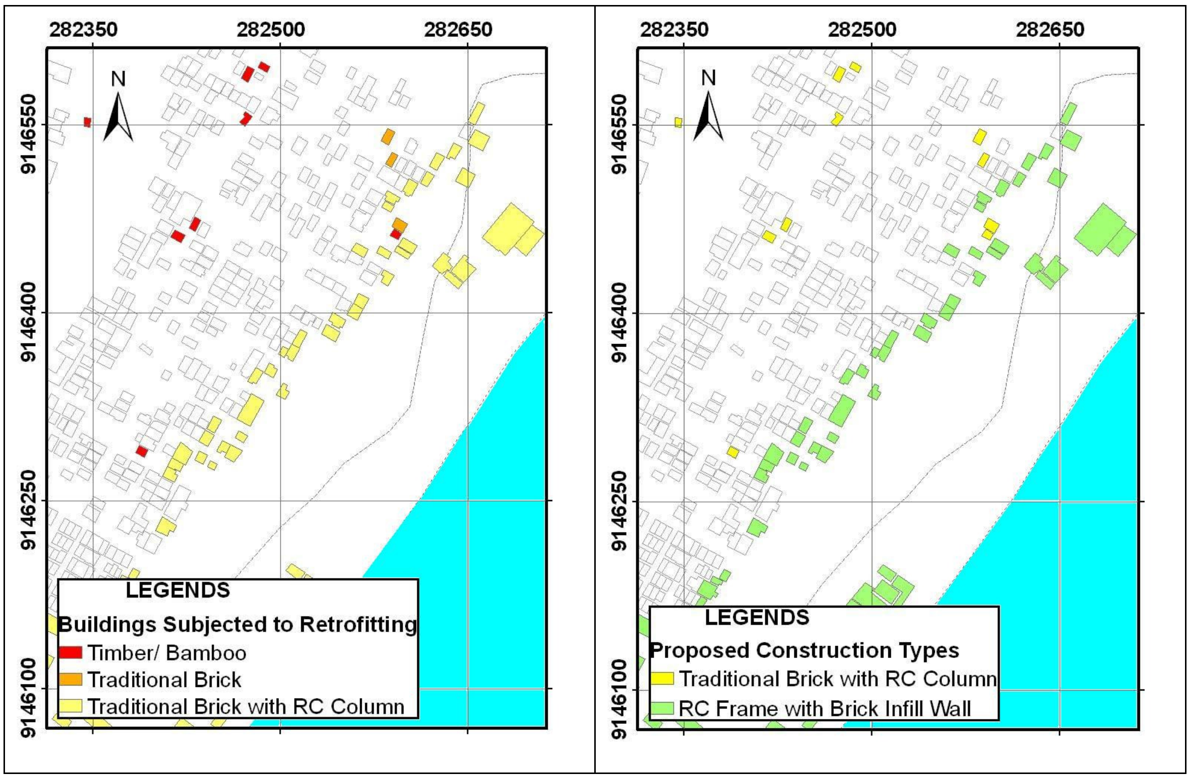

Figure 6-13. Buildings subjected to retrofitting because of the potential to contribute severe injuries and deaths (left), and the proposed changes on construction types to avoid death toll and severe injuries (right)

Retrofitting plan must also consider the number of threatened people inside or nearby a building. Upgrading the structural adequacy of a building is accepted as an effective way to lessen the vulnerability of people inside or nearby a building. Schemes for avoiding deaths and reducing severe injuries have been developed earlier. The next challenge is to reduce the rates of injuries. The rates of injuries are determined as the function of the people’s vulnerability (inside or nearby a building) and the occupancy rate of the building. When the occupancy rate of a threatened building is high, the rates of injuries to the given tsunami event will also be high. The potential rates of injury for day time scenario and night time scenario of each building after retrofitting are shown in Figure 6.14 below.

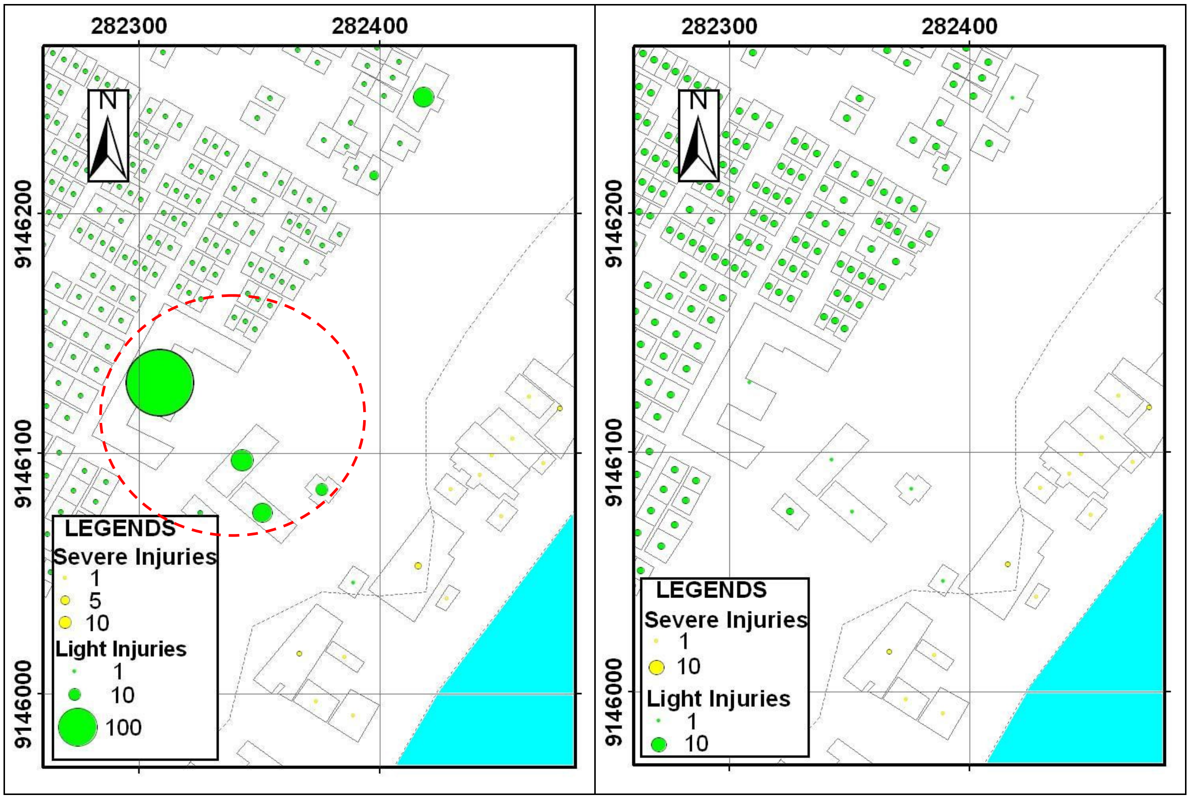

Figure 6-14. Estimated rates of severe injuries and light injuries in day time scenario after retrofitting (left), and estimated rates of severe injuries and light injuries in night time scenario after retrofitting (right)

Figure 6.14 above shows three office buildings of high occupancy rate and one school of very high occupancy rate in day time. Upgrading the construction type from *traditional brick with RC column* to *RC frame with brick infill wall* will reduce the vulnerability of people inside and nearby. The upper storey will provide refuge to people inside or nearby the building. Despite of the minimized vulnerability of people, the number of people potentially affected must be seriously considered. In day time, approximately 340 people are in the school; students, teachers, staffs, and merchants. In a sudden tsunami event without adequate early warning system, evacuating those people to the upper storey may lead to chaos.

A building shielded by other buildings will experience less effect of the tsunami flow. The tsunami wave will not hit the building directly. The velocity of the deflected tsunami flow that hit the building is assumed to be reduced. Since the aforementioned school and office are exposed to the sea, new artificial protecting shield can be built for those buildings. Constructing reinforced concrete wall surrounding the school or office complex will reduce the vulnerability of the people within the school or office complex to the minimum. The presence of the retaining wall is expected to reduce tsunami effect to the compound behind.

Figure 6-15. Reinforced concrete wall as protecting shield for high occupancy buildings (Dominey-Howes and Papathoma, 2007)

Figure 6-16. Proposed retaining wall for buildings of high occupancy rate

6.3. Post-tsunami reconstruction

Disasters can create enormous pressure to rebuild the community quickly and exactly as it was before the disaster (Eisner, 2001). Adequate post-tsunami reconstruction planning is expected to accelerate the reconstruction processes after a disaster occurrence. Many of the post-disaster rebuilding works are conducted in the basis of individual building or individual land parcel. For instance: rebuilding the damaged residential houses and public facilities. Unfortunately, tsunamis often cause damages to both buildings and the land parcel boundary marks.

Figure 6-17. Case where the buildings and parcels boundaries are completely disappeared (left) and case where the buildings and parcels boundaries are still identifiable (right) (Benny *et al.*, 2006)

The data on the initial condition of buildings and land parcel boundaries are available in the Land Office and Tax Office. Unfortunately, the existing data of the Land Office and the Tax Office are not reliable for post-tsunami reconstruction processes due to the inaccuracy and incompleteness of the data (see Sub-chapter 5.2). Such database of elements at risk developed in this research (see Chapter 5) is very useful and also reliable for post-tsunami reconstruction works.

The certainty in location of buildings and land parcels are urgently required to speed up the rehabilitation and reconstruction process after a disaster. Buildings are generally located in the basis of land parcels. Therefore, land parcel reconstruction process has to be completed as soon as possible in an effective and efficient manner. Tsunamis have the potential to destroy and wipe away the physical evidence of land parcel boundaries, man-made or natural objects. Sometimes there are no distinct clues available for parcel reconstruction in the field, as shown in Figure 6.17. Fake statements of land ownership may be made by some irresponsible peoples.

The absence of distinct physical evidences and the fake statements of land ownership will make the parcel reconstruction work more complicated. The land parcel layer in the database of elements at risk is extremely useful in order to conduct effective and efficient land parcel reconstruction.

Figure 6-18. Land parcel layer in the database overlaying the QuickBird imagery

The land parcels in the database are already in UTM coordinate system. Boundary reconstruction process using GPS technology is able to be performed. The general processes of land parcel reconstruction are revealed in Figure 6.19.

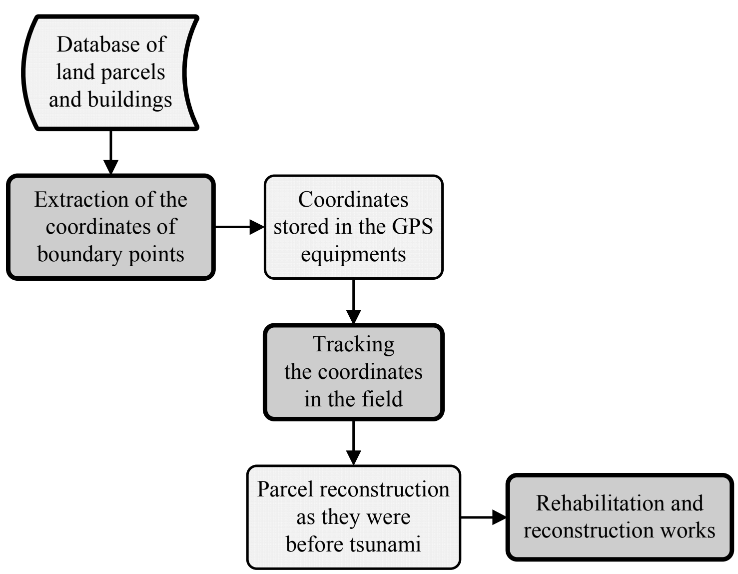

Figure 6-19. Parcel reconstruction utilizing the database of land parcel and buildings

Coordinates of the edges of land parcels are stored in the GPS equipment. By conducting the *Real Time Kinematic* differential GPS techniques, those coordinates can be accurately tracked in the field. The work is illustrated in Figure 6.20.

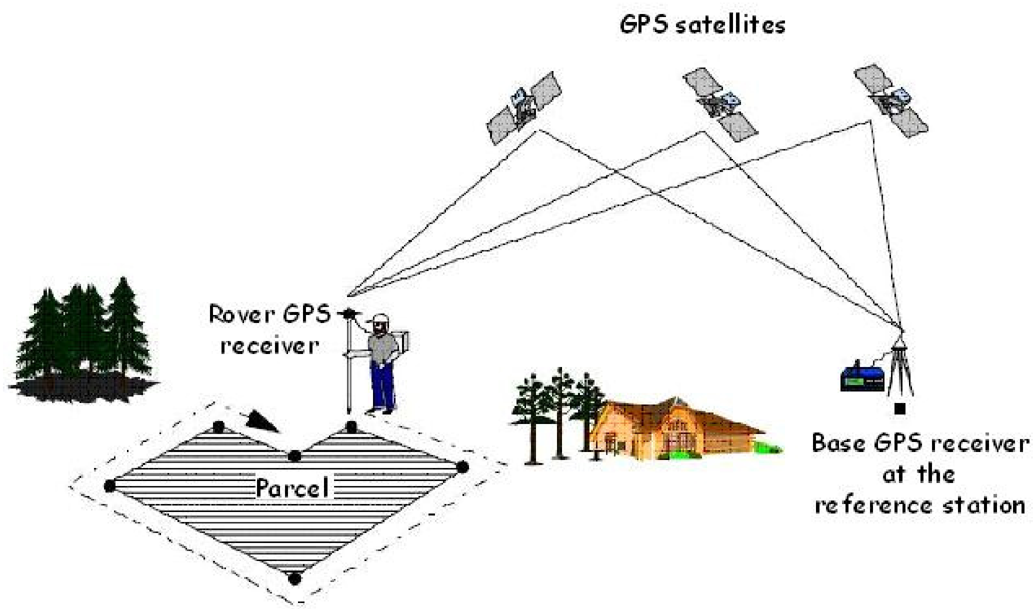

Figure 6-20. Real Time Kinematic GPS technique for parcel reconstruction (Abidin, 2007)

A base receiver is located at a reference station of a defined position. A rover receiver is used to track the coordinates in the field. In normal circumstances, the maximum distance between the base receiver and the rover receiver may reach up to 15 kilometers (Abidin, 2007). The accuracy of this method is in centimeters. Applying this method is expected to keep the cost and time for reconstruction at the minimum.

The existence of a reliable database of elements at risk and the implementation of *real time kinematic* GPS techniques will be a powerful combination for post-tsunami reconstruction processes in general. The initial positions of land parcels can be restored as it was before a tsunami occurrence in an effective and accurate way. Since many of the post-disaster rebuilding works are conducted in the basis of individual building or individual land parcel, the method is expected to speed up the rehabilitation and reconstruction process after the tsunami occurrence.

6.4. Conclusion

- The estimated losses of buildings in the urban sample area due to the given tsunami extent is Rp 4.949.353.710
- The estimated losses of buildings in the rural sample area due to the given tsunami extent is Rp 909.171.174
- The maximum death rate is in the urban sample area during night time scenario (252 deaths). It is assumed that all family members will stay at home during the night time. The badly damaged or collapsed houses will contribute to deaths.
- The maximum severe injury rate is in the urban sample area during day time scenario (533 severe injuries). A state school is assumed to be occupied to its maximum capacity during the day time (340 people, based on the architectural space requirement approach). The school contributes the highest for the severe injury rate.
- The estimated replacement cost for tsunami buffer zone acquisition in the urban sample area is Rp 1.163.542.000
- The estimated replacement cost for tsunami buffer zone acquisition in the rural sample area is Rp 5.204.914.00
- The numbers of buildings subjected to retrofitting to avoid deaths in the urban sample area are as follows:
    - 25 *timber/ bamboo* building to be upgraded to *traditional brick with RC column* construction type
    - 23 *traditional brick* building to be upgraded to *traditional brick with RC column* construction type
    - 36 *traditional brick with RC column* building to be upgraded to *RC frame with brick infill wall* construction type
- The numbers of buildings subjected to retrofitting to avoid deaths in the urban sample area are as follows:
    - 2 *traditional brick* building to be upgraded to *traditional brick with RC column* construction type
    - 11 *traditional brick with RC column* building to be upgraded to *RC frame with brick infill wall* construction type

7. Result and discussion

Loss estimation and mitigation planning were conducted two times, based on the original imagery and based on the corrected imagery. Comparison of the final results will reveal whether or not the geometrical correction applied upon the imagery changes the results of loss estimation and replacement cost estimation significantly. This chapter also reveals how the retrofitting scheme is expected to avoid deaths and to reduce the rate of severe injuries.

7.1. The contribution of image correction to change the result of loss estimation and replacement cost

7.1.1. Changes on the results of loss estimation

1. *Loss estimation of buildings*

Loss estimation on buildings was conducted two times utilizing two individual building maps, the one developed based on the original imagery and the other one developed based on the corrected imagery. Geometrical correction conducted upon the imagery shifts the positions of the buildings. Changes of relative positions to the flow depth classes are only experienced by the buildings located in the perimeter of flow depth classes. The buildings located far from the perimeter of flow depth classes will remain at the same flow depth class after image correction.

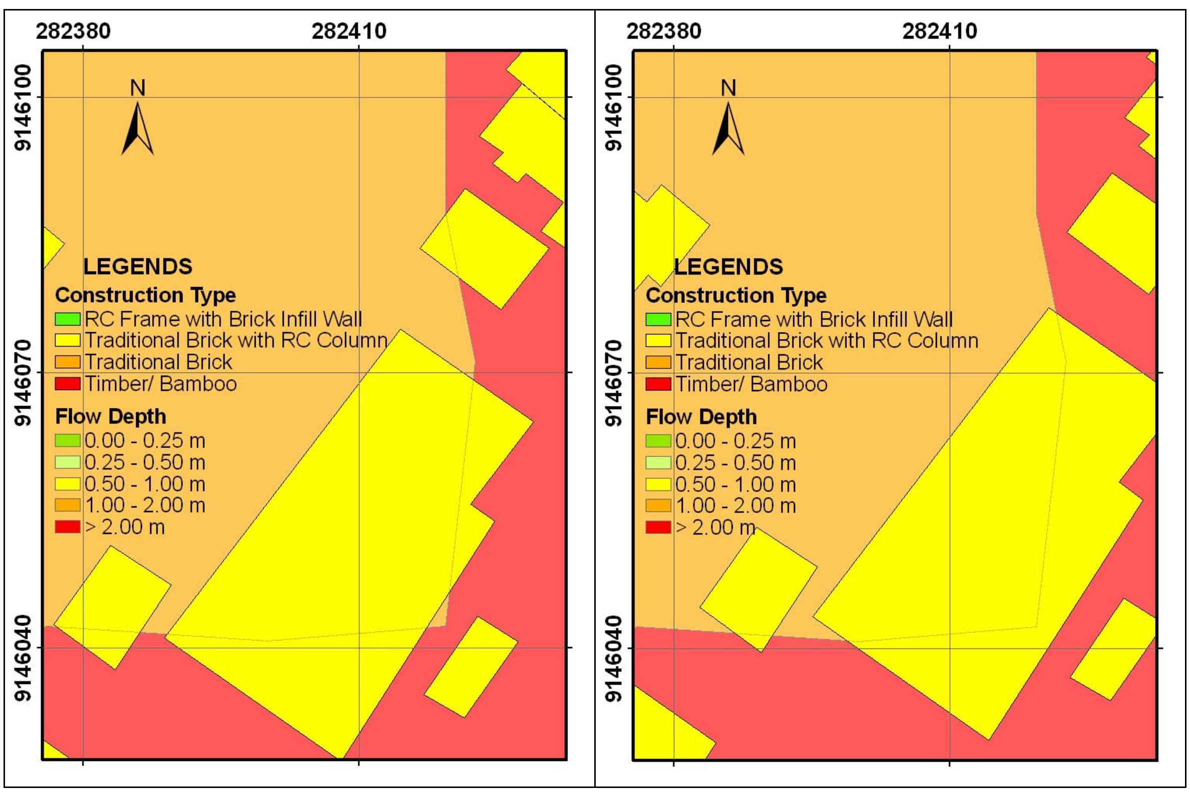

Figure 7-1. Relative positions of buildings to the flow depth classes based on original imagery (left) and corrected imagery (right)

Shifting of relative positions changed the estimated damage fractions, as shown in Figure 7.2.

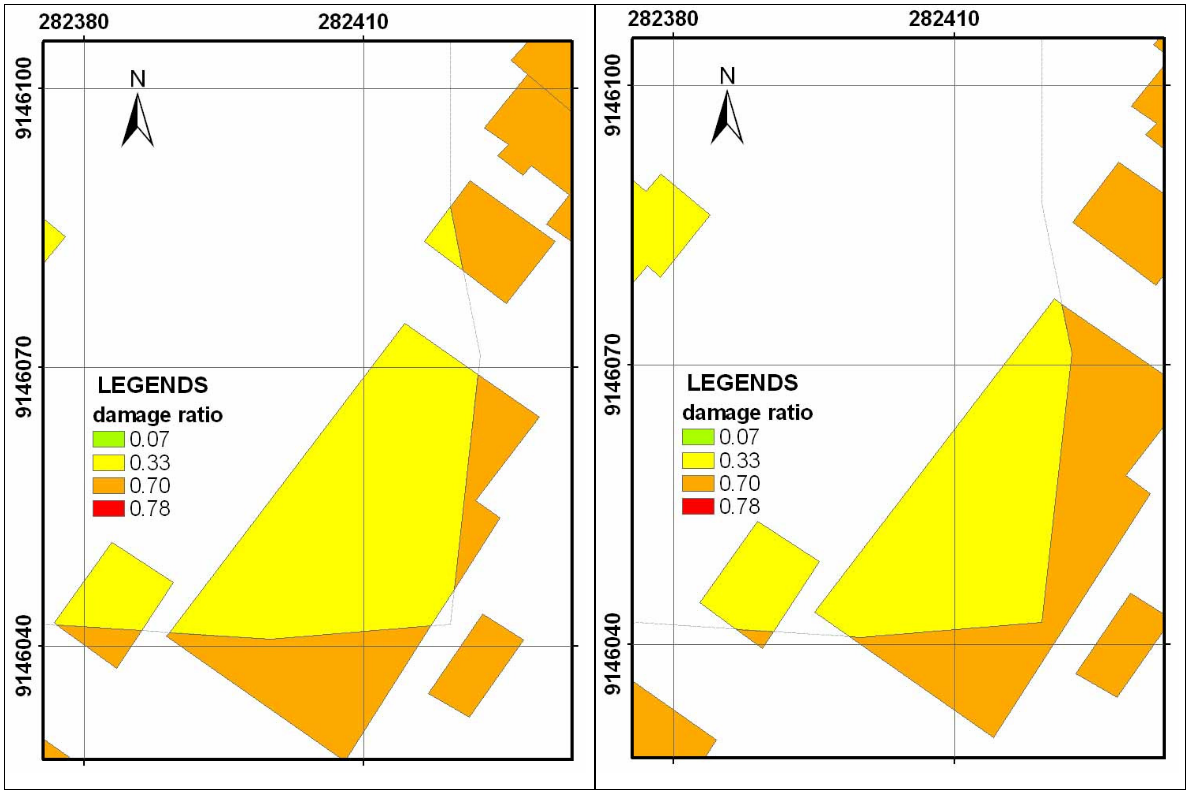

Figure 7-2. Damage fractions of buildings based on original imagery (left) and corrected imagery (right)

Changes of the estimated damage will change the result of loss estimation, as shown below:

Table 7-1. Final results of building loss estimation in the urban sample area

	Loss estimation (IDR)	Δ Loss estimation (IDR)	% Δ Loss estimation
Utilizing individual building maps developed based on original imagery	4.913.765.720	35.587.990	0.72%
Utilizing individual building maps developed based on corrected imagery	4.949.353.710		

Source: Data Analysis

Table 7-2. Final results of building loss estimation in the rural sample area

	Loss estimation (IDR)	Δ Loss estimation (IDR)	% Δ Loss estimation
Utilizing individual building maps developed based on original imagery	862.674.057	46.497.117	5.39%
Utilizing individual building maps developed based on corrected imagery	909.171.174		

Source: Data Analysis

As aforementioned, the changes of relative positions to the flow depth classes are only experienced by the buildings located in the perimeter of flow depth classes. Those are the buildings considered to experience changes on damage fraction and to change the final result of loss estimation.

Table 7-3. Final results of building loss estimation in the urban and rural sample area

	% of inundated buildings located in the perimeter of flow depth classes	% Δ building loss estimation after image correction
Urban sample area	16 out of 1141 buildings (1.40 %)	0.72 %
Rural sample area	11 out of 42 buildings (26.19 %)	5.39 %

Source: Data Analysis

Based on the data on Table 7.3, it can be concluded that image correction did not change the results of loss estimation significantly.

2. *Loss estimation of population*

Loss estimation on population was also conducted two times utilizing two individual building maps, the one developed based on the original imagery and the other one developed based on the corrected imagery. The changes of estimated population loss are as follows.

Table 7-4. Estimated losses of population for day time scenario in the urban sample area

	Losses of population in day time scenario		Δ Losses of population	% Δ Losses of population
	Based on original imagery	Based on corrected imagery		
Light injuries	2090	2096	6	0.29 %
Severe injuries	541	533	8	1.48 %
Deaths	150	152	2	1.33 %

Source: Data Analysis

Table 7-5. Estimated losses of population for night time scenario in the urban sample area

	Losses of population in night time scenario		Δ Losses of population	% Δ Losses of population
	Based on original imagery	Based on corrected imagery		
Light injuries	3944	3956	12	0.30 %
Severe injuries	253	237	16	6.32 %
Deaths	248	252	4	1.61 %

Source: Data Analysis

Table 7-6. Estimated losses of population for day time scenario in the rural sample area

	Losses of population in day time scenario		**Δ Losses of population**	**% Δ Losses of population**
	Based on original imagery	**Based on corrected imagery**		
Light injuries	14	14	0	0 %
Severe injuries	29	29	0	0 %
Deaths	19	19	0	0 %

Source: Data Analysis

Table 7-7. Estimated losses of population for night time scenario in the rural sample area

	Losses of population in night time scenario		**Δ Losses of population**	**% Δ Losses of population**
	Based on original imagery	**Based on corrected imagery**		
Light injuries	8	8	0	0 %
Severe injuries	21	21	0	0 %
Deaths	19	19	0	0 %

Source: Data Analysis

The vulnerability of the people inside or nearby a building can be estimated as functions of the building's vulnerability and depth of inundation (see Sub-chapter 5.7). After image correction, changes on the relative positions of various construction types to the flow depth classes will change their damage fractions. The changes of the building's damage fractions will change the final result of population loss estimation. In the urban sample area, image improvement resulted small changes on the estimated rates of light injuries, severe injuries, and deaths for day time or night time scenario (0.29 % - 6.32 %).

In the rural sample area, the direction of the building's shift after image correction is almost on a line with the boundary of the critical flow depth classes as shown in Figure 7.3. Vulnerability values of the buildings are not changed significantly after image correction. As the result, there are no changes on the estimated rates of light injuries, severe injuries, and deaths for day time or night time scenario. It can be concluded that geometrical correction on QuickBird imagery of 10 m horizontal accuracy will not give significant changes for population loss estimation.

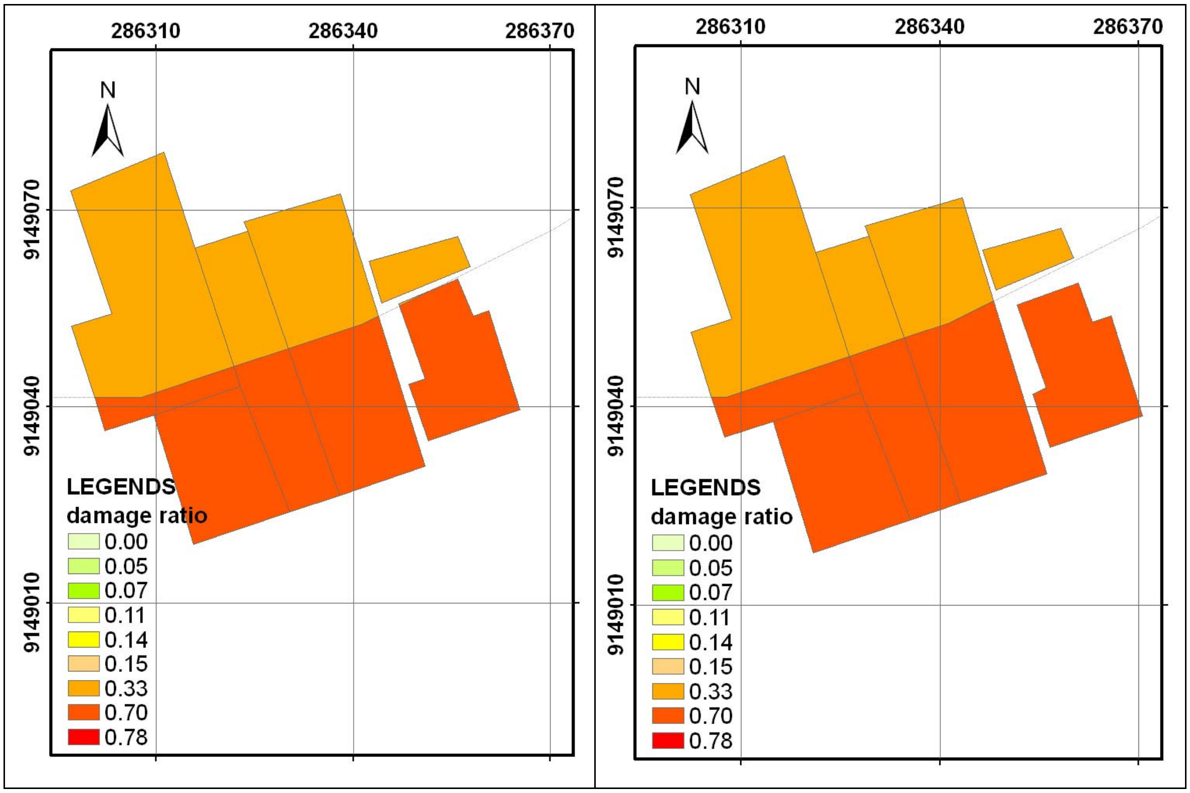

Figure 7-3. Damage fractions of buildings in rural sample area based on the original imagery (left), and based on the corrected imagery (right)

7.1.2. Changes on the results of replacement cost estimation

The existing land parcel maps and individual building maps are not reliable for mitigation planning (see Sub-chapter 5.2). Both of the proposed non structural mitigation measures are arranged by making use of the newly generated land parcel map and individual building map. Those maps are generated two times, based on the original imagery and the corrected imagery. The plans for non structural mitigation measures are developed two times, based on the original imagery and the corrected imagery.

As mentioned in Sub-chapter 5.1, geometrical correction conducted upon the imagery shifts the positions of the land parcels and buildings. The positions of land parcels and buildings in the new individual building map shift from their position in the previous individual building map. Some land parcels and buildings which are previously located out the tsunami buffer zone have become partially or completely located in the tsunami buffer zone after image correction.

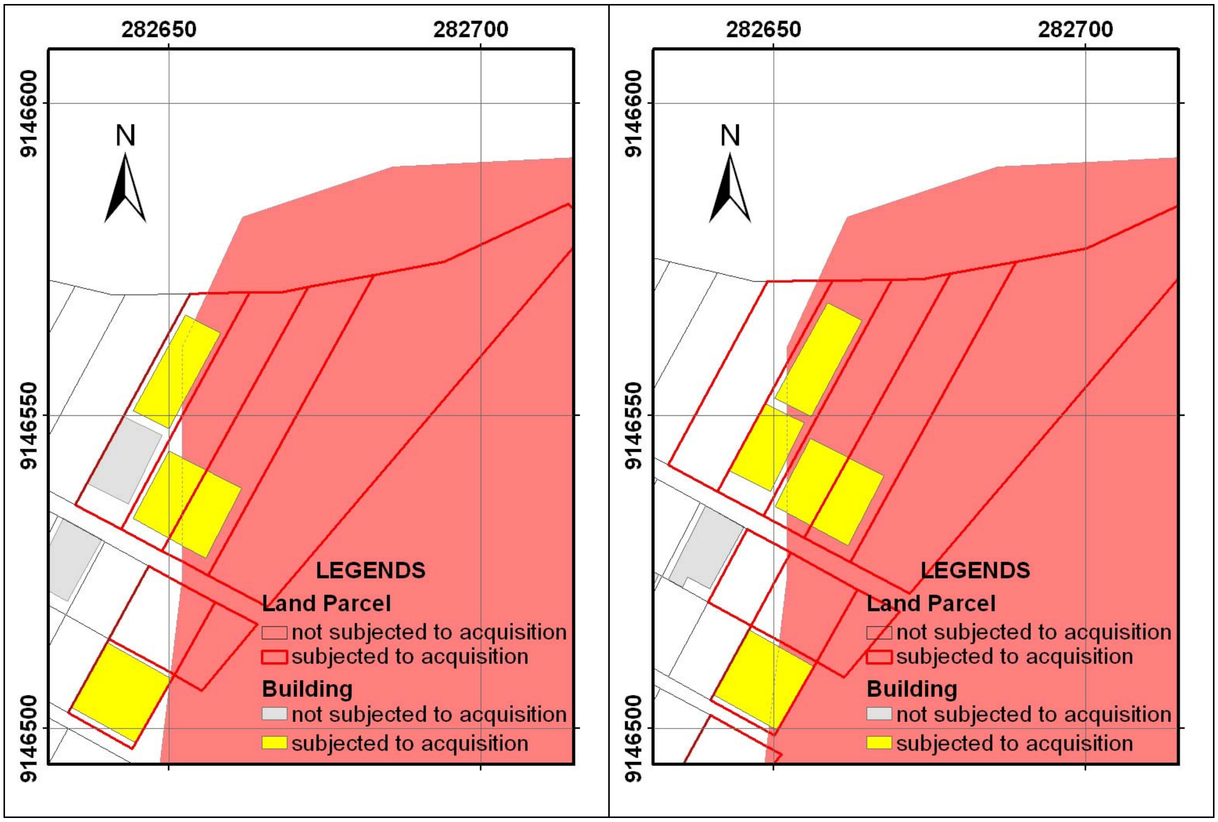

Figure 7-4. Land parcels and buildings subjected to acquisition based on original imagery (left), and based on the corrected imagery (right)

Some land parcels and buildings which are previously not subjected to acquisition have become subjected to acquisition after image correction as shown in Figure 7.4. The total number of land parcels and buildings subjected to acquisition will change due to image correction. The change of the number of buildings to acquire will change not only the total replacement cost but also the acquisition action plan.

1. *Replacement cost estimation in the urban sample area*

The results of the two acquisition plans are compared in terms of the number of private land parcels and buildings to acquire, as shown in Table 7.8 below.

Table 7-8. The number of land parcels and buildings to acquire for tsunami buffer zone acquisition in the urban sample area

	Number of land parcels and buildings subjected to acquisition		**Δ Number of land parcels and buildings subjected to acquisition**
	Based on original imagery	**Based on corrected imagery**	
Land parcel	13	16	3
Building	39	40	1

Source: Data Analysis

The changes of the number of land parcels and building to acquire will directly change the total replacement cost, as shown in Table 7.9.

Table 7-9. Replacement cost for tsunami buffer zone acquisition in the urban sample area

Acquisition of tsunami buffer zone		Replacement cost (IDR)		Δ Replacement cost (IDR)	% Δ Replacement cost
Utilizing maps developed based on *original* imagery	Land parcel	164.864.000	1.091.902.000	71.640.000	6.56 %
	Building	927.038.000			
Utilizing maps developed based on *corrected* imagery	Land parcel	208.384.000	1.163.542.000		
	Building	955.158.000			

Source: Data Analysis

Although the relative positions of the land parcels and buildings to the tsunami buffer zone are changed, there are only 3 land parcels and 1 building which were previously not subjected to acquisition have become subjected to acquisition. Since there are only a few land parcels and buildings located in the perimeter of tsunami inundation area which abuts the tsunami buffer zone, there are only a few of them have become located in the tsunami buffer zone after image correction. In fact, the total replacement cost for land parcels and buildings was changed significantly (6.56 %).

2. *Replacement cost estimation in the rural sample area*

The slight changes on the number of private land parcels and buildings to acquire are also found in the rural sample area. Geometrical correction on the imagery caused only 2 buildings which are previously not subjected to acquisition to be subjected to acquisition. The change on the number of land parcels and buildings subjected to acquisition is fewer than the change in the urban sample area. It can be understood because the number of land parcels and buildings in the rural sample area is very much smaller than that in urban sample area.

Table 7-10. The number of land parcels and buildings to acquire for tsunami buffer zone acquisition in the rural sample area

	Number of land parcels and buildings subjected to acquisition		Δ Number of land parcels and buildings subjected to acquisition
	Based on original imagery	Based on corrected imagery	
Land parcel	20	22	2
Building	17	17	0

Source: Data Analysis

Table 7-11. Replacement cost for tsunami buffer zone acquisition in the rural sample area

Acquisition of tsunami buffer zone		Replacement cost (IDR)		Δ Replacement cost (IDR)	% Δ Replacement cost
Utilizing maps developed based on original imagery	Land parcel	2.502.628.000	5.059.865.000	145.049.000	2.87 %
	Building	2.557.237.000			
Utilizing maps developed based on corrected imagery	Land parcel	2.642.569.000	5.204.914.000		
	Building	2.562.345.000			

Source: Data Analysis

The change of total replacement cost for land parcels and buildings in the rural sample area is 2.87 %. The values of land parcels and buildings are based on the data of the Tax Office for taxation purpose. They do not represent the market values. In fact, they are very much lower than the market values. When market values are used, the small percentage of the changes on the total replacement cost will mean a big amount of money. In conclusion, image correction is required in acquisition planning because it deals not only with safety goals but also with budgeting policies. The more reliable spatial data is expected to result more accurate acquisition scheme and more accurate calculation of replacement cost.

7.2. The contribution of retrofitting measures to avoid deaths and to reduce severe injuries

The retrofitting measures conducted upon buildings are expected to also reduce the vulnerability of people inside and nearby the building. Implementation of retrofitting schemes is expected to avoid death toll and reduce severe injuries. Loss estimation on population was conducted based on the initial building configuration and new building configuration after retrofitting. The changes of estimated population loss are as follows.

Table 7-12. Estimated losses of population for day time scenario in the urban sample area

	Losses of population in day time scenario		Δ Losses of population	% Δ Losses of population
	Before retrofitting	After retrofitting		
Light injuries	2096	2725	629	30.01%
Severe injuries	533	56	477	89.49%
Deaths	152	0	152	100.00%

Source: Data Analysis

Table 7-13. Estimated losses of population for night time scenario in the urban sample area

	Losses of population in night time scenario		**Δ Losses of population**	**% Δ Losses of population**
	Before retrofitting	**After retrofitting**		
Light injuries	3956	4385	429	10.84%
Severe injuries	237	60	177	74.68%
Deaths	252	0	252	100.00%

Source: Data Analysis

Table 7-14. Estimated losses of population for day time scenario in the rural sample area

	Losses of population in day time scenario		**Δ Losses of population**	**% Δ Losses of population**
	Before retrofitting	**After retrofitting**		
Light injuries	14	43	29	207.14%
Severe injuries	29	19	10	34.48%
Deaths	19	0	19	100.00%

Source: Data Analysis

Table 7-15. Estimated losses of population for night time scenario in the rural sample area

	Losses of population in night time scenario		**Δ Losses of population**	**% Δ Losses of population**
	Before retrofitting	**After retrofitting**		
Light injuries	8	29	21	262.50%
Severe injuries	21	19	2	9.52%
Deaths	19	0	19	100.00%

Source: Data Analysis

The retrofitting scheme is expected to completely avoid death toll. Severe injuries are reduced to the minimum. Contrary, the light injury rates highly increased. There are many people who are previously estimated to die or to suffer from severe injuries before building retrofitting. After retrofitting, they are less vulnerable to the given tsunami intensity. Those people are estimated to experience only light injuries.

8. Conclusion and recommendation

The conclusion whether or not the outcome of the works have met the objectives of the research is reveled in this chapter. Conclusion can also be drawn whether or not the research questions were answered. Recommendations are proposed for Cilacap City, other coastal cities, and further research.

8.1. Conclusion

The works conducted in the research have met the objectives of the research and also have answered the research questions stated in chapter 1. The main objective of the research is to develop a reliable database of elements at risk for accurate loss estimation and effective mitigation planning. The detailed conclusions related to each research objective are as follows:

1. *Methods in developing a reliable database of elements at risk*

- Existing maps related to the elements at risk are the Land Office's land parcel map and the Tax Office's block map. Poor positional accuracy and incompleteness of the feature data are the main flaws of the maps. In order to work in a detailed scale, the panchromatic QuickBird image of 0.60 m spatial resolution was used to generate new maps.
- Image validation and geometrical correction were conducted all at once. It was proven that the panchromatic ortho-rectified QuickBird imagery met the stated positional accuracy of 10 m. Ground control points (GCPs) of high accuracy were used to validate and to improve the positional accuracy of the image. Differential GPS measurement with post-processing correction have resulted 24 GCPs with horizontal precision ≤ pixel size (0.6 m).
- The land parcels and the buildings were on screen-digitized based on visual interpretation upon satellite imagery. The shapes and the spatial arrangements of buildings and parcels are extracted from the existing maps and are used as the pattern in digitizing the new individual building map and land parcel map.

2. *Loss estimation of buildings and population*

- Overlaying analysis of the tsunami inundation model and the improved individual building map will determine the relative positions of buildings to the flow depth classes accurately.
- The vulnerability curves established from the reconnaissance survey after South Java tsunami in 2006 were used as the basis in determining the vulnerability of buildings for this study. Whilst the economic values of buildings are available in the *Record of Land Parcel and Building Data* developed by the Tax Office.
- The dynamic distribution of the population in day time and night time were estimated in the basis of individual building. The occupancy rate of each building was determined based on architectural space requirements approach and several reasonable assumptions.
- The behavior of a building under the effects of certain hazards will determine whether the people inside or nearby the building might be injured or killed. The vulnerability of population is determined as the function of the vulnerability of a building to a given tsunami flow depth class.

3. *Non-structural mitigation planning through land use policy*

- The tsunami flow depth of ≥ 2 m was estimated to cause serious damage to buildings and to cause deaths to population. The area inundated by the tsunami flow depth of ≥ 2 m should be proposed as tsunami buffer zone.
- The land parcels and buildings located in tsunami buffer zone were determined by overlaying analysis of the tsunami inundation model, land parcel map, and individual building map. The economic values of land parcels buildings are available in the *Record of Land Parcel and Building Data* developed by the Tax Office. The replacement cost for tsunami buffer zone acquisition was calculated as the total compensation for land parcels and buildings located in the tsunami buffer zone.

4. *Structural mitigation planning; retrofitting*

- The behavior of a building under the effects of certain flow depth will determine whether the people inside or nearby the building might be injured or killed. Buildings that have the potential to contribute deaths or severe injuries should be subjected to retrofitting.
- The observed damages of buildings obtained from the reconnaissance survey after South Java tsunami in 2006 were used as the basis to determine the minimum structural adequacy to withstand each flow depth class. Sufficient retrofitting measures for the buildings were arranged to achieve the expected structural adequacy.

5. *The contribution of image correction for loss estimation and mitigation planning*

- Geometrical correction applied upon the original QuickBird imagery of 10 m positional accuracy results changes of building loss estimation as follows:
  - 0.72 % changes on building loss estimation in the urban sample area
  - 5.39 % changes on building loss estimation in the rural sample area

  The original imagery of 10 m positional accuracy is adequate for building loss estimation.
- Changes on the estimation of population losses due to image correction are as follows:
  - 1.33 % changes on estimated death rate for day time scenario in the urban sample area
  - 1.61 % changes on estimated death rate for night time scenario in the urban sample area
  - 0 % changes on estimated death rate for day time scenario in the rural sample area
  - 0 % changes on estimated death rate for night time scenario in the rural sample area

  The original imagery of 10 m positional accuracy does not need geometrical correction for population loss estimation purpose.
- Changes on the estimated replacement cost for tsunami buffer zone acquisition are:
  - 6.56 % changes on estimated replacement cost in the urban sample area
  - 2.87 % changes on estimated replacement cost in the rural sample area

When market values are used, the small percentage of the changes on the total replacement cost will mean a big amount of money. In addition, tsunami buffer zone acquisition deals with existing private land ownership. Accurate maps are required to determine the land parcels and building partially or completely located in the tsunami buffer zone. In the case of mitigation planning, geometrical correction utilizing differential GPS measurement must be applied upon the original QuickBird imagery of 10 m positional accuracy.

8.2. Recommendation

8.2.1. Recommendation for Cilacap City

There are several recommendations for Cilacap City based on the results of this study:

- The methods for developing reliable database of elements at risk have been conducted in the two sample areas; the urban sample area and the urban sample area. The similar methods can be conducted to generate the database of elements at risk for the whole area of Cilacap City.
- The area proposed for tsunami buffer zone has not experienced high development pressure until this time. Acquisition of the existing land parcels and buildings located in the tsunami buffer zone is still feasible.
- The retrofitting scheme conducted in the sample areas can also be implemented for the whole area of Cilacap City. The proposed construction configuration after retrofitting scheme can be used as the basis to establish local building code for the coastal area of Cilacap City.

8.2.2. Recommendation for other coastal cities

The proposed methods for developing reliable database of elements at risk are feasible to be conducted in many other coastal cities. Those methods will save significant cost and time span to result a useful and reliable database. Prices of high spatial resolution satellite imageries are revealed in sub-chapter 2.4. Prices of Trimble mapping grade GPS receivers range from US$ 6.000 to US$ 12.000. The prices of GPS receivers of the same grade from other producers are more or less the same. This equipment is useful not only for developing database of elements at risk, but also for many other works.

8.2.3. Recommendation for further research

- For similar studies in the future, it is recommended to assess the positional accuracy of the tsunami inundation model. The maps used as the basis to develop the tsunami inundation model should also be assessed in terms of positional accuracy.
- Loss estimation and calculation of replacement cost should use the market values instead of the values available in the document of the Tax Office. The prices of land parcels and buildings in for taxation purpose do not represent the actual values as the market values do.
- The proposed methods in generating reliable database of elements at risk can be conducted by making use of panchromatic QuickBird imagery of different positional accuracy or other high spatial resolution satellite imageries. Different findings may be resulted by making use of different types of satellite imageries.

List of References

Abidin, H. Z., 2007. *Penentuan Posisi Dengan GPS Dan Aplikasinya*. Third Edition. PT Pradnya Paramita. Jakarta, Indonesia. ISBN 978-979-408-377-2

Alpar, B., C. Gazioglu, Y. Altinok, Z. Y. Yücel and S. Dengiz, 2004. *Tsunami Hazard Assessment in Istanbul by Using High Resolution Satellite Data (IKONOS) and DTM*. XXth ISPRS Congress. 12-23 July 2004. Istanbul, Turkey. Proceedings of Commission VII.
http://www.isprs.org/congresses/istanbul2004/comm7/papers/137.pdf

Benny, H. Z. Abidin, T. S. Haroen and E. Heryani, 2006. *Post-Tsunami Land Parcel Reconstruction in Aceh: Aspects, Status and Problems*. Shaping the Change, XXIII FIG Congress. Munich, Germany. October 8-13, 2006

Boen, T., 2006. *Building A Safer Aceh, Reconstruction Of Houses, One Year After The Dec. 26, 2004 Tsunami*. World Seismic Safety Initiative. Jakarta, Indonesia.
http://www.unhabitat-indonesia.org/newsletter/02/files/02NL-08.pdf

BPN, 1996. *Peraturan Menteri Negara Agraria/ Kepala Badan Pertanahan Nasional Nomor 2 Tahun 1996 tentang Pengukuran Dan Pemetaan Untuk Penyelenggaraan Pendaftaran Tanah*. Badan Pertanahan Nasional (National Land Agency). Jakarta, Indonesia.
http://id.ndaru.net/wp-content/uploads/peraturan-menteri-negara-agraria-kepala-bpn-nomor-2-tahun-1996-ttg-pengukuran-dan-pemetaan-untuk-penyelenggaraan-pendaftaran-tanah.pdf

BPS, 2007. *Kecamatan Dalam Angka*. Badan Pusat Statistik. Cilacap, Indonesia.

Budiarjo, A., 2006. *Evacuation Shelter Building Planning for Tsunami-prone Area; a Case Study of Meulaboh City, Indonesia*. ITC, International Institute for Geo-Information Science and Earth Observation. MSc Thesis. Enschede, The Netherlands

Dall'Osso, F., M. Gonella, G. Gabbianelli, G.Withycombe and D. Dominey-Howes, 2009. *A Revised (PTVA) Model for Assessing The Vulnerability of Buildings to Tsunami Damage*. Natural Hazards and Earth System Sciences: 9: 1557–1565.
www.nat-hazards-earth-syst-sci.net/9/1557/2009/

Dial, G., 2000. *Ikonos Satellite Mapping Accuracy*. SpaceImaging:
http://www.gis.usu.edu/docs/protected/procs/asprs/asprs2000/pdffiles/papers/185.pdf

Digital-Globe, 2009. *QuickBird Imagery Products*. Product Guide. Digital Globe: Longmont, USA.
http://www.digitalglobe.com/index.php/48/Products?product_category_id=9

Dominey-Howes, D. and M. Papathoma, 2007. *Validating a Tsunami Vulnerability Assessment Model (the PTVA Model) Using Field Data from the 2004 Indian Ocean Tsunami*. Natural Hazards: 40: 113–136. DOI 10.1007/s11069-006-0007-9.

Dowman, I., 2005. *High Resolution Remotely Sensed Data And Spatial Data Infrastructure Development*. Eighth United Nations Regional Cartographic Conference for the Americas. 27 June -1 July 2005. New York, USA. http://unstats.un.org/unsd/geoinfo/8unrccaIP10e.pdf

Eisner, R., 2001. *Designing For Tsunamis: Seven Principles for Planning and Designing For Tsunami Hazards*. National Tsunami Hazard Mitigation Program (NTHMP).

ESRI-Canada, 2006. *Georeferencing an Image*. ESRI-Canada: Toronto, Canada. http://www.esricanada.com/k12_docs/georef_raster.pdf

Eurimage, 2009. *Eurimage Price List*. April 2009. Eurimage: Rome, Italy. http://www.eurimage.com/products/quickbird.html

Gerardi, F., M. S. Barbano, P. M. D. Martini and D. Pantosti, 2007. *Discrimination of Tsunami Sources (Earthquake Vs. Landslide) On The Basis Of Historical Data In Eastern Sicily and Southern Calabria*. http://www.earthprints.org/bitstream/2122/4119/2/Gerardi%20manuscript%202007192.pdf

ISDR, 2004. *Terminology of disaster risk reduction*. UN-International Strategy for Disaster Reduction http://www.unisdr.org/eng/library/lib-terminology-eng%20home.htm

Jones, S. A. and D. T. Jones, 2004. *Selecting The Right GPS For A Utility Infrastructure GIS*. http://www.gisdevelopment.net/proceedings/gita/2004/papers/013.pdf

Kerle, N. and M. Damen, 2009. *Multi Hazard Risk Assessment. Educational Guide Book Session 2: Spatial Data for Risk Management*. ITC. Enschede, The Netherlands

Kingma, N. C., 2009. *Multi Hazard Risk Assessment*. *Educational Guide Book Session 4: Elements at Risk*. ITC. Enschede, The Netherlands

Kingma, N. C. and C. J. V. Westen, 2009. *Multi Hazard Risk Assessment*. *Educational Guide Book Session 5: Vulnerability Assessment*. ITC. Enschede, The Netherlands

Knippers, R. A., 1999. *Geometric Aspects of Mapping*. Educational notes of ITC. Enschede, The Netherlands. http://www.kartografie.nl/geometrics/Map%20projections/body.htm

Lavigne, F., C. Gomez, M. Giffo, P. Wassmer, C. Hoebreck, D. Mardiatno, J. Priyono and R. Paris, 2007. *Field observations of the 17 July 2006 Tsunami in Java*. Natural Hazards and Earth System Sciences: 7: 177-183. www.nat-hazards-earth-syst-sci.net/7/177/2007/

Mardiatno, D., 2008. *Tsunami Risk Assessment Using Scenario Based Approach, Geomorphological Analysis, And Geographic Information System (A Case Study In South Coastal Areas of Java Island, Indonesia)*. Faculty of Geo- and Atmospheric Sciences. Universitat Innsbruck. Dissertation. Innsbruck, Austria

Murata, S., F. Imamura, K. Katoh, Y. Kawata, S. Takahashi and T. Takayama, 2010. *TSUNAMI: To Survive from Tsunami*. Advanced Series on Ocean Engineering. Volume 32. World Scientific. ISBN 13 978-981-4277-47-1

Papadopoulos, G. and F. Imamura, 2001. "*Tsunami Intensity Scale of 2001*." Retrieved 14th October 2009, from http://geology.about.com/library/bl/bltsunamiscalenew.htm.

Papathoma, M. and D. Dominey-Howes, 2003. *Tsunami Vulnerability Assessment and Its Implications for Coastal Hazard Analysis And Disaster Management Planning, Gulf of Corinth, Greece*. Natural Hazards and Earth System Sciences: 3: 733–747.

Papathoma, M., D. Dominey-Howes, Y. Zong and D. Smith, 2003. *Assessing Tsunami Vulnerability, an Example from Herakleio, Crete, Greece*. Natural Hazards and Earth System Sciences: 3: 377–389.

Post, J., K. Zosseder, G. Strunz, J. Birkmann, N. Gebert, N.Setiadi, H. Z. Anwar, H. Harjono, M. Nur and T. Siagian, 2007. *Risk and Vulnerability Assessment to Tsunami and Coastal Hazards in Indonesia: Conceptual Framework and Indicator Development*. GITEWS (German Indonesian Tsunami Early Warning System) Project: Publication no. 15.
http://www.hydroteam.de/Padang_Post_Zosseder_et%20al.pdf

Reese, S., W. J. Cousins, W. L. Power, N. G. Palmer, I. G. Tejakusuma and S. Nugrahadi, 2007. *Tsunami Vulnerability of Buildings and People in South Java – Field Observations after The July 2006 Java Tsunami*. Natural Hazards Earth and System Sciences: 7: 573–589.
www.nat-hazards-earth-syst-sci.net/7/573/2007/

ReliefWeb, 2006. *Indonesia: West Java Earthquake and Tsunami*. OCHA Situation Report No. 5.
http://www.reliefweb.int/rw/fullMaps_Sa.nsf/luFullMap/05C435428AA4B469852571B000670D43/$File/rw_EQ-TS_idn190706.pdf?OpenElement

Ruangrassamee, A., H. Yanagisawa, P. Foytong, P. Lukkunaprasit, S. Koshimura and F. Imamura, 2006. *Investigation of Tsunami-Induced Damage and Fragility of Buildings in Thailand after the December 2004 Indian Ocean Tsunami*. Earthquake Spectra: Volume 22, No. S3.
http://istim.ce.nd.edu/pubs/Thai_Damage_Anat.pdf

Santhanam, R., 2006. *Guidelines for Retrofitting of Buildings*. UNDP India:
http://www.un.org.in/untrs/reports/Retrofitting_Guidelien_16th_%20Nov_2006.pdf

Sieberg, A. and N. Ambraseys, 1962. "*Sieberg-Ambraseys Tsunami Intensity Scale*." Retrieved 14th October 2009, from http://geology.about.com/library/bl/bltsunamiscaleold.htm.

Taubenbock, H., J. Post, R. Kiefl, A. Roth, F. A. Ismail, G. Strunz and S. Dech, 2008. *Risk And Vulnerability Assessment To Tsunami Hazard Using Very High Resolution Satellite Data, The Case Study Of Padang, Indonesia*. Carsten Jurgens: Remote Sensing-New Challenges of High Resolution. http://www.earsel.org/workshops/HighRes2008/Artikel/09_Taubenboeck.pdf

UNDRO, 1991. *Mitigating Natural Disasters. Phennomena, Effects and Options. A manual Policy Makers and Planners*. Office of The United Nations Disaster Relief Co-ordinator: A publication within the Framework of the International Decade for Natural Disaster Reduction (IDNDR). http://desastres.usac.edu.gt/documentos/pdf/eng/doc1028/doc1028-indice.pdf

UNEP, 2005. *After The Tsunami*. United Nations Environment Programme (UNEP): National Rapid Environmental Assessment - Indonesia. http://www.unep.org/tsunami/reports/tsunami_indonesia_layout.pdf

Westen, C. J. V., 2009. *Multi Hazard Risk Assessment*. *Educational Guide Book Session 6: Risk Analysis*. ITC. Enschede, The Netherlands

Yeh, H., 2006. *Maximum Fluid Forces in the Tsunami Runup Zone*. Journal of Waterway, Port, Coastal, and Ocean Engineering: Vol. 132, No. 6: 496-500. https://web.engr.oregonstate.edu/~oshnackm/wiki/uploads/Main/YehH.pdf

Appendices

Appendix 1

The tsunami intensity scale proposed by Imammura and Papadopoulos (2001)

Tsunami intensity scale	Effects on humans (a), effects on objects including boats (b), and damage to buildings (c)
I. Not felt	
II. Scarcely felt	a. Felt by few people onboard small vessels. Not observed on the coast. b. No effect. c. No damage.
III. Weak	a. Felt by most people onboard small vessels. Observed by a few people on the coast. b. No effect. c. No damage.
IV. Largely observed	a. Felt by all onboard small vessels and by few people onboard large vessels. Observed by most people on the coast. b. Few small vessels move slightly onshore. c. No damage.
V. Strong (wave height 1 meter)	a. Felt by all onboard large vessels and observed by all on the coast. Few people are frightened and run to higher ground. b. Many small vessels move strongly onshore, few of them crash into each other or overturn. Traces of sand layer are left behind on ground with favorable circumstances. Limited flooding of cultivated land. c. Limited flooding of outdoor facilities (such as gardens) of near-shore structures.
VI. Slightly damaging (2 m)	a. Many people are frightened and run to higher ground. b. Most small vessels move violently onshore, crash strongly into each other, or overturn. c. Damage and flooding in a few wooden structures. Most masonry buildings withstand.
VII. Damaging (4 m)	a. Many people are frightened and try to run to higher ground. b. Many small vessels damaged. Few large vessels oscillate violently. Objects of variable size and overturn and drift. Sand layer and accumulations of pebbles are left behind. Few aquaculture rafts washed away. c. Many wooden structures damaged, few are demolished or washed away. Damage of grade 1 and flooding in a few masonry buildings.
VIII. Heavily damaging (4 m)	a. All people escape to higher ground, few are washed away. b. Most of the small vessels are damaged, many are washed away. Few large vessels are moved ashore or crash into each other. Big objects are drifted away. Erosion and littering of the beach. Extensive flooding. Slight damage in tsunami-control forests and stop drifts. Many aquaculture rafts washed away, few partially damaged. c. Most wooden structures are washed away or demolished. Damage of grade 2 in a few masonry buildings. Most reinforced-concrete buildings sustain damage, in a few damage of grade 1 and flooding is observed.

IX. Destructive (8 m)	a. Many people are washed away. b. Most small vessels are destroyed or washed away. Many large vessels are moved violently ashore, few are destroyed. Extensive erosion and littering of the beach. Local ground subsidence. Partial destruction in tsunami-control forests and stop drifts. Most aquaculture rafts washed away, many are partially damaged. c. Damage of grade 3 in many masonry buildings, few reinforced-concrete buildings suffer from damage grade 2.
X. Very destructive (8 m)	a. General panic. Most people are washed away. b. Most large vessels are moved violently ashore, many are destroyed or collide with buildings. Small boulders from the sea bottom are moved inland. Cars overturned and drifted. Oil spills, fires start. Extensive ground subsidence. c. Damage of grade 4 in many masonry buildings, few reinforced-concrete buildings suffer from damage grade 3. Artificial embankments collapse, port breakwaters damaged.
XI. Devastating (16 m)	b. Lifelines interrupted. Extensive fires. Water backwash drifts cars and other objects into the sea. Big boulders from sea bottom are moved inland. c. Damage of grade 5 in many masonry buildings. Few reinforced-concrete buildings suffer from damage grade 4, many suffer from damage grade 3.
XII. Completely devastating (32 m)	c. Practically all masonry buildings demolished. Most reinforced-concrete buildings suffer from at least damage grade 3.

Appendix 2

Format Conversion of the Land Office’s Land Parcel Map

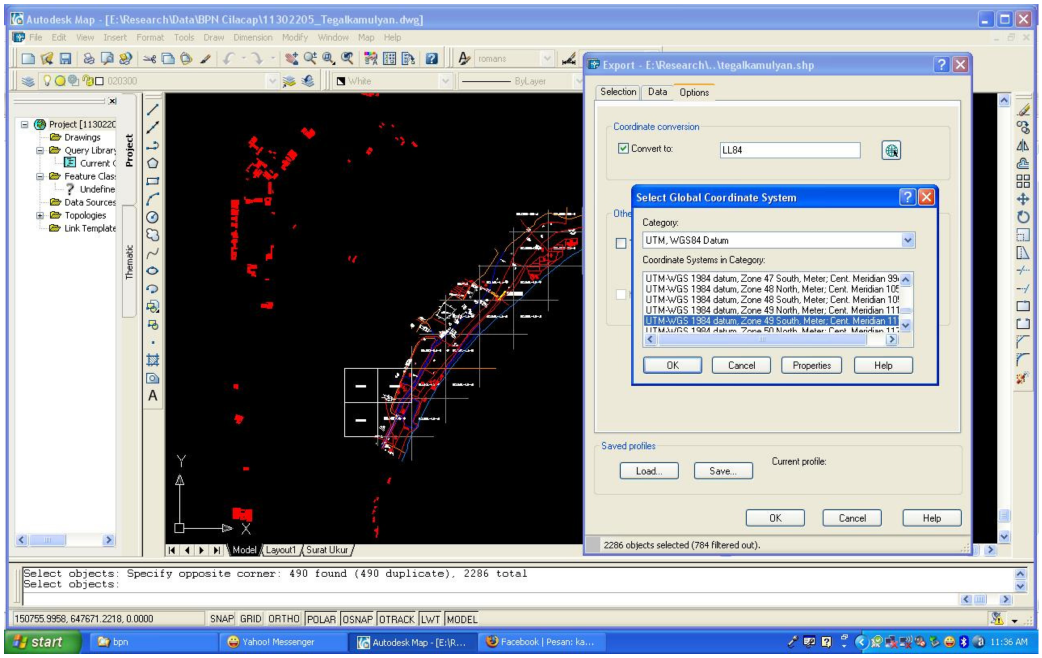

Setting the coordinate conversion

Cilacap city lies between longitude 108°59’27.21”E – 109°06’04.25”E. The whole city is located in UTM zone 49 (108º - 114º). Since the city is located in the southern hemisphere, the UTM zone is 49 S. In TM3º projection system, a 6 º zone in the UTM is divided into two 3 º zones. For the UTM 49 S zone, there will be TM3º 49.1 and TM3º 49.2 zones. Cilacap city is located in zone 49.1 (108º - 111º) in TM3º coordinate system.

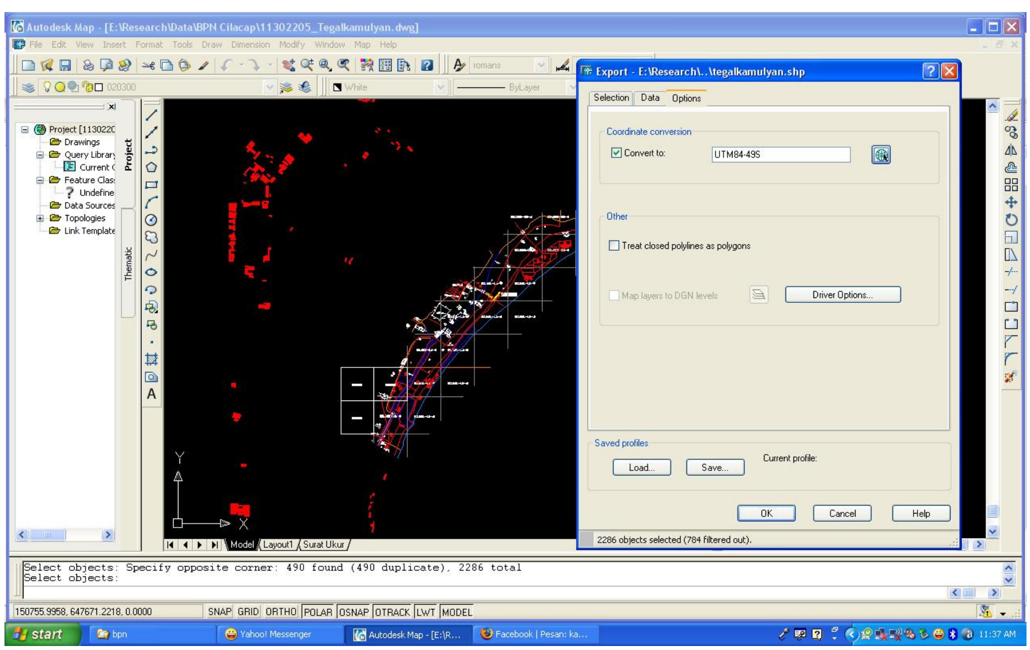

Converting the format and the coordinate system all at once

Appendix 3

The Record of Land Parcel and Building Data of the Tax Office

LAPORAN HASIL SURVEY LAPANGAN OLEH PETUGAS
DAFTAR HASIL REKAMAN DATA TANAH DAN BANGUNAN
URUT NOMOR OBJEK PAJAK
(Semua Objek Terdaftar)

KANWIL : 10 - JAWA TENGAH II
KANTOR PELAYANAN - PAJAK PRATAMA CILACAP
PROPINSI : 33 - JAWA TENGAH
KOTA/KAB : 01 - CILACAP

NOP	NO.FORMULIR	BNG	ALAMAT OBJEK PAJAK							RW/RT	NAMA WAJIB PAJAK					LUAS BUMI	ZNT
	NO.FORMULIR	NO. BNG	JENIS BNG	LUAS BNG	JML LNT	THN BNG	THN REN	DAYA LISTRIK	KONDISI UMUM	JENIS KONSTR	JENIS ATAP	JENIS DINDING	JENIS LANTAI	JENIS LANGIT	AC WINDOW	AC SPLIT	AC SENTRAL
020-0001.0	1996.0301.032	000	KP BLOK 020							00/000	SUTARDI					100 m2	BJ
020-0002.0	1996.0301.033	000	KP BLOK 020							00/000	MAHUR					100 m2	BJ
020-0003.0	1996.0301.034	002	KP BLOK 020							00/000	TABRANI					900 m2	BJ
	1913.4100.3	001	RMH	340 m2	2	1999		1300	BAIK	BETON	GT.BIA	BATA	KERAMIK	TRIPLEK	0	0	TD. ADA
	1913.4100.4	002	RMH	250 m2	1	1999		1300	SEDANG	BETON	GT.BIA	BATA	SEMEN	TD. ADA	0	0	TD. ADA
020-0014.0	1996.0301.045	000	KP BLOK 020							00/000	SANMURDI					100 m2	BJ
020-0015.0	1996.0301.046	000	KP BLOK 020							00/000	TUMINO					100 m2	BJ
020-0016.0	1996.0301.047	000	KP BLOK 020							00/000	M SOLICHIN					100 m2	BJ
020-0017.0	1996.0301.048	000	KP BLOK 020							00/000	DIDI HALININ					100 m2	BJ
020-0018.0	2005.0001.090	000	KP BLOK 020							00/000	HARYANTO EKO NUGROHO					100 m2	BJ
020-0019.0	2005.0002.020	000	KP BLOK 020							04/003	HARYANTO EKO NUGROHO					100 m2	BJ
020-0020.0	1996.0301.051	000	KP BLOK 020							00/000	NO KAV 20/1V					100 m2	BJ
020-0021.0	2003.0705.549	000	KP BLOK 020							00/000	HENI PRICHATININGSIH					100 m2	BJ
020-0022.0	2003.0705.581	000	KP BLOK 020							00/000	HENY PRICHATININGSIH					100 m2	BJ
020-0023.0	2003.0705.586	000	KP BLOK 020							00/000	HENY PRICHATININGSIH					100 m2	BJ
020-0024.0	2003.0705.578	000	KP BLOK 020							00/000	HENY PRICHATININGSIH					100 m2	BJ
020-0025.0	1996.0301.056	000	KP BLOK 020							00/000	NO KAV 25/1V					100 m2	BJ
020-0026.0	2001.1712.106	000	KP BLOK 020							00/000	HARYANTO EKO NUGROHO					100 m2	BJ
020-0027.0	2005.0001.090	000	KP BLOK 020							00/000	HARYANTO EKO NUGROHO					100 m2	BJ

Continued on next page..

KECAMATAN : 710 - CILACAP SELATAN
KELURAHAN : 005 - TEGALKAMULYAN

NILAI BUMI(xRp.1000)	NO. KTP	NPWP	STA.WP	PEK.WP	PERSIL	NIP PETUGAS	NIP OPERATOR
LUAS KOLAM RENANG FINISH. KOL.RNG	NILAI BANGUNAN (xRp.1000)	NILAI INDIVIDU (xRp.1000)				NIP PETUGAS	NIP OPERATOR
12,800	330171000502000010		1-PML	5-LNY		060046136	080500007
12,800	330171000502000020		1-PML	5-LNY		060046136	080500007
115,200	2337/02337/710004		1-PML	5-LNY		060046136	080500007
0	361,271	0				060046136	060009902
0	156,413	0				060046136	060009902
12,800	933.01.710.003.00720		1-PML	5-LNY		060046136	080500007
12,800	933.01.710.003.00725		1-PML	5-LNY		060046136	080500007
12,800	933.01.710.003.00729		1-PML	5-LNY		060046136	080500007
12,800	933.01.710.003.00730		1-PML	5-LNY		060046136	080500007
12,800	330171000502000180		1-PML	5-LNY		060046136	080500011
12,800	330171000502000190		1-PML	5-LNY		060046136	080500012
12,800	933.01.710.003.00741		1-PML	5-LNY		060046136	080500007
12,800	330171000502000210		1-PML	5-LNY		060046136	060073505
12,800	330171000502000220		1-PML	5-LNY		060046136	060073505
12,800	330171000502000230		1-PML	5-LNY		060046136	060073505
12,800	330171000502000240		1-PML	5-LNY		060046136	060073505
12,800	933.01.710.003.00766		1-PML	5-LNY		060046136	080500007
12,800	330171000502000260		1-PML	5-LNY		060046136	060085202
12,800	330171000502000180		1-PML	5-LNY		060046136	080500011

Appendix 4

Metadata of the QuickBird imagery according to ISO / TC211 2003

Metadata field	Description	Value
General Metadata		
Metadata Creation Date	Date that the metadata was created	2007-02-23
Language	Language used for documenting metadata	English
Identification		
Title	Identifies the location (URL) of the dataset to which the metadata applies	Quickbird Cilacap
Abstract	Brief narrative summary of the content of the resource(s)	Quickbird satellite image of Cilacap acquired on 2006-06-23
Descriptive Keywords	Provides category keywords, their type, and reference source	Quickbird satellite image, Cilacap on 2006-06-23
Citation	Citation data for the resource(s)	Digital Globe (2006): Quickbird Cilacap
Date	Reference date for the cited resource	2006-06-23
Dataset	Identifies the location (URL) of the dataset to which the metadata applies	
Lineage	Non-quantitative quality information about the lineage of the data specified by the scope	1. The data set was orthorectified by using rpb-files, 40 Ground control points derived from road-network- and coastline-information from topographic maps (1:25 000) and the SRTM-best-of dataset resampled down to 0.6 m.
Resource Format	Provides a description of the format of the resource(s)	GeoTiff
Data type	Type of spatial data (vector, raster, tin,)	Raster data
Equivalent Scale	Level of detail expressed as the scale of a comparable hardcopy map or chart	1 : 10 000
Distance	Ground sample distance	0,6 m (Panchromatic), 2,4 (Multispectral)

Continued on next page..

Metadata field	Description	Value
Positional Accuracy	Accuracy of the position of features	Horizontal accuracy: 10m The total RMS of the rectification of the panchromatic channel is 2.3287 The total RMS of the rectification of the multispectral channels is 0.5822
Thematic Accuracy	Accuracy of quantitative attributes and the correctness of non-quantitative attributes and of the classifications of features and their relationships	Not applicable
Imaging Condition	Conditions affected the image	Cloud Coverage is < 1% meanSatAz= 32.0, meanSunEl= 53.1, MeanSatAz= 111.0, MeanSatEl= 78.6, meanOffNadirAngle= 10.6
Spatial Representation		
Bounding Box	Earth location in the coordinate system defined by the Spatial Reference System and the grid coordinate of the cells at opposite ends of grid coverage along two diagonals in the grid spatial dimensions. There are four corner points in a georectified grid; at least two corner points along one diagonal are required	West Bounding Coordinate: 274012.741789 East Bounding Coordinate: 288100.141789 North Bounding Coordinate: 9153828.629013 South Bounding Coordinate: 9137520.029013
Resolution	Degree of detail in the grid dataset	0,6 m (Panchromatic), 2,4 (Multispectral)
Pixel Reference Point	Point in a pixel corresponding to the Earth location of the pixel	Pixel center
Reference System		
Reference System Identifier	Name of reference system (as EPSG code number)	UTM 49 South WGS 84
Content information		
Feature Catalogue Description	information identifying the feature catalogue or the conceptual schema	Not applicable

Continued on next page..

Metadata field	Description	Value
Spectral Band	Range of wavelengths in the electromagnetic spectrum	Blue Green Red NearInfrared Panchromatic
Bits Per Value	Maximum number of significant bits in the uncompressed representation for the value in each band of each pixel	Unsigned 16-bit
Dimension Size	Number of elements along the axis	5871 cols, 6797 rows (multispectral); 23480 cols, 27182 rows (panchromatic)
Specification	Name of a subset, profile, or product specification of the format	GEOTIFF
Processing Level Code	Image distributor's code that identifies the level of radiometric and geometric processing that has been applied	Orthorectified image

Appendix 5

Examples of construction types in the study area

No	Construction type	Image
1.	Timber/ Bamboo ▪ Wall material : Timber/ Bamboo ▪ Column material : Timber/ Bamboo ▪ Column dimension : 10 cm x 10 cm to 20 cm x 20 cm ▪ Floor material : Concrete ▪ Roof material : Corrugated steel sheets ▪ Number of storey : 1 storey	
2.	Traditional Brick ▪ Wall material : Brick infill concrete ▪ Column material : Timber ▪ Column dimension : 10 cm x 10 cm to 20 cm x 20 cm ▪ Floor material : Concrete ▪ Roof material : Corrugated concrete sheets ▪ Number of storey : 1 storey	
3.	Traditional Brick with RC column ▪ Wall material : Brick infill concrete ▪ Column material : Reinforced concrete ▪ Column dimension : 10 cm x 10 cm to 20 cm x 20 cm ▪ Floor material : Concrete ▪ Roof material : Clay tiles ▪ Number of storey : 1 storey	
4.	RC Frame with Brick Infill Wall ▪ Wall material : Brick infill concrete ▪ Column material : Reinforced concrete ▪ Column dimension : At least 20 cm x 20 cm ▪ Floor material : Concrete ▪ Roof material : Corrugated steel sheets ▪ Number of storey : 2 storeys	

Appendix 6

Example of building loss estimation

ID_Build	Construction Type	Flow Depth	Damage Fraction	Area Affected (m2)	Area Total (m2)	Percentage Area Affected	Building Price (Rp)	Building Losses (Rp)
737 *	Brick Traditional with RC-column	1,0 - 2,0 m	0.33	56.94	56.94	100.00%	8,795,000	2,902,350
738 *	Brick Traditional with RC-column	1,0 - 2,0 m	0.33	54.12	54.12	100.00%	10,805,000	3,565,650
739 *	Brick Traditional with RC-column	1,0 - 2,0 m	0.33	46.68	46.68	100.00%	8,795,000	2,902,350
740 *	Brick Traditional with RC-column	1,0 - 2,0 m	0.33	49.59	49.59	100.00%	7,745,000	2,555,850
741 *	Brick Traditional with RC-column	1,0 - 2,0 m	0.33	49.44	49.44	100.00%	7,745,000	2,555,850
742 *	Brick Traditional with RC-column	1,0 - 2,0 m	0.33	49.53	49.53	100.00%	12,275,000	4,050,750
743 *	Brick Traditional with RC-column	1,0 - 2,0 m	0.33	48.68	48.68	100.00%	11,876,000	3,919,080
744 *	Brick Traditional with RC-column	1,0 - 2,0 m	0.33	53.09	53.09	100.00%	12,275,000	4,050,750
745 *	Brick Traditional with RC-column	1,0 - 2,0 m	0.33	54.09	54.09	100.00%	10,805,000	3,565,650
750 *	Brick Traditional with RC-column	1,0 - 2,0 m	0.33	47.91	47.91	100.00%	8,795,000	2,902,350
751 *	Brick Traditional with RC-column	1,0 - 2,0 m	0.33	30.54	30.54	100.00%	12,275,000	4,050,750
752 *	Brick Traditional with RC-column	1,0 - 2,0 m	0.33	39.31	39.31	100.00%	8,795,000	2,902,350
754 *	Brick Traditional with RC-column	1,0 - 2,0 m	0.33	51.08	51.08	100.00%	8,795,000	2,902,350
755 *	Brick Traditional with RC-column	1,0 - 2,0 m	0.33	53.57	53.57	100.00%	7,745,000	2,555,850
1302 *	Brick Traditional with RC-column	1,0 - 2,0 m	0.33	81.70	81.70	100.00%	21,078,000	6,955,740
1303 *	Brick Traditional with RC-column	1,0 - 2,0 m	0.33	92.67	92.67	100.00%	23,941,000	7,900,530
1304 *	Brick Traditional with RC-column	1,0 - 2,0 m	0.33	82.45	82.45	100.00%	25,909,000	8,549,970
1305 **	Brick Traditional with RC-column	1,0 - 2,0 m	0.33	93.77	139.98	66.99%	36,171,000	7,996,366
1305 **	Brick Traditional with RC-column	>2,0 m	0.70	46.21	139.98	33.01%	36,171,000	8,357,635
1306 **	Brick Traditional with RC-column	1,0 - 2,0 m	0.33	79.49	89.01	89.31%	28,120,000	8,287,497
1306 **	Brick Traditional with RC-column	>2,0 m	0.70	9.52	89.01	10.69%	28,120,000	2,104,297
1307 **	Brick Traditional with RC-column	1,0 - 2,0 m	0.33	4.44	164.14	2.70%	51,818,000	462,169
1307 **	Brick Traditional with RC-column	>2,0 m	0.70	159.70	164.14	97.30%	51,818,000	35,292,365
1309 **	Brick Traditional with RC-column	1,0 - 2,0 m	0.33	4.67	112.09	4.16%	35,387,000	486,039
1309 **	Brick Traditional with RC-column	>2,0 m	0.70	107.42	112.09	95.84%	35,387,000	23,740,098

* Buildings completely located in a class of flow depth

** Buildings crossed by the boundary of two classes of flow depth

Appendix 7

Example of population loss estimation

Vulnerability of People	Building Type	Occupants Day Time	Occupants Night Time	Light Injuries Day Time	Light Injuries Night Time	Severe Injuries Day Time	Severe Injuries Night Time	Deaths Day Time	Deaths Night Time
Severe injuries	House	2	4	0	0	2	4	0	0
Deaths	House	2	4	0	0	0	0	2	4
Deaths	House	2	4	0	0	0	0	2	4
Light injuries	House	2	4	2	4	0	0	0	0
Deaths	House	2	4	0	0	0	0	2	4
Light injuries	House	2	4	2	4	0	0	0	0
Light injuries	House	2	4	2	4	0	0	0	0
Light injuries	House	2	4	2	4	0	0	0	0
Severe injuries	House	2	4	0	0	2	4	0	0
Light injuries	House	2	4	2	4	0	0	0	0
Severe injuries	House	2	4	0	0	2	4	0	0
Light injuries	House	2	4	2	4	0	0	0	0
Severe injuries	House	2	4	0	0	2	4	0	0
Severe injuries	House	2	4	0	0	2	4	0	0
Severe injuries	House	2	4	0	0	2	4	0	0
Light injuries	House	2	4	2	4	0	0	0	0
Deaths	House	2	4	0	0	0	0	2	4
Deaths	House	2	4	0	0	0	0	2	4
Severe injuries	House	2	4	0	0	2	4	0	0
Severe injuries	Office	36	1	0	0	36	1	0	0
Severe injuries	Office	29	1	0	0	29	1	0	0
Severe injuries	Office	11	1	0	0	11	1	0	0
Deaths	Warehouse	2	2	0	0	0	0	2	2
Deaths	Warehouse	1	1	0	0	0	0	1	1
Deaths	Warehouse	2	2	0	0	0	0	2	2